Translated from Russian by J. G. Adashko

Reviews of Plasma Physics

Edited by Acad. B. B. Kadomtsev

Volume 13

CONSULTANTS BUREAU · NEW YORK-LONDON

The Library of Congress cataloged the first volume of this title as follows:

Reviews of plasma physics. v. 1–
New York, Consultants Bureau, 1965–
/v. illus. 24 cm.
Translation of Voprosy teorii plazmy.
Editor: v. 1– M. A. Leontovich.

1. Plasma (Ionized gases)–Collected works. I. Leontovich, M. A., ed. II. Consultants Bureau Enterprises, Inc., New York. III. Title: Voprosy teorii plazmy. Eng.
QC718.V63 64-23244

The original text, published by Energoatomizdat in Moscow in 1984,
has been corrected and updated by the authors.

ISBN 0-306-11003-2

A Division of Plenum Publishing Corporation
233 Spring Street, New York, N.Y. 10013

Printed in the United States of America

CONTENTS

PARTICLE DYNAMICS IN MAGNETIC TRAPS

B. V. Chirikov

TRANSPORT PROCESSES IN AXISYMMETRIC OPEN TRAPS

D. D. Ryutov and G. V. Stupakov

CLASSICAL LONGITUDINAL PLASMA LOSSES FROM OPEN ADIABATIC TRAPS

V. P. Pastukhov

SPECTRAL-LINE BROADENING IN A PLASMA

V. I. Kogan, V. S. Lisitsa, and G. V. Sholin

ELECTRON CYCLOTRON PLASMA HEATING IN TOKAMAKS

A. D. Piliya and V. I. Fedorov

PARTICLE DYNAMICS IN MAGNETIC TRAPS

B. V. Chirikov

1. Introduction. Budker's Problem [1]

The investigation of the dynamics of individual (noninteracting) charged particles in a magnetic trap is probably the simplest of the problems of prolonged plasma containment for controlled thermonuclear fusion. Nonetheless, even this "simple" problem is quite rich in content and is far from completely solved, notwithstanding many years' efforts in this direction (see, e.g., [2-4]). In addition, the dynamics of an individual particle is an integral part of the more complicated problem of collective processes in a plasma. Finally, the problem of containing a single particle in a magnetic trap must be faced every time when a new scheme or a substantial modification of an old method of magnetic confinement of a plasma appears.* An example is Dimov's ambipolar (tandem mirror) trap [7]. It is one of the so-called open systems of plasma confinement, or traps with "magnetic mirrors," which will be discussed below. We shall refer to them for brevity simply as traps.

The dynamics of a particle in a trap can be regarded as a problem of nonlinear oscillations induced possibly by some external perturbation in a system having, generally

*Certain very simple particle-interaction effects can be accounted for also within the scope of the single-particle problem, for example the change of the magnetic-field configuration on account of plasma diamagnetism or particle scattering in a plasma.

speaking, three degrees of freedom. The term "oscillations" is used here in a broad sense as a synonym for finite motion of a particle in a bounded region of space (particle containment). In other words, we assume here that the construction of the trap (the magnetic-field configuration) ensures "locking" of the particle for a time equal at least to several passes of the particle through the trap. Under these conditions, the main factor that determines the character of a prolonged evolution of the oscillations are the resonances, or the commensurability of the periods of various degrees of freedom of the oscillations, as well as commensurability with the external perturbation. The mechanism whereby the resonances act is particularly clear (and well known) in the simplest case of linear oscillations. Nonlinear dynamics is much more complicated, but in this case resonant processes are unique for the very same reason: small resonant perturbations repeat in time and accumulate, leading to a greater long-time effect than nonresonant perturbations. This important property can be used to define resonant processes in a broad sense.

Such a "resonant" approach means, figuratively speaking, that before some dynamic problem is solved it must be checked for the presence of resonances, even if it seems obvious at first glance that none exist here. A splendid example of such a situation is the action exerted on a system by an adiabatic (i.e., a very-low-frequency) perturbation, and is in fact the subject of this article.

We shall accordingly pay principal attention below to a fullest possible analysis of various resonances and to the interaction between them. The latter means the effect of the joint action of several resonances, which does not add up simply to the sum of the effects due to individual resonances, since the equations of motion are nonlinear and the superposition rule is thus invalid.

It turns out that, under certain conditions, the interaction of the resonances alters radically the character of the motion and transforms it from the well-known regular or quasiperiodic oscillations into the relatively little-known "random (stochastic) walk" of the particle in its phase space (see, e.g., [8, 9]). The latter is very similar to (and in some cases indistinguishable from) random oscillations, i.e., oscillations caused by some external (relative to the dynamic system) random perturbation or "noise," although such a perturbation need not necessarily be present. Strange as it may seem, this unusual motion regime is quite widespread for nonlinear oscillations in general, and for a particle in a magnetic field in particular. From the standpoint of prolonged containment of particles in a trap, the onset of random oscillations is harmful, since it leads as a rule to particle loss through diffusion in phase space.

We confine ourselves in this review to a discussion of the simplest case of nonlinear oscillations with two degrees of freedom, when a random regime of motion in a conservative system is still possible. For particle motion in a trap this presupposes some symmetry of the magnetic field, meaning an additional integral of motion (besides the energy). In the case of axial symmetry, for example, the additional integral is the component of the particle's canonical momentum along the symmetry axis. The motion is then over the intersection, in phase space, of the constant-energy surface and the constant-value surface of the additional integral.

We actually consider below a certain quite special case, when the connection between the two degrees of freedom is adiabatic, i.e., the ratio of the fundamental unperturbed frequencies is very large (or small). This special problem, which stems from an analysis of the operation of a trap with magnetic mirrors (the Budker problem), is nonetheless connected with one classical problem of mechanics, viz., adiabatic invariance of the action variables. It is worthwhile noticing that it is precisely research into particle containment in traps which made possible considerable progress toward the solution of this general problem, too. It became clear, in particular, that, under certain conditions, an adiabatic invariant becomes an exact integral of the motion [10].

These and other results are discussed below using as an example particle dynamics in several quite simple yet typical modifications of a magnetic trap. The problem can be solved in some cases completely; i.e., it is possible to obtain in explicit form the particle containment conditions, on the one hand, and the statistical properties of the motion in the unstable region, on the other [2].

The author is indebted to G. I. Dimov, D. D. Ryutov, and D. L. Shepelyanskii for interesting discussions of the questions touched upon in the article, and to G. B. Minchenkov for help with the numerical simulation.

2. Choice of Unperturbed System

As a rule, an analytic investigation is possible only by using some approximate methods or perturbation theory. The first step is therefore to divide the investigated system into an unperturbed part and a perturbed one. This division is not unique and is dictated by the type of physical problem.

In the present case we might, for example, choose as the unperturbed system a particle in a uniform magnetic field, and include the spatial inhomogeneity of the field as a whole in the perturbation. Although the unperturbed motion is in this case extremely simple, this is not the best choice. The point is that such an unperturbed motion is infinite and, therefore, differs qualitatively from the actual (perturbed) motion. The unperturbed motion is said in this case to be degenerate (one of the fundamental frequencies of the system is zero), and an arbitrarily small perturbation (field inhomogeneity of suitable configuration) leads to bifurcation.

To choose an unperturbed system more suitable for investigation we recall that particle containment in an open trap is the result of approximate conservation of the particles' magnetic moment $\mu = mv_\perp^2/2B$, which is proportional to an adiabatic invariant (the action variable $J_\perp$ of the Larmor rotation). Taking as the basic units the speed of light, the charge, and the particle mass ($c = e = m = 1$), we get

$$J_\perp = \frac{1}{2\pi}\oint(\mathbf{p}_\perp + \mathbf{A})\,d\mathbf{r} = v_\perp^2/2\omega = \mu. \tag{2.1}$$

The subscript $\perp$ labels here quantities that characterize motion in a plane perpendicular to the magnetic field $\mathbf{B} = \mathrm{rot}\,\mathbf{A}$; $\omega = B$ is the Larmor frequency. We shall be interested below in the nonrelativistic case ($v \ll 1$), but all the relations remain in force at arbitrary velocities if the substitution $m \to \gamma m$, $\gamma = (1 - v^2)^{-1/2}$ is made. Expression (2.1) for the action $J_\perp$ is exact only in a uniform field. We can, however, define the unperturbed system by stipulating just this quantity to be an exact integral:

$$\mu \equiv \mathrm{const}. \tag{2.2}$$

The identity sign indicates that the last condition is an arbitrary choice of the unperturbed system rather than the property of the quantity μ. We refer all the changes of μ to the perturbation, which we assume to be small enough. The last condition is known to be met for a sufficiently strong magnetic field or, equivalently, for a sufficiently small Larmor radius of the particle (see Section 4 below).

For an axisymmetric magnetic trap, neglecting the particle drift velocity, the unperturbed Hamiltonian is

$$H^0(p, s) = v^2/2 = p^2/2 + \mu\omega(s), \tag{2.3}$$

where s is the coordinate along the magnetic line, and $p = v_{\parallel} = \dot{s}$ is the conjugate momentum (and the longitudinal velocity) of the particle. It can be seen that an unperturbed system defined with the aid of (2.2) is convenient also because the effective potential energy of the longitudinal motion turns out, in this case, to be simply proportional to the specified magnetic field strength. Knowing the Hamiltonian (2.3), we can, in principle, obtain the unperturbed longitudinal motion of the particle.

3. A Few Examples

1. Auxiliary System. To demonstrate most simply the main features of particle dynamics in a magnetic trap, we consider, besides different trap variants, also an auxiliary model with two degrees of freedom, specified by the Hamiltonian

$$H(x, y, p_x, p_y) = \frac{p_x^2 + p_y^2 + (1 + x^2)^2 y^2}{2}, \tag{3.1}$$

where $p_x = \dot{x}$; $p_y = \dot{y}$. The equipotentials of this system $[(1 + x^2)y = \text{const}]$ are not closed, so that the energy conservation law does not by itself ensure as yet that the motion is finite. Nonetheless, as will be shown below (Section 10), the oscillations of this system turn out under certain conditions to be rigorously bounded. If the frequency of the oscillations along x (the x oscillations) is much lower than that of the y oscillations, the system (3.1) simulates approximately the motion of a particle in an axisymmetric magnetic trap. Indeed, y oscillations with variable frequency $\omega_y = 1 + x^2$ correspond to Larmor rotation in an inhomogeneous magnetic field $B = 1 + s^2$. The action variable for these oscillations is

$$J_y = \omega_y a_y^2/2 = (1 + x^2)\, a_y^2/2 \equiv \text{const}, \tag{3.2}$$

where a_y is the amplitude of the y oscillations. The last condition, just as (2.2), defines an unperturbed system whose Hamiltonian we obtain with the aid of the condition

$$\frac{p_y^2}{2}+\frac{\omega_y^2 y^2}{2}\equiv\omega_y J_y, \tag{3.3}$$

which is equivalent to (3.2). From (3.1) we get

$$H^0=p_x^2/2+J_y(1+x^2)=J_y+J_x\sqrt{2J_y}\,. \tag{3.4}$$

The unperturbed Hamiltonian depends only on the action variables, which are therefore integrals of the motion, and describes independent oscillations in two degrees of freedom, with frequencies

$$\omega_x=\partial H^0/\partial J_x=\sqrt{2J_y}\,,\qquad \langle\omega_y\rangle=\partial H^0/\partial J_y=1+J_x/\sqrt{2J_y}\,. \tag{3.5}$$

The quantity $\langle\omega_y\rangle$ has the meaning of the time-averaged frequency of the y oscillations and can, of course, be obtained also by directly averaging the quantity $(1 + x^2)$.

An important property of the considered unperturbed oscillations is that they are not isochronous – the oscillation frequencies depend on the actions (or amplitudes), although both the x and the y oscillations are almost harmonic (the frequency of the y harmonics varies slowly with time).

2. Short Magnetic Trap. Assume that the trap field has not only a symmetry axis ($r = 0$ in the cylindrical coordinates z, r, φ) but also a symmetry plane ($z = 0$). Let the field on the trap axis be given as

$$B_z(z,0)=B_{00}f(z),\quad f(0)=1,\qquad f(-z)=f(z),\quad B_r(z,0)=0, \tag{3.6}$$

where B_{00} is the field at the trap ($z = r = 0$). The field configuration $f(z)$ on the axis depends generally speaking both on the external currents in the trap windings and on the currents in the plasma. In a sufficiently close vicinity of the axis, the vector potential of the field (3.6) can be written in the form

$$A_\varphi(z,r)\approx B_{00}\left[\frac{rf(z)}{2}+r^3g(z)\right]. \tag{3.7}$$

There is no term proportional to the r^2 because of the axial symmetry of the field. Given $f(z)$, the function $g(z)$ can be arbitrary, depending on the currents in the plasma. In the absence of the latter ("vacuum" field) we have $g(z) = -f''/16$ from $\Delta\mathbf{A} = 0$ or rot $\mathbf{B} = 0$. At the accuracy assumed, the field next to the axis is

$$\left.\begin{aligned} B_z(z, r) &\approx B_{00}[f(z) + 4r^2 g(z)], \\ B_r(z, r) &\approx -B_{00}\left[\frac{rf'}{2} + r^3 g'\right]. \end{aligned}\right\} \quad (3.8)$$

It is important that, given the field on the axis, the currents in the plasma add only small corrections of order r^2. Neglecting these, we can write for the dependence of the field strength along a magnetic line

$$B(s) \approx B_0 f(s), \quad B_0 \approx B_{00}[f(0) + 4r_0^2 g(0)] \approx B_{00}. \quad (3.9)$$

The zero subscripts denote here and elsewhere the values of the corresponding quantities in the symmetry plane $z = 0$.

An example of a short trap is a field configuration corresponding to

$$f(s) = 1 + (s/L)^2, \quad (3.10)$$

where L is the longitudinal scale of the trap. This configuration is a good approximation of the central part of a classical trap with magnetic mirrors. The meaning of the term "short trap" will be explained below (see Subsection 3).

Using the results of Subsection 1 of the present section, we can write right away the unperturbed Hamiltonian for the field (3.10):

$$H^0 = p^2/2 + \mu\omega_0\left(1 + \frac{s^2}{L^2}\right) = \mu\omega_0 + J\sqrt{2\mu\omega_0}/L \quad (3.11)$$

and the frequencies

$$\left.\begin{aligned} \Omega(\mu) = \partial H^0/\partial J = \sqrt{2\mu\omega_0}/L, \quad \langle\omega(\mu, J)\rangle &= \omega_0 + \frac{J\sqrt{\omega_0}}{L\sqrt{2\mu}} \\ &= \omega_0\left(1 + \frac{a^2}{2L^2}\right) = \frac{\omega_0}{2}\left(1 + \frac{1}{\sin^2\beta_0}\right). \end{aligned}\right\} \quad (3.12)$$

Here a is the amplitude of the longitudinal oscillations of the particle; $J = \Omega a^2/2$ is the longitudinal action; β_0 is the angle between the particle-velocity vector and the magnetic line (at $s = 0$).

The foregoing example (3.10) could be called also a harmonic trap (in view of the waveform of the longitudinal oscillations).

3. Long Magnetic Trap. This configuration is different in that the field is almost constant over most of the trap, whose mirrors are relatively short and steep. Such a field is a feature of Dimov's ambipolar trap [7]. We describe it by the relation [4]

$$f(s) = 1 + (s/L)^n, \tag{3.13}$$

where n is some even number. As before, L is the length of the entire trap, whereas the length of the mirror is of the order of

$$l = L/n \tag{3.14}$$

(a short trap corresponds to $n = 2$ and $\ell \sim L$, while for a long one we have $n \gg 1$ and $\ell \ll L$); i.e., the mirrors are much shorter than the entire trap. This is the distinction between "short" and "long" traps.

At $n \gg 1$, the effective potential energy of the longitudinal motion can be approximately represented by a rectangular well of length 2L. The unperturbed Hamiltonian (2.3) takes then the form

$$H^0 = p^2/2 + \mu\omega_0 f(s) \approx J^2/2M + \mu\omega_0. \tag{3.15}$$

Recall that ω_0 does not depend on s on the given magnetic line. We have $M = (2L/\pi)^2$, and the longitudinal action is

$$J = \frac{1}{2\pi}\oint p\,ds \approx \frac{2L}{\pi}p. \tag{3.16}$$

The fundamental unperturbed frequencies are

$$\Omega = \frac{J}{M} = \frac{\pi}{2L}p, \quad \langle\omega\rangle \approx \omega_0. \tag{3.17}$$

4. Multimirror Trap [11]. Such a trap is a chain of ordinary traps; in other words, a long trap with a corrugated magnetic field whose strength varies along the trap periodically (in the simplest case). We specify the field configuration in such a trap in the form

$$f(s) = \frac{1}{2}\left[(\lambda+1) - (\lambda-1)\cos\left(\frac{\pi s}{L}\right)\right], \tag{3.18}$$

where $\lambda = f_{max}/f_{min}$ is the mirror ratio. The unperturbed Hamiltonian (2.3) now becomes

$$H^0 = \frac{p^2}{2} + \frac{\mu\omega_0}{2}\left[(\lambda+1) - (\lambda-1)\cos\left(\frac{\pi s}{L}\right)\right]. \tag{3.19}$$

The equations of motion of such a system are known to be fully integrable in terms of elliptic functions (see, e.g., [8, 12-14]). The modulus k of the elliptic integrals is given in terms of the system parameters in the form

$$k^2 = \begin{cases} \dfrac{W}{\mu\omega_0(\lambda-1)}, & H^0 < \lambda\mu\omega_0, \\ \dfrac{\mu\omega_0(\lambda-1)}{W}, & H^0 > \lambda\mu\omega_0, \end{cases} \tag{3.20}$$

where $W = H^0 - \mu\omega_0$ is the unperturbed energy reckoned from the minimum of the potential ($\mu\omega_0$). The first regime of the motion corresponds to trapped particles that execute oscillations limited in s, and the second to untrapped particles. The limiting trajectory that separates the two regimes ($H^0 = \lambda\mu\omega_0$) is called the separatrix. A diagram of the phase trajectories of the system (3.19) is shown in Fig. 1.

For trapped particles, the longitudinal-oscillation frequency is

$$(H^0) = \frac{\pi\Omega_0}{2\mathscr{K}(k)}, \tag{3.21}$$

where $\mathscr{K}$ is a complete elliptic integral of the first kind, and

$$\Omega_0 = \frac{\pi}{L}\sqrt{\frac{\mu\omega_0(\lambda-1)}{2}} \tag{3.22}$$

is the frequency of the small oscillations. For untrapped (denoted by subscript "un") particles the fundamental frequency of the longitudinal motion can be represented in a form similar to (3.21):

$$\Omega_{un} \equiv 2\pi/T_{un} = \pi\Omega_r/2\mathscr{K}(k), \tag{3.23}$$

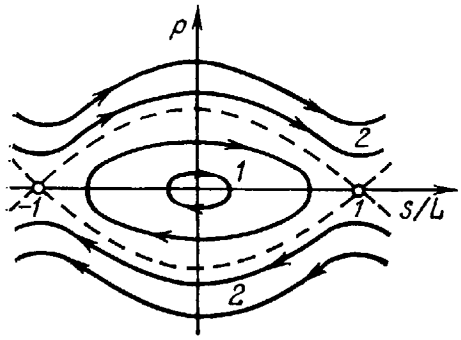

Fig. 1. Diagram of unperturbed phase trajectories in a multimirror trap: 1) trapped particles; 2) untrapped particles; the separatrix is shown dashed.

where T_{un} is the time to travel over one period of the field (3.18), and

$$\Omega_r = \frac{\pi}{L}\sqrt{2W} \tag{3.24}$$

is the free motion frequency (at $\lambda = 1$). Note that, in the case considered, we have $k = 2\Omega_0/\Omega_r$ (3.20).

We shall hereafter be particularly interested in motion near the separatrix, the energy distance to which will be characterized by the dimensionless quantity

$$w = (H^0 - \lambda\mu\omega_0)\frac{2}{(\lambda - 1)\,\mu\omega_0}. \tag{3.25}$$

A close proximity to the separatrix corresponds to $|w| \ll 1$, with $w < 0$ and $w > 0$ for trapped and untrapped particles, respectively. In both regimes we have $k^2 \to 1 - |w|/2$, $\Omega_r \to 2\Omega_0$, and

$$\Omega(w) \approx \frac{\Omega_{un}(w)}{2} \to \frac{\pi\Omega_0}{\ln\left(\frac{32}{|w|}\right)}. \tag{3.26}$$

Although the frequencies in the two regimes differ by a factor of 2 [the period of the untrapped particle is exactly half that of the trapped (see Fig. 1)], the motions in both cases are close to each other and to the motion along the separatrix, the latter expressed in terms of elementary functions:

$$\left.\begin{aligned} \dot{s}_c &= p_c(s) = \pm \frac{2}{\pi} L\Omega_0 \cos\left(\frac{\pi s}{2L}\right), \\ \frac{s_c(t)}{L} &= \frac{4}{\pi}\arctan\left(e^{\Omega_0 t}\right) - 1. \end{aligned}\right\} \qquad (3.27)$$

The phase trajectory on the separatrix (the first expression) is shown in Fig. 1. In the second expression, the time origin ($t = 0$) corresponds to the minimum of the field ($s = 0$). The significant difference between the motion along the separatrix from that along neighboring trajectories reduces only to the frequency, which is exactly zero on the separatrix [cf. (3.21) and (3.23)].

The action is easiest to determine by integrating expression (3.21) for the frequency. In the case of trapped particles

$$J(H^0, \mu) = \int_0^W \frac{dW}{\Omega(W, \mu)} = \frac{8}{\pi^3} L^2\Omega_0 [E(k) - (1 - k^2)\mathscr{K}(k)], \qquad (3.28)$$

where we have transformed to integration with respect to dk with the aid of (3.20); $E(k)$ is a complete elliptic integral of the second kind. This expression defines implicitly the function $H^0(J, \mu)$. As $W \to 0$ (small oscillations), we have $J \to W/\Omega_0$ [cf. (3.11)]. The derivative $\partial H^0(J, \mu)/\partial J = [\partial J(H^0, \mu)/\partial H^0]^{-1}$ yields, of course, again the frequency (3.21). To calculate the average Larmor-rotation frequency $\langle\omega\rangle = \partial H^0(J, \mu)/\partial\mu$, we write the differential

$$dJ(H^0, \mu) = \frac{\partial J}{\partial H^0} dH^0 + \frac{\partial J}{\partial \mu} d\mu = 0.$$

Hence

$$\langle\omega\rangle = -\frac{\partial J/\partial\mu}{\partial J/\partial H^0} = \omega_0\left[\lambda - (\lambda - 1)\frac{E(k)}{\mathscr{K}(k)}\right] \to \lambda\omega_0\left[1 - \frac{2(\lambda - 1)/\lambda}{\ln(32/|w|)}\right]. \qquad (3.29)$$

The later expression gives the asymptote of $\langle\omega\rangle$ near the separatrix ($|w| \ll 1$). For small oscillations we have $\langle\omega\rangle \to \omega_0 + W/2\mu$ [cf. (3.12)]. When calculating (3.29) it must be recognized that $\partial W(H^0, \mu)/\partial\mu = -\omega_0$.

For the untrapped particles we obtain analogously the action in the form

$$J_{un}(H^0, \mu) = J^c_{un} + \int_{W_c}^{W} \frac{dW}{\Omega_{un}(W, \mu)} = \frac{4L^2\Omega_0}{\pi^3}\frac{E(k)}{k}. \quad (3.30)$$

Here $W_c = \mu\omega_0(\lambda - 1)$ and $J_{un} = 4L^2\Omega_0/\pi^3$ are the energy and action on the separatrix. We note that the second of these quantities is half the value (3.28) for trapped particles. The action as a function of the energy has thus a discontinuity on the separatrix, for the same reason as the frequency [see (3.26)]. The mean value of the Larmor frequency is

$$\langle\omega\rangle = \omega_0\left[1 + \frac{\lambda - 1}{k^2}\left(1 - \frac{E(k)}{\mathcal{K}(k)}\right)\right] \to \lambda\omega_0\left[1 - \frac{2(1 - 1/\lambda)}{\ln(32/|w|)}\right]. \quad (3.31)$$

We point out that the asymptote of $\langle\omega\rangle$ as $w \to 0$ is the same on both sides of the separatrix [cf. (3.29)]. At $W \gg W_c$ we have $\langle\omega\rangle \approx \omega_0(1 + \lambda)/2$; i.e., it is simply equal to the average over s.

5. Field-Reversed Mirrors, Planar Geometry. A diagram of the magnetic lines of such a field is shown in Fig. 2a. The vector **B** is in the (x, y) plane ($B_z = 0$) and does not depend on z. We note that owing to this symmetry we have here, as in an axisymmetric trap, an additional exact integral of motion (z component of the canonical momentum of the particle), and the problem reduces to two degrees of freedom. The configuration of the considered field is the same in all four quadrants of the (x, y) plane, so that it suffices to consider one of them, say the first (x, y > 0). In addition, the field is symmetric about the bisector of the angles between the coordinate axes ($y = \pm x$). We specify the magnetic line in terms of the minimum distance r_0 to the origin (Fig. 2a). The vector potential of this field can be chosen in the form (see, e.g., [15])

$$A_z(x, y) = Cxy, \quad (3.32)$$

where C is a certain constant to be determined below. Then

$$B_x = Cx; \quad B_y = -Cy; \quad B = Cr; \quad r^2 = x^2 + y^2. \quad (3.33)$$

We denote by B_0 the minimum field along the magnetic line at the point r_0; then $C = B_0/r_0$; i.e., the minimum field is proportional to r_0. In the case considered, the paraxial approximation used in the preceding magnetic-trap examples is quite unsuitable, since the field on the trap axis (x, y =

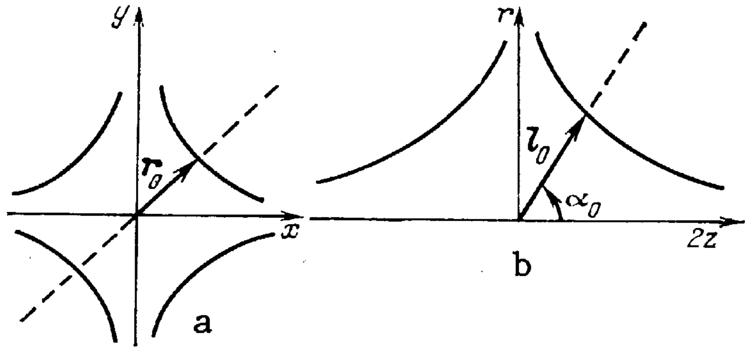

Fig. 2. Diagram of magnetic lines of field-reversed mirrors: a) planar geometry (the field is independent of z); b) cylindrical (axisymmetric) geometry $r^2 = x^2 + y^2$, $\tan\alpha_0 = \sqrt{2}$ ($\alpha_0 \approx 55°$). The field-maximum line is shown dashed. The vectors $\mathbf{r}_0$ and $\mathbf{l}_0$ specify the magnetic line.

0) is zero. To find the function B(s) along the magnetic line we determine first the length of the line s, measured from the point $\mathbf{r}_0$. The equation of the line is A_z = const or $2xy = r_0^2$, or else $r_0^2 = r^2 \sin 2\varphi$ (in the polar coordinates r, φ). The coordinate along the line is

$$s(r) = \int_{r_0}^{r} \frac{r^2 dr}{\sqrt{r^4 - r_0^4}} \to \begin{cases} \sqrt{r_0(r - r_0)}, & r - r_0 \ll r_0, \\ r + \frac{r_0}{6} \approx r, & r \gg r_0. \end{cases} \qquad (3.34)$$

This integral can be expressed in terms of elliptic functions, but we confine ourselves to the two indicated extreme situations. The first corresponds to the central section of the magnetic line near the field minimum. Taking (3.33) into account, we get in this region

$$f(s) \approx 1 + \frac{s^2}{r_0^2}, \qquad \omega(s) = \omega_0 f(s), \qquad \omega_0 = B_0, \qquad (3.35)$$

i.e., the field of the short trap (3.10) with characteristic length $L = r_0$. The second expression in (3.34) describes the edges of the magnetic lines. Here

$$f(s) \approx |s|/r_0. \qquad (3.36)$$

This configuration is new to us, and we shall examine it in greater detail. The unperturbed Hamiltonian is of the form

$$H^0 = \frac{p^2}{2} + \frac{\mu\omega_0 |s|}{r_0} = \left(\frac{3\pi}{4\sqrt{2}} \frac{\omega_0}{r_0} \mu J\right)^{2/3}, \qquad (3.37)$$

where J is the longitudinal action. The unperturbed frequencies are

$$\left.\begin{aligned} \Omega &= \frac{2}{3}\left(\frac{3\pi}{4\sqrt{2}} \frac{\omega_0}{r_0}\right)^{2/3} \frac{\mu^{2/3}}{J^{1/3}} = \frac{\pi}{2}\sqrt{\frac{\mu\omega_0}{2r_0 a}}, \\ \langle\omega\rangle &= \frac{2}{3}\left(\frac{3\pi}{4\sqrt{2}} \frac{\omega_0}{r_0}\right)^{2/3} \frac{J^{2/3}}{\mu^{1/3}} = \frac{2}{3}\frac{\omega_0 a}{r_0}, \end{aligned}\right\} \qquad (3.38)$$

where a is the amplitude of the longitudinal oscillations.

6. Field-Reversed Mirrors, Cylindrical Geometry. We consider now the magnetic-field configuration produced by axisymmetric field-reversed mirrors, say by two identical cylindrical coils with oppositely directed currents and magnetic fields (Fig. 2b). The vector potential of such a field can be chosen in the form (see, e.g., [15])

$$A_\varphi = Czr,$$

whence

$$B_z = C2z, \quad B_r = -Cr, \quad B = Cl, \qquad (3.39)$$

where the vector $\mathbf{l}$ with components (2z, r) characterizes the position of the point on the (2z, r) plane (see Fig. 2b).

The main difference between this trap and the preceding one is that the magnetic lines are not symmetric about the field on the line. The minimum-field line is, as before, a straight line, but it makes now an angle $\alpha_0 \approx 55°$ [$\tan \alpha_0 = \sqrt{2}$ with the z axis on the (2z, r) plane]. The equation of the magnetic line is obtained from rA_φ = const, or

$$zr^2 = (l_0/\sqrt{3})^3, \qquad (3.40)$$

where the vector $\mathbf{l}_0$ defines the position of the field minimum on this line. Accordingly, the constant is $C = B_0/\ell_0$.

The coordinate s along the magnetic line is reckoned as before from the point $\mathbf{l}_0$:

$$s = \int_{z_0}^{z} dz \sqrt{1 + \frac{b^3}{4z^3}} \to \begin{cases} -\frac{b^{3/2}}{\sqrt{z}}, & z \ll z_0, \\ \sqrt{3}\,(z - z_0), & z \approx z_0, \\ z, & z \gg z_0. \end{cases} \tag{3.41}$$

Here $z_0 = b/2$; $b = \ell_0\sqrt{3}$. Combining this with the expression $B = \omega = C\ell$ (3.39), we get

$$f(s) \approx \begin{cases} |s|/l_0, & z \to 0, \\ 1 + 2s^2/l_0^2, & z \approx z_0, \\ 2\,|s|/l_0, & z \to \infty. \end{cases} \tag{3.42}$$

As in the preceding case, near the minimum of the field ($z \approx z_0$) we can use the short-trap approximation with scale $L = \ell_0/\sqrt{2}$, while far from the minimum the effective potential is linear in s. It is significant, however, that in contrast to the preceding example the slope of the potential curve (i.e., the effective longitudinal force) is different on the two sides of the minimum of the potential. This is the result of the aforementioned asymmetry of the trap's cylindrical geometry. The cause of the symmetry can be illustratively explained in the following manner: as $z \to \infty$ the bundle of magnetic lines is compressed in two directions (x, y), whereas as $r \to \infty$ the compression is only along one direction (z).

To calculate the frequencies $\langle\omega\rangle$ and Ω, we can use expressions (3.38), taking the arithmetic means of $\langle\omega\rangle$ and $1/\Omega$ for both slopes of the potential at one and the same energy H^0.

4. Adiabatic Perturbation

Our principal task is to investigate the effect of the perturbation, i.e., of the change of the particle's magnetic moment μ, which was assumed in the unperturbed system to be constant [Eq. (2.2)]. In this section we obtain an equation for $\dot{\mu}$.

We begin with the simple model system (3.1). We obtain an expression for $\dot{J}_y$ by differentiating (3.3) and using the exact equations of motion from the Hamiltonian (3.1):

$$\dot{J}_y = \dot{x}x\left(y^2 - \frac{\dot{y}^2}{\omega_y^2}\right) = 2J_y \frac{\dot{x}x}{1 + x^2}\cos(2\theta). \tag{4.1}$$

Here $\omega_y = 1 + x^2$, and we have put

$$y \equiv a_y \cos\theta, \quad \dot{y} \equiv \omega_y a_y \sin\theta, \tag{4.2}$$

defining by the same token new variables a_y and θ (the amplitude and phase of the y oscillations), in terms of which $J_y = \omega_y a_y^2/2$ [see (3.2) and (3.3)]. Expression (4.1) is indeed the sought-for equation for $J_y(t)$. It will be integrated in Sec. 7. It is useful, however, to note right away some of its properties. The right-hand side of the equation is the product of functions that vary with time at different frequencies: low [the factor $S(t) = \dot{x}x/(1 + x^2)$ has the same frequency Ω as the longitudinal oscillations] and high [the factor $F(t) = \cos(2\theta)$ has double the frequency of the Larmor rotation, viz., $2\langle\omega\rangle$]. In first-order approximation J_y will therefore execute bounded and small (if the ratio $\Omega/2\langle\omega\rangle$ is small) oscillations. The cumulative changes of J_y, all that interests us here, are made possible only by the resonance between the two motions, i.e., by the sufficiently high harmonics of the low frequency Ω. The smaller the frequency ratio $\Omega/2\langle\omega\rangle$, the higher the harmonics needed for the resonance and the smaller their amplitudes and, consequently, a certain average rate of change of J_y. It is natural, therefore, to choose in this problem as the parameter characterizing the smallness of perturbation simply the frequency ratio:

$$\varepsilon = \Omega/\langle\omega\rangle. \tag{4.3}$$

This quantity is usually called the adiabaticity parameter, since its smallness is in fact the main condition for adiabatic invariance of the action variables, i.e., the condition for their approximate conservation with time. This question will be discussed in greater detail below (see Section 10).

Proceeding to the discussion of the magnetic traps themselves, we note first that the small adiabaticity parameter (4.3) is determined by the second derivative of the magnetic field with respect to the coordinates; this derivative determines the frequency Ω of the longitudinal oscillations. The first derivative (field gradient) used sometimes for estimates has by itself no physical meaning as an adiabaticity parameter. Thus, for example, in the case of converging or diverging straight magnetic lines, the magnetic moment of the particle is exactly conserved, although the field gradient differs from zero. What is essential is the bending of the magnetic lines, their curvature. It turns out that in a mag-

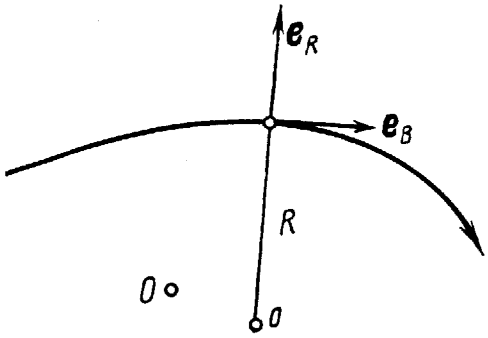

Fig. 3. Geometry of planar magnetic line: $\mathbf{e}_B$, $\mathbf{e}_R$ are the tangential and normal unit vectors; O is the center of the trap; 0 is the curvature center corresponding to the given point of the magnetic line; R is the curvature radius at this point (negative in this case; see the text).

netic trap it is precisely the curvature of the magnetic line that makes the main contribution to the change of μ, as was first elucidated in [16].

Let us examine this mechanism in greater detail. Bending (turning) of the magnetic line alters μ even if the velocity vector $\mathbf{v}$ remains constant, since μ depends only on the projection of v on a plane perpendicular to the vector $\mathbf{B}$, and this plane rotates independently of $\mathbf{v}$. Let us find the derivative $\dot{v}_\perp^2$ due to this effect. Assume that the magnetic line is a planar curve (has no torsion), and let $\mathbf{e}_B = \mathbf{B}/B$ be a unit tangent vector and $\mathbf{e}_R$ a unit outward normal (relative to the trap center) to the magnetic line (Fig. 3). We then have, from the expression $v_\perp^2 = v^2 - (\mathbf{v}, \mathbf{e}_B)^2$,

$$\dot{v}_\perp^2 \to -2v_\parallel (\mathbf{v}, \dot{\mathbf{e}}_B) = -2v_\parallel^2 v_n/R,$$

where we have assumed $\mathbf{v}$ = const; $v_\parallel = \mathbf{v}, \mathbf{e}_B$; $v_n = \mathbf{v}, \mathbf{e}_R = \mathbf{v}_\perp, \mathbf{e}_R$, and R is the curvature radius of the magnetic line and is assumed positive if the line is convex relative to the trap center. The instantaneous angular velocity $\mathbf{e}_B$ of the rotation as the particle moves along the magnetic line is

$$\mathbf{\Omega} = \mathbf{e}_B \times \mathbf{e}_R \frac{v_\parallel}{R}.$$

At a sufficiently small Larmor radius, the projection of the particle velocity is $v_n \approx -v_\perp \sin\theta$, where θ is the Larmor phase reckoned from the direction of the vector $\mathbf{e}_R$ (a more accurate expression for v_n is given in [8]). We ultimately get

$$\dot{\mu} \to \sqrt{2\mu}\,\frac{v_\parallel^2}{R\sqrt{\omega}}\sin\theta. \tag{4.4}$$

The arrow indicates here that the equation given here for $\dot{\mu}$ contains only the principal term that determines the cumulative resonance changes of μ. The complete equation for $\dot{\mu}$ is given in [5]. It includes, in particular, also terms of form (4.1), which are proportional to $\cos(2\theta)$. It will be shown below, however (see Section 7), that they make only exponentially small additions, since the adiabaticity parameter (4.3) is only half as large. A detailed discussion of the separation of the principal term of the perturbation (4.4) is contained in [5]. We shall return to this question in Section 7.

5. Insignificant Effect of Perturbation

Our principal task is to integrate a perturbed equation such as (4.4) or (4.1), i.e., to determine the effect of the perturbation, meaning the change of the unperturbed integral of motion μ (or J_y). Such equations are quite frequently integrated by some asymptotic method [12], i.e., by constructing the solution in the form of an asymptotic series in powers of a small parameter of the problem, which in our case is the adiabaticity parameter (4.3). The term "asymptotic" means that the remainder term of such a series does not decrease in general with increasing number of its terms, and decreases only together with the smallness parameter. This approach was used in many studies also to investigate the dynamics of a particle in a magnetic trap (see, e.g., [17, 18]). As applied to equations such as (4.4) or (4.1), it means, roughly speaking, integration by parts. During each step the high-frequency factor F(t) of the right-hand side is integrated and the low-frequency side S(t) is differentiated. As a result, each step increases the degree of the small parameter (4.3) by unity. For Eq. (4.1), for example, the first step yields

$$\delta J_y = J_y\,\frac{\dot{\omega}_y}{2\omega_y^2}\sin(2\theta). \tag{5.1}$$

As soon as the unperturbed solution, which is substituted in the right-hand side of (4.1), becomes quasiperiodic, the variations of $J_y(t)$ given by the asymptotic series also become quasiperiodic, with fundamental frequencies Ω and $\langle\omega\rangle$ that are close the unperturbed ones. These variations are consequently bounded and small at a sufficiently small adiabaticity parameter. In this sense, such quasiperiodic variations of the unperturbed action are an insignificant effect of the perturbation. What is meant by insignificant? In the language of asymptotic expansions what is significant is the remainder term of such an expansion, and we shall proceed to determine it.

To conclude this section, we note that quasiperiodic oscillations of the unperturbed action (5.1) can be used to introduce a "more precise" action $J_y^{(n)}$, whose nonresonant changes will be smaller than for J_y (n is the order of the precision). In first order, for example, we obtain from (5.1)

$$J_y^{(1)} = J_y - \delta J_y = J_y\left(1 - \frac{\dot{\omega}_y}{2\omega_y^2}\sin(2\theta)\right)$$

$$= J_y\left(1 \mp \sqrt{2}\,\frac{x\sqrt{H^0 - J_y(1+x^2)}}{(1+x^2)^2}\sin(2\theta)\right). \qquad (5.2)$$

In the last expression we used the unperturbed relation $\dot{x} = \pm\sqrt{2(H^0 - J_y\omega_y)}$ [see (3.4)]. The derivative is $\dot{J}_y^{(1)} \sim \varepsilon^2$, i.e., it is already of second order in the adiabaticity parameter (4.3). Introduction of a more precise action is equivalent to the canonical transformation of variables, which is widely used in nonlinear mechanics and eliminates the nonresonant terms of a perturbation. This procedure was first used for magnetic traps in [19] for a model of type (3.1) and in [17] for an arbitrary magnetic field (see also [18, 20]). A more precise μ is useful for a comparison of the theory with results of numerical simulation (see [20] and Section 7 below).

6. Nonlinear Resonances

As already noted, nonperiodic changes of μ, which can be cumulative, are due to resonances between the Larmor precession of the particle and the higher harmonics of the longitudinal oscillations. To analyze these resonances we transform in the right-hand side of Eq. (4.4) for $\dot{\mu}$ to the unperturbed action variables μ and J and to their canonically conjugate phases φ, ψ. Taking the Fourier transforms with respect to the phases, we get

$$\dot{\mu} = \frac{1}{2} \sum_n f_n(\mu, J) e^{i(\varphi - n\psi)} + \text{c.c.}, \tag{6.1}$$

where $\dot{\varphi} = \langle\omega\rangle$; $\dot{\psi} = \Omega$, and n is an arbitrary integer. Generally speaking, this is a double Fourier series; i.e., it includes also harmonics of the phase φ. Since, however, $\langle\omega\rangle / \Omega \gg 1$, the amplitudes of the resonance harmonics $m\varphi$ become quite small compared with f_n, and we neglect them. The resonance conditions are (n is a positive integer)

$$\langle\omega\rangle = n\Omega. \tag{6.2}$$

Generally speaking, this condition is not met. Since, however, the unperturbed oscillations are not isochronous, i.e., their frequencies ($\langle\omega\rangle$, Ω) depend on the actions μ, J (see Section 3), there are always special (resonant) values $\mu = \mu_r$, $J = J_r$, for which the resonance condition (6.2) will be satisfied with some n = r.

If the amplitudes f_n are small enough (a smallness condition will be obtained below; see Section 10), we need retain in (6.1) only the resonant term

$$\dot{\mu} \approx |f_r(\mu_r, J_r)| \cos\psi_r, \tag{6.3}$$

where we have introduced the resonant phase

$$\psi_r = \varphi - r\psi + \psi_r^0, \tag{6.4}$$

and $\psi_r^0(\mu_r, J_r)$ is some constant: $f_r = |f_r| \exp(i\psi_r^0)$. At exact resonance (6.2) we have ψ_r = const. However, in view of the change of μ and of the dependence of the frequencies $\langle\omega\rangle$, Ω on μ and J, the resonant phase also varies with time. The equation for ψ_r can be written as

$$\dot{\psi}_r \approx \langle\omega\rangle - r\Omega. \tag{6.5}$$

This equation is approximate, since ψ_r is altered not only by the frequency change but also directly by the perturbation. The latter effect, however, is small if the perturbation is small, and we shall neglect it (this question is discussed in greater detail in [8]).

The perturbation alters not only μ but also J. In a purely magnetic field, however, the particle energy is conserved and the change of J can be expressed in terms of the change of μ. We assume, therefore, that both the frequencies $\langle\omega\rangle$ and Ω, and the Fourier amplitudes f_n depend only on μ. Equations (6.3) and (6.5) constitute then a complete system that describes the dynamics of one resonance. Equation (6.5) can be simplified by expanding the right-hand side near the resonance:

$$\dot{\psi}_r \approx \left.\frac{d\omega_r}{d\mu}\right|_{\mu=\mu_r} (\mu-\mu_r), \quad \omega_r(\mu) = \langle\omega\rangle - r\Omega. \tag{6.6}$$

Introducing the quantity $\nu = \mu - \mu_r$, and noting that $\dot{\nu} = \dot{\mu}$, we obtain a pair of canonical equations

$$\left.\begin{aligned} \dot{\nu} &= |f_r(\mu_r)| \cos\psi_r, \\ \dot{\psi}_r &= \omega_r'\nu, \quad \omega_z' \equiv \left.\frac{d\omega_r}{d\mu}\right|_{\mu=\mu_r} \end{aligned}\right\} \tag{6.7}$$

with a Hamiltonian

$$H_r(\psi_r, \nu) = \frac{\omega_\nu'\nu^2}{2} - |f_r| \sin\psi_r. \tag{6.8}$$

It can be easily seen that this is the Hamiltonian of a pendulum, say of unit length with mass $1/\omega_r'$ in a gravitational field $mg = |f_r|$, where ν is the angular momentum of the pendulum and ψ_r is the angle of its inclination from the horizontal. The Hamiltonian (6.8) is therefore said to describe a nonlinear resonance in the pendulum approximation [8]. The conditions of this simple approximation are discussed in detail in [8]. What matters is just that the perturbed oscillations are not isochronous: $\omega_r' \neq 0$. The oscillations of ν are therefore bounded near resonance ($|\Delta\nu| \leq 2\sqrt{|f_r|/|\omega_r'|}$), and are small at small $|f_r|$, so that one can use for $\dot{\psi}_r$ the expansion (6.6) in terms of ν.

The limited size of the oscillations of ν (hence of μ), and the ensuing limited (and insignificant) energy exchange between the degrees of freedom of the system in question, constitute the essential difference between a nonlinear and a linear resonance. In the latter case, the exchange would be complete. The nonlinearity (nonisochronism) of the oscillations is said to stabilize the resonant perturbation. A transition to linear resonance in the Hamiltonian (6.8) corresponds to $\omega_r' \to 0$ and $\Delta\nu \to \infty$ (the pendulum approximation, naturally, then becomes invalid). We note also that the dynamics of a nonlinear resonance are similar to unperturbed motion of a particle in the periodic field of a multimirror trap [cf. (6.8) and (3.19)]. We shall need this analogy later (see Section 10).

Returning to our problem, we see that one nonlinear resonance cannot inhibit particle containment in a magnetic trap, since the oscillations of μ on it are bounded. In fact, however, there are many resonances (6.1). If the remaining terms in (6.1) are not neglected, the Hamiltonian (6.8) takes the more complicated form

$$H_r(\psi_r, \nu) \approx \frac{\omega_r' \nu^2}{2} - \sum_n |f_n| \sin(\psi_r - (n-r)\Omega t + \psi_n^0 - \psi_r^0), \qquad (6.9)$$

where we have put approximately $\psi \approx \Omega t$. Although different terms of the last sum cause resonances under different initial conditions (different μ), is it always possible to neglect the nonresonant perturbation, as was done in (6.8)? We shall consider this important and, in essence, central question somewhat later (see Section 10), and proceed now to calculate the resonant amplitudes f_n. We can use for this purpose the relation

$$\Delta\mu = T |f_r| \cos\psi_r, \qquad (6.10)$$

which is obtained by integrating (6.1) over the period $T = 2\pi/\Omega$ of the longitudinal oscillations. On the other hand, we can obtain $\Delta\mu$ by directly integrating Eq. (4.4) for $\dot{\mu}$. We shall name the quantity (6.10) the resonance $\Delta\mu$.

7. Resonant $\Delta\mu$

Thus, our next task is to calculate the total change of the unperturbed action ($\Delta\mu$) within the period of the low-frequency (longitudinal) oscillations. We shall do this below for the set of typical examples described in Section 3. We begin, as usual, with the simple auxiliary system (3.1). In this case we must calculate the integral [see (4.1)]

$$\frac{\Delta J_y}{J_y} \approx \Delta \ln J_n = 2\int dt \frac{\dot{x}x}{1+x^2} \cos 2\theta \approx 2\mathrm{Re}\int d\theta e^{2i\theta} \frac{\dot{x}x}{(1+x^2)^2}, \qquad (7.1)$$

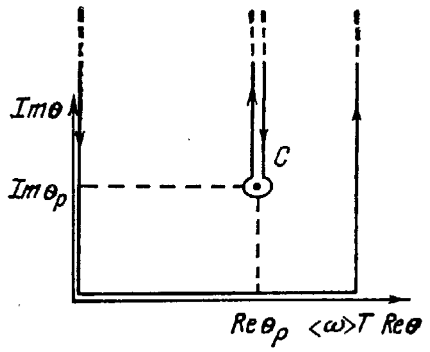

Fig. 4. Integration contour in the complex θ plane when calculating ΔJ_y and $\Delta\mu$; C – bypass of the singularity along the cut; θ_p – location of singularity.

furthermore not asymptotically in terms of the small adiabaticity parameter $\varepsilon = \Omega/\langle\omega\rangle$ (4.3), but in a certain sense "exactly." Let us formulate the problem more accurately. Since we do know the integrand as a function of time, the use of some successive-approximation method is unavoidable. We therefore replace the integrand by an unperturbed solution, in particular J_y = const, something already taken into account in the relation $d\theta = (1 + x^2)dt$ for the last representation of the integral (7.1). In the integration by parts in Section 5 we have integrated in essence only the high-frequency factor, "lumping" all the effects of the low-frequency part (including its high harmonics) in the remainder term which was left undetermined. Now, however, we integrate the unperturbed integrand exactly (with all its harmonics). This can be done in a number of cases by analytically continuing the integrand into the complex plane of the integration variable. If the latter is chosen to be the phase θ, as was done, e.g., in [5], we can close the integration contour in the upper half-plane of θ and neglect the contribution made to the integral by the infinitely remote part of this contour ($\mathrm{Im}\,\theta \to +\infty$). The value of the integral is then determined by the singularities of the integrand, which are bypassed by branch cuts (Fig. 4).

If the resonance condition (6.2) is satisfied, the sum of the integrals over the two vertical lines is also zero, since the quasiperiodic time dependence of the unperturbed solution (the two incommensurate frequencies $\langle\omega\rangle$ and Ω) becomes at resonance periodic with a period T ($\langle\omega\rangle T = 2\pi n$). Off resonance, this sum is generally speaking not zero because of the different values of the function $\exp(2i\theta)$ on the two straight lines. This leads to a quasiperiodic increment to $\Delta\mu$ (see Section 5) which, however, is of no interest to us.

For the integral (7.1), the only singularity in the upper θ half-plane is a pole at $x_p = i$. We note right away that the frequency at this singularity is $\omega_y = 0$, and the singularity is also a saddle point (col) of the function $\exp(2i\theta)$.

Since the singularity is bypassed twice during one period of the x oscillations, it suffices to calculate the integral over the half-period T/2. Near the singularity we have $\omega_y(x_p) = 1 + x_p^2 = 0$ and $\theta = \theta_p$:

$$\theta - \theta_p \approx \left(\frac{d\theta}{dx}\right)_p (x - x_p) + \frac{1}{2}\left(\frac{d^2\theta}{dx^2}\right)_p (x - x_p)^2 = \frac{x_p}{v_0}(x - x_p)^2, \quad (7.2)$$

since $(d\theta/dx)_p = \omega_y(x_p)/\dot{x}_p = 0$, while $(d^2\theta/dx^2)_p = (d\omega_y/dx)_p/\dot{x}_p$ and $\dot{x}_p = \sqrt{2H0} = v_0$ [see (3.4)], where $v_0^2 = \dot{x}_0^2 + \dot{y}_0^2$ is the total velocity at the minimum of the potential energy (x = 0). Next,

$$(1 + x^2)^2 \approx (2x_p)^2 (x - x_p)^2 \approx 4x_p v_0 (\theta - \theta_p).$$

Substituting this expression in (7.1) and calculating the residue at the pole, we obtain

$$\Delta \ln J_y = \pi \operatorname{Re}\left(ie^{2i\theta_p}\right). \quad (7.3)$$

Note that were we to calculate the integral in the complex t or x plane, we would obtain the different (incorrect) result:

$$\Delta \ln J_y = 2 \operatorname{Re} \int \frac{x\,dx}{1 + x^2} e^{2i\theta} = 2\pi \operatorname{Re}\left(ie^{2i\theta_p}\right).$$

The reason for the difference is that the function $\exp(2i\theta \cdot (x))$, generally speaking, does not vanish as $\operatorname{Im} x \to \infty$, so that the integral does not reduce to a residue at a pole. Finally, we can proceed as follows. We assume that the last integral is taken along a contour in the θ plane, but we simply replace the integration variable by x. As $x - x_p \propto \sqrt{\theta - \theta_p}$, when the singularity is bypassed in the θ plane [the complex vector $(\theta - \theta_p)$ is rotated through an angle

2π], the vector $(x - x_p)$ is rotated only through an angle π. Therefore, the value of the integral over dx is equal to half the residue at the pole, and this coincides exactly with (7.3).

We now find θ, which we can represent in the form

$$\theta_p = \theta_0 + \int_0^{t_p} \omega_y dt = \theta_0 + \int_0^{x_p} \frac{\omega_y dx}{\dot{x}}, \tag{7.4}$$

where $\theta_0 = \mathrm{Re}\,\theta_p$. To calculate this integral we use an unperturbed solution, for example in the form [see (3.4)]

$$\dot{x} = \sqrt{2J_y(a_x^2 - x^2)}\,, \tag{7.5}$$

where a_x is the amplitude of the longitudinal oscillations. Recognizing that $\omega_y = 1 + x^2$ and $x_p = i$, we obtain from (7.4)

$$\theta_p = \theta_0 + \frac{i\chi(\sin\beta_0)}{2v_0}, \qquad \chi(u) = \frac{1}{u^2}\left(\frac{1+u^2}{2u}\ln\frac{1+u}{1-u} - 1\right), \tag{7.6}$$

where $\sin\beta_0 = \dot{y}_0/v_0$. In this form, the expression for the exponent that determines the order of the resonant perturbation was obtained (for a magnetic trap) in [21] and later in [5]. It is valid, of course, only for harmonic longitudinal oscillations, a fact used explicitly in the integration of (7.4). On the other hand, relation (7.6) is too complicated and inconvenient for further use. A simple approximation for θ_p is obtained by putting $\dot{x} \approx \dot{x}_0 = \text{const}$ in (7.4). Then

$$\theta_p \approx \theta_0 + \frac{2i}{3v_0\cos\beta_0}. \tag{7.7}$$

The condition $\dot{x} \approx \dot{x}_0$ will be called the small β_0 approximation since it is valid only if $\dot{x}_0 = v_0\cos\beta_0 \approx \dot{x}_p = v_0$. Hence $\cos\beta_0 \approx 1$ or $\beta_0 \ll 1$. Expression (7.7) can, of course, be obtained also directly from (7.6) as $\sin\beta_0 \to 0$. In a more general case, however, the expression for θ_p in the small β_0 approximation depends on the form of the function $\omega_y(x)$ (see below). For the harmonic oscillations considered here, a comparison of (7.6) and (7.7) shows that the difference between them does not exceed 10% at $\beta_0 \leq 50°$. We confine ourselves hereafter, for simplicity, to the small-β_0 approximation.

In this approximation we obtain from (7.3) for the considered model system

$$\Delta \ln J_y = -\pi \exp\left[-\frac{4}{3v_0 \cos\beta_0}\right]\sin(2\theta_0). \qquad (7.8)$$

If the singularity of the integrand is more complicated than a pole, for example a branch point, the integration method described above cannot be used. A more general method, used in particular in [15], is to reduce the integral along the cut (see Fig. 4) to a Γ function with the aid of the relation (see, e.g., [22]):

$$\int\limits_C \frac{e^{-u}du}{(-u)^p} = \frac{2\pi i}{\Gamma(p)}, \qquad (7.9)$$

where, in our case, $u = -i(\theta - \theta_p)$, $p > 0$, and the integration contour C is shown in Fig. 4 (it is drawn in the negative direction). Using (7.2), we reduce the integral (7.1) (with respect to $d\theta$) to the form (7.9) with $p = 1$, obtaining again (7.3).

In the problem of particle motion in a magnetic trap we must calculate the integral [see (4.4)]

$$\frac{\Delta\mu}{\sqrt{2\mu}} \approx \Delta\sqrt{2\mu} = \int dt \frac{v_\parallel^2}{R\sqrt{\omega}}\sin\theta \approx \operatorname{Im}\int d\theta e^{i\theta}\frac{v_\parallel^2}{R\omega^{3/2}}. \qquad (7.10)$$

The singularities of the integrand are determined now not only by the function $\omega(s)$ but also by the function $R(s)$. It is therefore necessary first to find a sufficiently simple expression for the curvature radius of the magnetic line.

In the paraxial approximation, the vector potential of the field is given by relation (3.7), and the equation of the magnetic lines is $rA_\varphi = \text{const}$, or

$$r^2 f(s) = r_0^2, \qquad (7.11)$$

where r_0 is the distance from the symmetry axis to the magnetic line at the minimum of the field [$s = 0$, $f(0) = 1$]. Hence

$$\frac{1}{R} \approx \frac{d^2r}{ds^2} = \frac{3r_0}{4}\frac{(f')^2}{f^{5/2}} - \frac{r_0}{2}\frac{f''}{f^{3/2}} \to \frac{3r_0}{4}\frac{(f')^2}{f^{5/2}}, \qquad (7.12)$$

assuming that $(dr/ds)^2 \ll 1$ (paraxial approximation). We note first that in this approximation the singularity of R coincides with the singularity of ω, since both quantities are proportional to f_p. It is furthermore clear that the main contribution is made by the term with the strongest singularity (maximum p, see below). We have therefore retained in (7.12) only the first term. Relation (7.2) near the singularity now takes the form

$$\theta - \theta_p \approx \left(\frac{d\theta}{ds}\right)(s - s_p) + \frac{1}{2}\left(\frac{d^2\theta}{ds^2}\right)_p (s - s_p)^2$$

$$= \frac{\omega_0 f_p'}{2v}(s - s_p)^2 \approx \frac{\omega_0}{2vf_p'} f^2, \qquad (7.13)$$

since $d\theta/ds = \omega/\dot{s} = 0$ at $s = s_p$; $(d^2\theta/ds^2)_p = (d\omega/ds)_p/\dot{s}_p = \omega_0 f'_p/v$ [see (2.3)]. In (7.13) we used the relation $f(s) \approx f(s_p) + f_p'(s - s_p) = f_p'(s - s_p)$. Note that the factor $\omega_0/vf_p' \sim \omega_0 L/v \sim 1/\varepsilon$ in (7.13) is $\gg 1$ [see (4.3)]. Therefore, each extra power of f in the denominator of the integral (7.10) increases its value by $\sim\varepsilon^{-1/2}$. This is why allowance for only the principal singularity of the integrand is justified.

This explains also why the remainder term of the asymptotic series in ε for $\delta\mu$ (see Section 5) does not decrease with increasing number of terms of such a series. On the one hand, the time derivative of each succeeding more precise $\mu^{(n)}$ decreases by a factor ε, but, on the other hand, the denominator of the expression for $\dot{\mu}^{(n)}$ acquires thereby an extra ω^2 [one ω on account of integration of $\exp(i\theta)$, and the other on account of the differential denominator]. As a result, the integral of $\dot{\mu}^{(n)}$ does not depend on the degree of precision and it is simplest to calculate it with unperturbed μ.

Gathering together all the relations, we reduce the integral (7.10) to the form (7.9) with p = 2 and obtain

$$\left.\begin{aligned} \Delta\sqrt{\mu} &= -\frac{3\pi}{8\sqrt{2}} r_0 \sqrt{\omega_0}\, \mathrm{Im}\,(e^{i\theta_p}); \\ \frac{\Delta\mu}{\mu} &\approx -\frac{3\pi}{4}\frac{r_0\omega_0}{v_{\perp 0}} \mathrm{Im}\,(e^{i\theta_p}). \end{aligned}\right\} \qquad (7.14)$$

Since p is an integer in this case, the integral can, of course, be expressed also in terms of a residue at a pole.

Note that in the considered paraxial approximation the magnetic-field configuration influences only the value of θ_p (if f'_p is finite; see below). A more general and correspondingly more complex expression for $\Delta\mu$, not restricted to the paraxial region, was obtained in [5] [see Eq. (32)]. Its analysis shows that the main condition of the paraxial approximation is the inequality

$$\frac{r_0^4}{L\rho_m^3} \ll 1, \tag{7.15}$$

where $\rho_m = v/\omega_0$ is the maximum Larmor radius of the particle (at $\beta_0 = \pi/2$) and L is the longitudinal scale of the trap (see Section 3). Expression (4.4), on which the derivation of (7.14) is based, was obtained under the additional simplifying assumption that $\rho_m \ll r_0$ (see Section 4). A more detailed analysis [8] shows, however, that in the paraxial approximation all the relations remain unchanged also for $r_0 < \rho_m$. In particular, at $r_0 = 0$, when the center of the Larmor circle moves along the symmetry axis of the field, we have $\Delta\mu = 0$, for in this case μ coincides with an exact integral, viz., the canonical angular momentum conjugate to the azimuthal angle φ [see (2.1)]:

$$(\mathbf{r} \times (\mathbf{p} + \mathbf{A}))_z = r(\mathbf{p}_\perp + \mathbf{A})_\varphi = \frac{v_\perp^2}{2\omega} = \mu.$$

Note also that expressions (7.14) are equally valid during both half-cycles of the longitudinal oscillations.

The calculation of θ_p in (7.14) is in accordance with an equation similar to (7.4):

$$\theta_p = \theta_1 + \omega_0 \int_{s_1}^{s_p} \frac{f(s)\,ds}{\dot{s}(s)}, \tag{7.16}$$

where $\theta_1 = \theta(s_1)$ and $s_1 = \mathrm{Re}(s_p)$. In the general case we have $s_1 \neq 0$ (see below).

For a short trap (see Subsection 2 of Section 3), $f(s) = 1 + s^2/L^2$ and $s_p = iL$; $s_1 = 0$; $\theta_1 = \theta_0$. In the small-β_0 approximation [$\dot{s}(s) \approx \dot{s}_0$] we obtain, in analogy with (7.7),

$$\theta_p \approx \theta_0 + \frac{2i}{3}\frac{L}{\rho_m \cos\beta_0}. \tag{7.17}$$

The same expression is valid (with a certain effect L_{ef}) also in the case of a multimirror trap (see Subsection 4 of Section 3). The value of L_{ef} is obtained by expanding f(s) in the vicinity of s = 0. From (3.18) we have

$$f(s) \approx 1 + (\pi s/2L)^2(\lambda - 1), \tag{7.18}$$

whence

$$L_{ef} = \frac{2L}{\pi\sqrt{\lambda - 1}}. \tag{7.19}$$

Since the singularity is located at the point $s_p = iL_{ef}$, at a larger mirror ratio $\lambda \gg 1$ we have $|s_p| \ll L$ and the expansion (7.18) can actually be used. The same condition ($\lambda \gg 1$) ensures smallness of β_0 for particles near the separatrix of a multimirror trap, for which $\sin\beta_0 = 1/\sqrt{\lambda} \ll 1$ (see Section 3). It is important that, in this case, there are no singularities other than $s_p \approx iL_{ef}$. This can be seen from the exact expression for s_p:

$$\cos(\pi s_p/L) = (\lambda + 1)/(\lambda - 1) \text{ [see (3.18)]}.$$

The situation is different for a long trap in the model (3.13). The upper s plane has in this case n/2 singularities (n is even) at the points

$$s_k = L\exp\left[i\frac{\pi}{n}(1 + 2k)\right], \tag{7.20}$$

where k takes on integer values from 0 to (n/2 − 1). The largest contribution to $\Delta\mu$ is made by the two singularities closest to the real axis and corresponding to k = n/2 − 1 and k = 0:

$$s_p = \mp L\cos(\pi/n) + iL\sin(\pi/n) \approx \mp L + i\pi L/n. \tag{7.21}$$

The last approximate expression is valid at $n \gg \pi$, i.e., precisely for a long trap.

From the connection (7.16) between θ and s in the small-β_0 approximation ($\dot{s} \approx v$),

$$\theta = \frac{\omega_0 s}{v}\left[1 + \frac{1}{n+1}\left(\frac{s}{L}\right)^n\right] + \text{const} \tag{7.22}$$

it can be seen that the singularities θ_k in the θ plane also lie on the circle ($s_k^n = -L^n$), and the singularities closest to the real axis are well separated from one another. Thus, for the singularity (7.21) which neighbors on s_p, the value of Im θ_k is three times larger than for s_p. This justifies the neglect of all singularities except s_p (7.21). The constant in (7.22) is determined by the values of θ_1 and $s_1 \approx \mp L$. We ultimately get

$$\theta_p \approx \theta_1 \pm \frac{2n}{n+1} \frac{l}{\rho_m} + i\pi \frac{n}{n+1} \frac{l}{\rho_m} \approx \theta_1 \pm \frac{2l}{\rho_m} + i\pi \frac{l}{\rho_m}. \quad (7.23)$$

We see that the order of $\Delta\mu$ is determined now by the size $\ell = L/n$ of the mirror, and not by that of the whole trap. In addition, the phase on which $\Delta\mu$ depends is no longer equal to the Larmor phase θ_1 at $s = s_1$, but is shifted by the large value $2\ell/\rho_m \gg 1$, and furthermore to opposite sides for the two singularities. Expression (7.14) for $\Delta\mu$ remains valid also in this case for each of the two main singularities. In contrast to the preceding examples, however, the changes of μ on two half-cycles of longitudinal oscillations (i.e., after a round trip of the particle over the trap) are not fully symmetric. Namely, the sign of the additional phase shift $2\ell/\rho_m$ is reversed.

In place of a phase shift by $\pm 2\ell/\rho_m$ at the point $s = s_1$ one can shift by a distance s the point at which the phase θ_1 is chosen:

$$\left.\begin{aligned} &\theta_1(s_1) \pm 2l/\rho_m \to \theta_1(s_1 + \Delta s_1), \\ &\Delta s_1 \approx \pm (2l/\rho_m)/(d\theta/ds) \approx \pm 2l, \quad \Delta\,|\,s_1\,| \approx -2l. \end{aligned}\right\} \quad (7.24)$$

The point of each mirror shifts toward the center of the trap. The field at the shifted points

$$\omega_1/\omega_0 \approx 1 + (1 - 2/n)^n \approx 1 + e^{-2} \approx 1 \quad (7.25)$$

differs little from the field at the center of the trap. It can be stated that the shifted points are located at the inner edges of the mirrors.

For traps with field-reversed mirrors (see Subsections 5 and 6 of Section 3), there is no paraxial approximation, and $\Delta\mu$ must be calculated anew. This problem was solved in [15].

We consider initially a planar geometry of opposing mirrors (see Subsection 5 of Section 3). In contrast to a multi-mirror trap (see Subsection 4), the quadratic expansion of the field (3.35) near the minimum is not suitable in this case, since its singularity is too far away, at $|s_p| = r_0$, where the expansion is no longer valid [see (3.34)]. To get around this difficulty, we note that although the integration contour (7.10) should be taken in the θ plane, the integration variable and (or) the argument of the integrand can be arbitrary. To choose the most suitable variable, we express the Larmor frequency in the form [see (3.33)]

$$\omega = \frac{\omega_0}{r_0}\sqrt{x^2+y^2} = \frac{\omega_0 r_0}{2x}\sqrt{1+\frac{4x^4}{r_0^4}}, \tag{7.26}$$

where we use the magnetic-line equation $2xy = r_0{}^2$. If we now choose the argument of the function $\omega(\xi)$ to be, for example,

$$\xi = 2x^2/r_0^2, \quad \omega(\xi) = \omega_0\sqrt{(1+\xi^2)/2\xi}, \tag{7.27}$$

the position of the singularity in the complex ξ plane will be $\xi_p = i$, and $\xi_0 = 1$ [at the minimum of $\omega(\xi)$ on the given magnetic line].

We find first the connection between the new variable ξ and the phase θ. We have

$$\theta = \int \omega dt = \int \frac{\omega(\xi)}{\dot{s}(\xi)}\frac{ds}{d\xi}d\xi \approx \frac{q_2}{2}\left(\xi - \frac{1}{\xi}\right). \tag{7.28}$$

The last expression is valid in the approximation of small β_0, when $\dot{s}(\xi) \approx \dot{s}_0 \approx v$, and we have used the relation

$$\frac{ds}{d\xi} = \frac{ds}{dx}\frac{dx}{d\xi} = \frac{r_0}{2\sqrt{2}}\frac{\sqrt{1+\xi^2}}{\xi^{3/2}}, \tag{7.29}$$

while $q_2 = \omega_0 r_0/2v = r_0/2\rho_m$ is the large parameter of the problem. In the same approximation we have

$$\theta_p = \theta_0 + iq_2. \tag{7.30}$$

The curvature of the magnetic line is obtained from the equation $2xy = r_0{}^2$ of the line:

$$\frac{1}{R(\xi)}=\frac{d^2y/dx^2}{\left[1+\left(\frac{dy}{dx}\right)^2\right]^{3/2}}=\frac{r_0^2}{(x^2+y^2)^{3/2}}=\frac{\omega_0^3}{r_0\omega^3(\xi)}. \qquad (7.31)$$

Just as in the preceding examples, the curvature is expressed in terms of the field, and has a singularity at the very same point $\xi = \xi_p = i$. At the minimum of the field the curvature radius is $R_0 = r_0$; i.e., it is equal to the minimum distance from the line to the center $x = y = 0$ of the trap (see Fig. 2a).

We choose the same integration variable as before:

$$u=-i(\theta-\theta_p)\approx\frac{iq_2}{2\xi_p^3}(\xi-\xi_p)^2. \qquad (7.32)$$

The last expression is obtained by expanding the function $\theta(\xi)$ (7.28) near the singularity. In the same region we have

$$\omega\approx\omega_0(\xi-\xi_p)^{1/2}\approx\left(-\frac{2u}{q_2}\right)^{1/4} \qquad (7.33)$$

[see (7.27)]. Substituting all these expressions in the integral (7.10) for $\Delta\mu$, we reduce it to the form (7.9) with $p = 9/8$. We obtain ultimately

$$\Delta\sqrt{\mu}=\frac{\pi}{2^{13/8}\Gamma(9/8)}\frac{v}{\sqrt{\omega_0}}q_2^{1/8}e^{-q_2}\sin\theta_0\approx 1.08\frac{v}{\sqrt{\omega_0}}q_2^{1/8}e^{-q_2}\sin\theta_0. \qquad (7.34)$$

This is exactly the result of [15] (at $\beta_0 \ll 1$) corrected for the misprints there. We note that Howard [15] used a somewhat different method in which the integration variable was the scalar potential of the magnetic field.

In the case of cylindrical geometry of the field-reversed mirrors (Subsection 6), the procedure for calculating $\Delta\mu$ remains the same. We choose as the argument of the integrand the quantity $\xi = r^3/2b^3$, where b is a parameter of the magnetic line $zr^2 = b^3 = (\ell_0/\sqrt{3})^3$ (see Fig. 2b). Then

$$\omega(\xi)=\omega_0\frac{2^{1/3}}{\sqrt{3}}\frac{\sqrt{1+\xi^2}}{\xi^{2/3}} \qquad (7.35)$$

and

$$\theta(\xi) = 2^{-1/3} q_3 \xi^{2/3} \left(1 - \frac{1}{2\xi^2}\right), \qquad (7.36)$$

and $q_3 = \omega_0 \ell_0 / 3v = \ell_0 / 3\rho_m \gg 1$. Using the same integration variable $u = -i(\theta - \theta_p)$, we arrive at a singularity of the same order $p = 9/8$ and get

$$\Delta\sqrt{\mu} = \frac{\pi \cdot 3^{1/8}}{2^{11/6}\Gamma\left(\frac{9}{8}\right)} \frac{v}{\sqrt{\omega_0}} q_3^{1/8} e^{-\alpha q_3} \sin(\theta_0 - \Delta)$$

$$= 1.07 \frac{v}{\sqrt{\omega_0}} q_3^{1/8} e^{-\alpha q_3} \sin(\theta_0 - \Delta), \qquad (7.37)$$

$$\Delta = \frac{11}{48}\pi + 0.155 q_3, \qquad \alpha = 1.031 \approx 1.$$

We note first of all that, at a suitable choice of the parameters q, the expressions for $\Delta\mu$ are very close to each other for field-reversed mirrors of both types. The strongest difference is due to the phase shift Δ in the last case. Its cause is the same as for a long trap, viz., the asymmetric configuration of the field relative to the singularity. Here, too, one can introduce an equivalent shift of the point at which one takes the Larmor phase that determines $\Delta\mu$: $\theta_0(s = 0) \to \theta_1(s = s_1)$, where

$$s_1 \approx -v\Delta/\omega_0 \approx -l_0/19. \qquad (7.38)$$

Note that in both cases the shift is toward a smaller field gradient.

Expression (7.37) agrees with the results of [15], except for a constant phase shift $11\pi/48$, which differs in [15] by $+\pi/4$. This difference is possibly due to the fact that in [15] the integration is over a contour in the complex plane of z and not θ.

In all the cases considered, the change of $\Delta\mu$ turns out to be exponentially small relative to the adiabaticity parameter $\varepsilon = \Omega/\langle\omega\rangle \sim \Omega/\omega_0 \sim \rho_m/L$. This raises the serious question of how reliable are estimates of so small a quantity, especially in view of the neglect of the much larger ($\sim\varepsilon$) quasiperiodic variations of μ. Similar misgivings were raised many times in the literature concerning this problem and similar ones. This is seemingly confirmed by the fact that different preexponential factors in the expression for resonant $\Delta\mu$ were obtained by different workers. Some differ greatly enough to doubt the validity of the power-law (in ε) correction to $\Delta\mu$. The latter, however, is excluded completely for the following reasons. It is shown in [17] that asymptotic corrections to μ, in any order in ε, are quasiperiodic. Consequently, the nonperiodic (resonant) change of μ decreases with ε more rapidly than any power of ε, i.e., exponentially. The same conclusion can also be reached in much simpler fashion, by starting from the exact expression (4.4) for $\Delta\mu$. Indeed, in the case of an analytic time dependence of the right-hand side on the time or on the phase θ (and this is always the case for real field), we can shift the integration contour (with respect to θ) along the imaginary axis ($\mathrm{Im}\,\theta = 0 \to \mathrm{Im}\,\theta = \theta_s = \mathrm{const}$), and this leads to the appearance of a constant factor $\exp(-\theta_s)$ [after making the substitution $\sin\theta \to \mathrm{Im}\exp(i\theta)$]. But since $\theta_s \propto \omega \propto 1/\varepsilon$, we have $\Delta\mu \propto \exp(-A/\xi)$; i.e., it decreases exponentially as $\varepsilon \to 0$.

A more complicated problem is that of the accuracy of the expressions obtained above for resonant $\Delta\mu$. The difficulty lies here in the fact that in the higher approximations the harmonics of the low frequency Ω are, generally speaking, enhanced, and can in principle alter somehow the argument of the exponential and (or) the preexponential factor. Nonetheless, it can apparently be stated that the relative correction to $\Delta\mu$ is small as $\varepsilon \to 0$. This is due to the specific structure of the integral for $\Delta\mu$ in (7.10). Although we do not know the integrand as a function of t, we can express it in terms of the exactly known functions $\omega(s)$ and $R(s)$ (the specified configuration of the magnetic field) and, generally speaking, the (exactly) unknown function $\mathbf{v}(s)$. But the latter is needed only in the singularities, where $\omega = \omega(s_p) = 0$ and $v_{\parallel}(s_p) = v$; $v_{\perp}(s_p) = 0$ in view of $v_{\perp}^2 = 2\mu\omega$. It is important that this result [$v_{\perp}(s_p) = 0$] does not depend on the corrections to μ, provided they are small, i.e., at sufficiently low ε. In this way all the complexities of the $v(s)$ dependence in the higher approximations do not affect the integral value of $\Delta\mu$. This means physically that the contributions of the higher approximation to the $\mu(t)$ dependence cancel out over the half-period T/2. We note incidentally that, owing to $v_{\perp}(s_p) = 0$, we can discard in the equation for $\dot{\mu}$ not only the terms with $\sin(2\theta)$, but also the terms of form $v_{\perp} \sin\theta$, as was done in (4.4) (cf. the total expression in [5]).

It remains to discuss the calculation of θ_p by means of (7.16). In the small-β_0 approximation, the corrections to $\dot{s}$ are immaterial. In the general case [see, e.g., (7.6)], the correction to θ_p is proportional to the integral of $\delta\mu$. The latter is described by an expression such as (5.1), so that $|\delta\mu| \sim \varepsilon$ and is proportional to the rapidly oscillating function $\cos\theta$ (for a particle in a trap). The integral of $\delta\mu$ is therefore of the order of ε^2, and the correction to θ_p, notwithstanding the large factor $1/\varepsilon$ in (7.16), turns out to be small ($\lesssim\varepsilon$).

Results of numerical simulation show that the typical first-approximation error of $\Delta\mu$ is of order 10% (see, e.g., [5]). In some special cases the accuracy can be even higher [15]. These figures include also the errors in the separation of the resonant $\Delta\mu$ against the background of much larger, generally speaking, quasiperiodic, oscillations $\delta\mu$ (see Section 5). As already noted above, the use of explicit expressions for a more precise μ greatly facilitates this task (see [15, 20]). An even more effective method can be the use of resonant trajectories for numerical simulation. In this case, the quasiperiodic variations cancel out at both reflection points.

Note that an exponentially small resonant $\Delta\mu$ was first obtained in [16] from the solution of the corresponding quantum-mechanical problem. The relatively simple classical-mechanics technique described above was proposed in [20] and then developed in a number of papers (see, e.g., [5, 15, 21]). The most extensive calculations were carried out in [5].

8. Mapping

Taken by itself, the quantity $\Delta\mu$ obtained in the preceding section not only fails to solve the problem of prolonged particle confinement in a trap, but is meaningless, for in typical cases it is much smaller than the quasiperiodic oscillations $\delta\mu$ of μ. The central question in the problem of prolonged containment of particles in a trap is the accumulation of successive changes of μ. This problem can be answered in two ways. The first is to analyze the Hamiltonian (6.9) that describes a system of interacting resonances with amplitudes determined by the quantity $\Delta\mu$(6.10). The second is to describe the particle motion by mapping or transforms, i.e., not continuously but at certain finite time intervals. We use below the second way, which turned out to be simpler and more convenient (see [2]). It is convenient to choose as the characteristic time interval the longitudinal-oscillation half-period T/2 to which the quantity $\Delta\mu$ pertains. This very quantity characterizes the variation of one of the dynamic variables of the system, that of the action μ in this interval. This, however, is not enough for a complete description of the motion since $\Delta\mu$ depends on another dynamic variable, the Larmor phase θ at a certain point of the magnetic line (in the simplest case – at the minimum of the field). We must therefore first find the change of θ between successive passes through this point. This problem is generally solved in various ways, depending on the actual magnetic-field configuration.

We begin with the model (3.1). According to the results of Section 7, the quantity ΔJ_y is determined in this case by the value of the phase θ at the minimum of the potential ($x = 0$). The change of θ between successive passes through this minimum, during the half-period of the x oscillations, can therefore be written in the form

$$\Delta\theta_0 \approx \frac{\pi}{\omega_x} \langle\omega_y\rangle = \pi\left(\frac{1}{\sqrt{2J_y}} + \frac{J_x}{2J_y}\right). \tag{8.1}$$

In the last expression we used the connection between the frequencies ω_x, $\langle\omega_y\rangle$ and the actions J_x, J_y (3.5).

In this form, however, relation (8.1) still does not solve our problem, since a new dynamic variable appears (J_x), and calls for one more equation. Instead of finding an equation for ΔJ_x, however, we can express J_x in terms of J_y by using the energy conservation law $H^0(J_x, J_y) =$ const. From (3.4) we get

$$J_x = (H^0 - J_y)/\sqrt{2J_y} = (v_0^2 - 2J_y)/2\sqrt{2J_y}, \tag{8.2}$$

whence

$$\Delta\theta_0 = \frac{\pi}{2}\left(\frac{1}{\sqrt{2J_y}} + \frac{v_0^2}{(2J_y)^{3/2}}\right). \tag{8.3}$$

Now let J_y and θ_0 be the values of the dynamic variables at some pass through the minimum of the potential, and $\overline{J_y}$, $\overline{\theta_0}$ the values of the same variables during the next pass. Mapping is defined as the connection between these two pairs: $J_y, \theta_0 \to \overline{J_y}, \overline{\theta_0}$. Introducing for convenience a new phase $\vartheta = 2\theta$, we can write this connection, in our case, in the form

$$\left.\begin{aligned}\bar{J}_y &= J_y + (\Delta J_y)_m \sin\vartheta_0,\\ \bar{\vartheta}_0 &= \vartheta_0 + G(\bar{J}_y),\\ (\Delta J_y)_m &\approx -\pi J_y \exp[-4/3v_0 \cos\beta_0],\end{aligned}\right\} \quad (8.4)$$

[see (7.8)], and take the function $G(J_y) = 2\Delta\theta_0(J_y)$ at $J_y = \bar{J}_y$, i.e., for the value of J_y after the first pass, the very thing that determines the difference between two successive values of the phase ϑ_0.

Mapping should describe completely the evolution of the considered model in its phase space (J_y, ϑ_0). This space is, in this case, a semicylinder, since $J_y \geq 0$, while the phase ϑ_0 is defined accurate to an integer multiple of 2π. Given the energy $H^0 = v_0^2/2$, the motion is confined to the region $J_y \leq H^0$ (8.2). The term mapping stems from the fact that the difference equations (8.4) transform (or map) the phase semicylinder on itself; i.e., each point of this semicylinder goes over into one of the points of the very same surface.

The mapping (8.4) is not canonical; i.e., it does not conserve the measure (area) of the phase surface. Indeed, if we put for simplicity $\cos\beta_0 = 1 (\beta_0 \ll 1)$, the Jacobian of the mapping is

$$\frac{\partial(\bar{J}_y, \bar{\vartheta}_0)}{\partial(J_y, \vartheta_0)} = 1 + \frac{\partial(\Delta J_y)_m}{\partial J_y}\sin\vartheta_0 \neq 1. \quad (8.5)$$

Since the initial system (3.1) is canonical, or Hamiltonian, the result (8.5) means simply that the mapping (8.4) is not exact. In fact, relation (7.8) defines the change not of J_y but of $\ln J_y$. If we assume as before that $\cos\beta_0 = 1$ and introduce a new variable $P = \ln J_y$, the mapping

$$\bar{P} = P + (\Delta P)_m \sin\vartheta_0, \quad \bar{\vartheta}_0 = \vartheta_0 + G(\bar{P}) \quad (8.6)$$

now becomes canonical, since $(\Delta P)_m = \pi\exp(-4.3v_0)$ is independent of P.

Note that were we to retain the dependence of the argument of the exponential in $(\Delta P)_m$ on β_0 [$\cos\beta_0$ or, in the general case, the dependence (7.6)] and, consequently, also on J_y, the last mapping would again become noncanonical, since $\partial(\Delta P)_m/\partial J_y \neq 0$. This is one more advantage of the small-β_0 approximation. In this approximation it is possible to choose, in all the examples considered above, the variable P such that $\partial(\Delta P)_m/\partial P = 0$, and the mapping of form (8.6) (see below) turns out to be canonical.

Canonicity of the mapping is essential for the use of certain general ergodic-theory theorems and is necessary in numerical simulation, for otherwise the errors can accumulate rapidly because the phase area is not conserved.

For certain magnetic-field configurations, the mapping that describes particle motion in a trap turns out to be the same as (8.6). For example, for a certain trap (see Subsection 2 of Section 3), we introduce the variable $P = \sqrt{\mu}$ [see (7.14) and (7.17)] and obtain

$$\overline{P} = P + (\Delta P)_m \sin\theta_0;\ \bar{\theta}_0 = \theta_0 + G(\overline{P}), \tag{8.7}$$

where

$$(\Delta P)_m = -\frac{3\pi}{8\sqrt{2}} r_0 \sqrt{\omega_0}\, e^{-q} \tag{8.8}$$

and

$$G(P) = \frac{\pi\langle\omega\rangle}{\Omega} = \frac{\pi}{2\sqrt{2}} L\sqrt{\omega_0}\left(\frac{1}{P} + \frac{v^2}{2\omega_0 P^3}\right). \tag{8.9}$$

The last expression can be obtained directly from (8.3) in view of the complete analogy between (3.4), (3.11) and (3.5), (3.12). The adiabaticity parameter is, in this case, $\varepsilon \sim 1/q = 3\rho_m/2L$.

The mapping takes the same form as well for a multimirror trap (see Subsection 4), and also for planar geometry of field-reversed mirrors (Subsection 5). In all these cases there is only one singularity on a half-period of the longitudinal oscillations (in one pass of the particle through the trap), and the motion is symmetric about the field minimum. The mapping for the remaining examples of Section 3 will be constructed later (see Section 14). We note right away that in all the magnetic-trap examples the variable is $P = \sqrt{\mu}$, since we have always used Eq. (4.4) in the calculation of $\Delta\mu$.

In the case of a multimirror trap, we confine ourselves to the region near the separatrix (see Subsection 4 of Section 3). The frequencies $\langle\omega\rangle$ and Ω are specified here as functions of the parameter w [Eqs. (3.26), (3.29), (3.31)] that depends only on μ [see (3.25), H^0 = const]. As a result we obtain for the function G(P) in the mapping (8.7):

$$\left.\begin{aligned} G(P) &= \frac{\sqrt{2}}{\pi}\,\frac{\lambda}{\sqrt{\lambda-1}}\,\frac{L\sqrt{\omega_0}}{P}\left(\ln\frac{32}{|w|}-2\frac{\lambda-1}{\lambda}\right); \\ w &= \frac{v^2}{(\lambda-1)\,\omega_0 P^2}-\frac{2\lambda}{\lambda-1}. \end{aligned}\right\} \quad (8.10)$$

The expression for $(\Delta P)_m$, however, remains (8.8) as before, with the parameter

$$\frac{1}{q}=\frac{3\pi}{4}\sqrt{\lambda-1}\,\frac{\rho_m}{L}, \quad (8.11)$$

where 2L is the distance between neighboring mirrors [see (3.18) and (7.19)].

In the case of field-reversed mirrors we use for the field the asymptotic expression (3.36), which corresponds to large amplitudes of the longitudinal oscillations, since we assume, as before, that β_0 is small. In our case, the frequencies are given by relations (3.38) and we get

$$G(P) \approx \frac{2}{3}\,\frac{r_0 v^3}{\omega_0 P^4}. \quad (8.12)$$

The quantity $(\Delta P)_m$, on the other hand, is given by (7.34).

The mappings obtained in this section can be used directly for numerical simulation of prolonged motion of a particle in a magnetic trap of suitable configuration. These mappings are quite simple, and each iteration of a mapping corresponds to one complete pass of the particle through the trap between reflection points in the mirrors.

For analytic study, the mappings obtained can be further simplified and "standardized."

9. Standard Mapping

The mapping (8.7) obtained in the preceding section is equivalent to the Hamiltonian (6.9) in the sense that it describes the same system of nonlinear resonances. The resonance condition (in first approximation – see Section 10 below) for the mapping can be written as

$$G(P_r) = 2\pi r, \tag{9.1}$$

where r is an arbitrary integer. This condition determines the resonance values $P = P_r$ and, accordingly, $\mu = \mu_r = P_r^2$, for which the successive values of the phase θ_0 remain unchanged. The latter is correct, of course, if μ also remains unchanged, i.e., if $\theta_0 = 0$ or π. It can be easily seen that one of these phase values is unstable, depending on the sign of $(\Delta P)_m$ [at $(\Delta P)_m > 0$, for example, the unstable point is $\theta_0 = 0$].

Since $G(P) = \pi\langle\omega\rangle/\Omega$ (see Section 8), the resonance condition can also be written in the form $\langle\omega\rangle = 2r\Omega$. It differs from the condition (6.2) by a factor of two which is connected with the symmetry of the motion described by the mapping (8.7) about the minimum of the field. In this case, the amplitudes of all the odd harmonics of the longitudinal oscillations vanish in the Fourier expansion (6.1).

We linearize the function G(P) near one of the resonant values of P and introduce a new variable p:

$$G(P) \approx G(P_r) + \frac{dG}{dP}\bigg|_{P=P_r}(P - P_r) \rightarrow G_r'(P - P_r) \equiv p. \tag{9.2}$$

Here $G_r' \equiv (dG/dP)_{P=P_r}$, and we have discarded the term $G(P_r) = 2\pi r$, which does not change the mapping. In terms of the variables p and θ (we drop the zero subscript of the phase), the mapping (8.7) takes the form

$$\begin{aligned} \bar{p} &= p + K\sin\theta, \\ \bar{\theta} &= \theta + \bar{p} = \theta + p + K\sin\theta. \end{aligned} \tag{9.3}$$

It was introduced similarly in [8] and named the standard mapping, since many (although by far not all) actual problems of nonlinear dynamics of Hamiltonian systems are reducible to it. In particular, all the magnetic trap types considered in the preceding section reduce to this mapping. Any actual system is distinguished only by a single standard-mapping parameter that can be represented in the form

$$K = G_r'(\Delta P)_m. \tag{9.4}$$

Note that if even the quantity $(\Delta P)_m$ depended on P, it would have to be taken in (9.4) at $P = P_r$ (just as G'). Consequently, K is simply a constant, and the standard mapping turns out to be canonical. The canonicity of the initial mapping (8.7) is therefore immaterial if this mapping is to be analytically investigated by changing to a standard mapping.

The first-approximation resonances for a standard method are defined by the conditions

$$p = p_r = 2\pi r, \tag{9.5}$$

i.e., they are infinite in number, and all are located at equal distances $\delta p = 2\pi$ from one another. From a comparison of the last expression with (9.1) it can be seen that the standard mapping describes the initial system (in particular, its resonant structure) locally with respect to P (and μ). Indeed, the initial system is a particle in a trap, and the mapping (8.7) that describes it has, generally speaking, a finite number of resonances (in view of the limited range of $\mu \leq v^2/2\omega_0$), which are not uniformly distributed with respect to μ (or P). A standard mapping transforms this section of the resonant structure and makes it homogeneous and infinite. For this reason, the standard mapping is also called the homogeneous model of a resonant structure.

For the local model to have meaning, it is necessary that the number of resonances be large, and that their characteristics, particularly K, differ little from neighboring resonances. This is in fact the condition under which linearization of (8.7) with respect to P is admissible. This condition can be written in the form

$$\frac{\delta P}{P} \approx \frac{2\pi}{|PG'|} \sim \frac{2\pi}{|G|} \sim \varepsilon \ll 1, \tag{9.6}$$

where $\delta P = |P_{r+1} - P_r|$ is the distance in P between neighboring resonances.

10. Limit of Global Stability

As already noted, the central question of prolonged confinement of a particle in a magnetic trap is whether or not successive resonant changes $\Delta\mu$ of the particle magnetic moment are cumulative. In the language of standard mapping, the same question reads: Is the motion of this system finite, limited in p, or infinite?

The only parameter K of the standard mapping has the meaning of a perturbation parameter. In fact, at K = 0 we have p = const and hence also μ = const. Since we are dealing in this case with an adiabatic perturbation, K can be regarded as a new adiabaticity parameter. More accurately speaking, the dimensionless adiabaticity parameter should be taken to be $|K|/(2\pi)^2$, the square of the ratio of the perturbation-induced oscillation frequency [$\sim\sqrt{|K|}$; see Eq. (10.2) below] to the perturbation frequency (equal to 2π, with the period of the perturbation equal to 1). The new parameter is connected with the old (ε) by the estimate

$$k = \frac{|K|}{4\pi^2} \sim \frac{e^{-1/\varepsilon}}{\varepsilon}. \tag{10.1}$$

The exponential factor stems here from the expression for $(\Delta P)_m$ (or $\Delta\mu$), and the preexponential one from $G_r' \sim G/P \sim 1/\varepsilon P$. For understandable reasons we shall call k the resonant adiabaticity parameter.

Since the function $k(\varepsilon)$ has a singularity at $\varepsilon = 0$, the new parameter k cannot be obtained, as we have verified also directly, from the asymptotic expansion in ε. Once, however, we have found it by exact integration of the perturbation and have arrived thus ultimately at the standard mapping, we can now use for the analysis an asymptotic expansion in k and, in particular, a very simple averaging method (see, e.g., [12]). Thus, for sufficiently small $k \to 0$ and nonresonant $p \neq 2\pi r$ we can expect the variation of p to be quasiperiodic and bounded. In exactly the same manner, for $k \to 0$ and resonant p (for example, $p \approx 0$) we can neglect all the resonances except the given one (r = 0). The standard-mapping difference equations can then be replaced by differential ones:

$$\bar{p} - p \approx \frac{dp}{dt} \approx K \sin\theta; \qquad \bar{\theta} - \theta \approx \frac{d\theta}{dt} = p, \tag{10.2}$$

which turn out to be canonical with a Hamiltonian

$$H_r(\theta, p) = \frac{p^2}{2} + K\cos\theta. \tag{10.3}$$

The time t is measured here in numbers of iterations of the mapping, or in units of T/2.

The resonant Hamiltonian (10.3) is equivalent to the Hamiltonian (6.8) – both describe one nonlinear resonance. As already noted in Section 6, motion in this case is finite under all initial conditions. The maximum amplitude of the p oscillations corresponds to motion near the separatrix ($H_r = |K|$). The separatrix has two branches:

$$p_c = \pm 2\sqrt{K}\sin\frac{\theta}{2}. \qquad (10.4)$$

This expression is valid at $K > 0$: reversal of the sign of K is equivalent to a shift of the phase θ by π: $\theta \to \theta + \pi$ [see (10.3)]. The maximum change $(\Delta p)_m$ of p is equal to the width of the separatrix, i.e., to the largest distance between the branches of the separatrix (at $\theta = \pi$):

$$(\Delta p)_m = 4\sqrt{|K|} = 8\pi\sqrt{k}. \qquad (10.5)$$

The dynamics of one nonlinear resonance (10.3) is perfectly similar to the motion of an ordinary pendulum or of a particle in a field with a harmonic potential, particularly in a multimirror trap of type (3.19). The picture of the phase trajectories in all these cases has the form shown schematically in Fig. 1. Consequently, as already noted in Section 6, the oscillations of p, meaning also of μ, are bounded in the case of one resonance. Up to which K is this simple picture of the motion preserved? The usual condition of asymptotic theory requires that the frequency ($\sim|K|^{1/2}$) of the averaged (smoothed) system (10.2) be much lower than the frequency of discarded perturbation in the initial system (9.3), which is equal to 2π (one iteration is taken as the unit of time), i.e., that $|K| \ll (2\pi)$ or $k \ll 1$ (10.1). The critical value of the perturbation is therefore

$$k_{cr} \sim 1, \quad |K|_{cr} \sim (2\pi)^2 \approx 40. \qquad (10.6)$$

A much better estimate can be obtained by using the criterion called the overlap of nonlinear resonances [8]. The simplest variant of this criterion is obtained in the following manner. All integer $[p_r/2\pi = r]$ resonances of the standard mapping are identical and are described by the same Hamiltonian (10.3) with shifted momentum $p \to p - p_r$. In particular, each of them has the same width (10.5). The simplest resonance-overlap criterion is determined from the condition that the separatrices of neighboring resonances be tangent. Since the distance between them is $\delta p = 2\pi$ (9.5), the tangency condition is $\delta p = (\Delta p)_m$, whence

$$k_{cr} = 1/16, \quad |K|_{cr} = \pi^2/4 \approx 2.5. \qquad (10.7)$$

This is already much closer to the numerical simulation of the standard mapping [8], which yields

$$|K|_{cr} \approx 1, \; k_{cr} \approx 1/40 \tag{10.8}$$

accurate to several percent. Note that at the stability limit the adiabaticity parameter is $k = k_{cr} \ll 1$, thereby justifying the use of an asymptotic expansion in this region.

A very simple criterion thus permits a correct estimate of the order of a critical perturbation. Moreover, the picture of the overlap of the resonance is clear enough to gain a qualitative idea of what happens when the perturbation is larger. Clearly, when the resonances overlap, the trajectory of the system can move over from the region of one resonance to that of a neighboring and the motion becomes infinite, at least for certain initial conditions. The character of this motion will be considered below (Section 11). We note here merely that the overestimate of the critical value by the simple resonance-overlap criterion is due mainly to the fact that in this form the criterion takes into account only resonance of first-order approximation in the adiabaticity parameter k. In the second order in this parameter there appear half-integer resonances $p_r/2\pi = r/2$; in third order we get resonances $p_r/2\pi = r/3$, etc. The complete system of resonances turns out to be everywhere dense in p:

$$p_{rq} = 2\pi r/q, \tag{10.9}$$

where r and q are arbitrary integers. This does not mean, of course, that the resonances always overlap (for any $k \to 0$), since their widths decrease rapidly with increasing denominator q. Indeed, resonances with a denominator q appear only in the q-th (and higher) approximations, i.e., in perturbation terms whose amplitudes are of order of k^q, and the resonance width is $\sim k^{q/2}$. Recognizing that the number of q-resonances in a given p interval (for example 2π between neighboring integer resonances) is proportional to q, we find that the overlap of resonances in all approximations is estimated by the sum

$$S = \sum_{q=1}^{\infty} q\eta^q = \eta \frac{d}{d\eta} \sum_{q=1}^{\infty} \eta^q = \frac{\eta}{(1-\eta)^2} = \frac{1}{4}. \tag{10.10}$$

Here $\eta = \sqrt{k}$, and the overlap condition $S = 1/4$ is obtained from the critical value $\eta_1 = 1/4$ (10.7) with account taken of only integer resonances. The higher-approximation resonances increase S (at a given η) and accordingly decrease η_{cr} to

$$\eta_{cr} = 3 - \sqrt{8} \approx 0.17, \quad k_{cr} \approx \frac{1}{34}, \quad |K|_{cr} \approx 1.16. \qquad (10.11)$$

This is already quite close to the stability limit (10.8), although the estimate (10.10) cannot, of course, be regarded beforehand as reliable, since the terms of the sum in (10.10) contain unknown numerical coefficients. According to the data of [8], the coefficients of the second and third powers of η are equal to $\pi/2 \approx 1.57$ and $(2.2)^2$, respectively. At any rate, expression (10.10) demonstrates that a system of resonances that is everywhere dense does not necessarily lead to overlap and instability.

This fundamentally and practically important conclusion can nevertheless not be regarded as sufficiently convincing, since it is based in final analysis on an asymptotic expansion in the parameter k. The result of numerical simulation is also limited, in view of the finite computation time (up to $\sim 10^7$ iterations of the standard mapping). A rigorous proof of existence of a critical perturbation below which the particle remains perpetually (i.e., at $-\infty < t < \infty$) in a magnetic trap was obtained in [10] by constructing converging (and not asymptotic) perturbation-theory series. Unfortunately, technical difficulties prevent us from obtaining, in this manner, an effective estimate of the magnitude (and even of the order) of the critical perturbation. With allowance for second- and third-order perturbation-theory approximations, as well as for higher approximation effects, a value $|K|_{cr} \approx 1.1$ was obtained in [8]. An entirely different method [23] leads to $|K|_{cr} \approx 0.97$ (this method is discussed in [24]). In sum, it can be concluded that the values (10.8) for the critical perturbation are reliable enough and can be used to solve specific nonlinear-dynamics problems that are reducible to standard mapping.

Bounded oscillations of the action μ for subcritical perturbation are sometimes called superadiabaticity (see [25], where a related problem was solved). In essence, in this case the adiabatic invariant becomes an exact integral of the motion, albeit nonanalytic and even singular in the dynamic variable and in the initial small parameter ε [10]. It should be noted in this connection that the famous Poincaré theorem that a Hamiltonian system has in the general case no analytic integrals of motion other than the energy is not as significant as heretofore assumed.

The onset of instability of motion for overlapping resonances can be regarded as an interaction of resonances, i.e., as joint action of several resonances; the result of this action differs (radically in this case) from the sum of actions of individual resonances. This situation might be described as interference of resonances, an interference with catastrophic aftereffects. At any rate, resonance overlap is a clear example of the profound difference between linear and nonlinear mechanics.

Since standard mapping describes the initial system locally, the critical value of the parameter K determines the stability boundary in the phase space of the system. We express the position of this boundary in terms of the parameters of the initial system.

For the model (3.1) the standard-mapping parameter is [see (7.8), (8.3), (9.4)]:

$$K \approx \frac{\pi^2}{2}\left(\frac{3}{\sin^3\beta_0}+\frac{1}{\sin\beta_0}\right)\frac{\exp\left[-\dfrac{4}{3v_0\cos\beta_0}\right]}{v_0}$$

$$\approx \frac{3\pi^2}{2}\,\frac{\exp\left(-\dfrac{4}{3v_0}\right)}{v_0\beta_0^3}, \quad \beta_0 \ll 1. \tag{10.12}$$

The critical value $|K| = 1$ (10.8) determines the stability boundary on the plane of the dynamic variables β_0 and $v_0 = \sqrt{2H^0}$, which is a two-dimensional projection of the four-dimensional phase space of the model under consideration.

This boundary can also be represented in the form

$$\beta_0^{cr} \approx 2.5 v_0^{-1/3}\exp(-4/9v_0). \tag{10.13}$$

On the velocity plane $(\dot{x}_0, \dot{y}_0)$ the quantity $\beta_0{}^{cr}$ defines an unstable-motion sector $\beta_0 < \beta_0{}^{cr}$, in which the amplitude of the longitudinal oscillations increases without limit. The adiabatic regime corresponds here to small $v_0 \ll 1$, since the frequency ratio is $\omega_x/\langle\omega_y\rangle \sim v_0\beta_0{}^3 \sim \exp(-4/3v_0)$ [the last estimate is valid at the stability boundary (10.13)].

For a short magnetic trap, using (8.8) and (8.9), we obtain in analogy with the preceding case

$$K \approx \frac{81\pi^2}{64}\,\frac{r_0}{L}\,\frac{q^2 e^{-q}}{\beta_0^4}, \tag{10.14}$$

where $q = 2L/3\rho_m \gg 1$ and $\beta_0 \ll 1$. The critical angle is therefore

$$\beta_0^{(cr)} \approx \frac{3\sqrt{\pi}}{4}\left(\frac{r_0}{L}\right)^{1/4}\sqrt{q}\, e^{-q/4}. \tag{10.15}$$

It defines in the trap an instability cone in the particle-velocity space at the magnetic-field minimum. In the assumed short-trap model (3.10), the field increases along the magnetic line without limit, and an instability cone exists for all $q \to \infty$, although its width does decrease very rapidly with increasing q. In real traps the field is bounded by some maximum value $\omega_m = \lambda\omega_0$, where λ is the mirror ratio. There therefore exists the known adiabatic particle-departure cone $\beta_0^{(a)} \approx \lambda^{-1/2}$ (at $\lambda \gg 1$), even if μ = const. The instability of the particle motion in a magnetic trap is significant only if $\beta_0^{(cr)} > \beta_0^{(a)}$, or

$$\lambda > \frac{8}{9\pi}\left(\frac{L}{r_0}\right)^{1/2}\frac{e^{q/2}}{q}. \tag{10.16}$$

This estimate can also have another meaning – an upper bound on the amplitude of the stable longitudinal oscillations ($a < a_{cr}$). Actually, the minimum stable β_0^{cr} ($\ll 1$) occurs when the particle reaches a field $\omega_{cr} \approx \omega_0\lambda_{cr} \approx \omega_0(\beta^{cr}_0)^{-2}$. Consequently, $\lambda_{cr} = 1 + a_{cr}^2/L^2$ (for our short-trap model) and is equal to the right-hand side of inequality (10.16).

An estimate of the stability is obtained quite similarly as well for opposing mirrors (in planar geometry). From (8.12) and (7.34) we obtain, with the aid of (9.4),

$$K \approx -\frac{64\sqrt{2}}{3}\,\frac{q^{9/8}e^{-q}}{\beta_0^5}. \tag{10.17}$$

Here $q = r_0\omega_0/2v = r_0/2\rho_m$ and $\beta_0 \ll 1$. The width of the unstable sector is

$$\beta_0^{(cr)} \approx 2q^{9/40}e^{-q/5},$$
$$\lambda_{cr} \approx \frac{e^{0,4q}}{4q^{9/20}} \approx \frac{|s|_{cr}}{r_0} \approx \frac{x_{max}}{r_0} \approx \frac{y_{max}}{r_0}, \tag{10.18}$$

where $x_{max} = y_{max} \approx |s|_{max} \gg r_0$ is the maximum deflection of the particle along the coordinate axes (see Fig. 2a), at which its oscillations are still stable.

The location of the stability boundary on the (x, y) intersection plane of the magnetic field can be obtained in the following manner. Since $\omega_0(r_0) = Cr_0$, where C is a certain constant (see Subsection 5 of Section 3), we have

$$\frac{r_0 v}{\omega_0} = r_0 \rho_m = \frac{v}{C} = L^2 = \text{const}, \quad q = \frac{r_0 \omega_0}{2v} = \frac{r_0^2}{2L^2} \tag{10.19}$$

and the length L is a certain physical parameter of the given trap. Substituting these expressions in the second relation of (10.18) and using the magnetic-line equation $2xy = r_0^2$, we obtain the equation of the stability boundary in the form

$$y_b \approx \frac{1}{2\sqrt{2}} q^{1/20} e^{0.4q} \approx \frac{e^{0.4x_b y_b}}{2\sqrt{2}}$$

or

$$y_b \approx \frac{5}{2} \frac{1 + \ln x_b}{x_b}. \tag{10.20}$$

Here x_b and y_b are measured in units of L. This expression is valid only at $x_b \gg 1$, since the asymptotic form (3.36) of the field was used in (10.18). Curve (10.20) symmetrized relative to the line x = y is shown in Fig. 5 (the lower hatched line) together with one of the magnetic lines it intersects. Formally, curve (10.20) intersects the line x = y at the point $x_b = y_b \approx 2.08$, where $r_0^{min} = 2.9$ and $q^{min} \approx 4.3$. The unstable region is located below the curve.

In a multimirror trap we take explicitly into account an adiabatic loss cone with aperture angle $\beta_0^{(a)} \approx \lambda^{-1/2} \ll 1$. Therefore, the unstable region takes the form of a conical layer adjacent to the loss cone. We characterize this layer by its width, which we assume to be small (see below):

$$\Delta\beta_0 = \beta_0^{cr} - \beta_0^{(a)} \ll \beta_0^{(a)} \ll 1. \tag{10.21}$$

The main parameter of the function G(P) [Eq. (8.10)] is then equal to

$$w \approx -4\sqrt{\lambda}\, \Delta\beta_0. \tag{10.22}$$

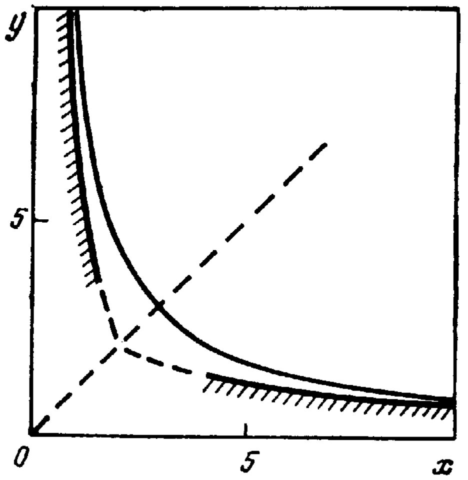

Fig. 5. Motion-stability boundary (lower hatched curve) for planar geometry of opposing mirrors; the instability region is below this curve. Upper curve – one of the magnetic lines. The unit of length is defined by the condition $r_0 \rho_m(r_0) = 1$ (see text).

Since $|w| \ll 1$, it suffices to differentiate in the expression for $G'(p)$ only w:

$$G' \approx -\frac{2\sqrt{2}}{\pi} \frac{L\lambda\omega_0^{3/2}}{\Delta\beta_0 v^2}. \tag{10.23}$$

Using for $(\Delta P)_m$ the relation (8.8) with the parameter q from (8.11), we get

$$K \approx \frac{27\pi^2}{64} \frac{r_0}{L} \frac{\lambda^2}{\Delta\beta_0} q^2 e^{-q}. \tag{10.24}$$

The stable-motion layer therefore is

$$|\Delta\beta_0| \approx 4.2 \frac{r_0}{L} (\lambda q)^2 e^{-q}. \tag{10.25}$$

In a multimirror trap the layer consists of two halves, each of width $|\Delta\beta_0|$: "upper," in which the particles are untrapped ($w > 0$; $\Delta\beta_0 < 0$), and "lower," with trapped particles ($w < 0$; $\Delta\beta_0 > 0$).

A similar layer is produced, of course, in any other real trap, since the field has maxima in the mirrors. A model of such a "real" trap can be one section of a multimirror trap (two mirrors). In this case the upper half of the layer plays no role, since a particle landing there will leave the trap in one pass. In the lower half, however, the particle can stay for an arbitrarily long time (see Section 11), so that the existence of a layer is perfectly observable. Of course, the presence of this layer is of no importance whatever for prolonged confinement of the particles in a trap, since it hardly increases the adiabatic loss cone.

11. Local Diffusion

We consider the character of the motion in the unstable region defined by the condition $|K| > 1$ (see Section 10). We start from the standard mapping (9.3), which describes the motion of the particle at relatively small changes of μ. A characteristic feature of the standard-mapping dynamics is local instability of the motion, i.e., the rapid "scatter" of almost all very close trajectories. This instability must not be confused with the global instability considered in Section 10, which means simply unrestricted motion, i.e., an unbounded variation of p over a sufficiently long time. To investigate the behavior of close standard-mapping trajectories we consider the derivatives [see (9.3)]

$$\frac{d\bar{\theta}}{d\theta} = 1 + K\cos\theta \approx K\cos\theta. \tag{11.1}$$

The last expression is valid at $|K| \gg 1$, i.e., deep in the region of global instability. Exactly the same expression is obtained also for the derivative $(d\bar{p}/dp)$ if it is recognized that the phase θ in the first equation of (9.3) is connected with the preceding value of $\underline{\theta}$ by the relation $\theta = \underline{\theta} + p$. It is clear, therefore, that the average distance between very close trajectories (in the linear approximation) will increase exponentially with time:

$$|\,\delta\theta(t)\,| \approx |\,\delta\theta\,|_0 e^{-ht}, \tag{11.2}$$

where the velocity h of the local instability is (per iteration)

$$h = \langle \ln |\,K\cos\theta\,| \rangle = \ln\frac{|K|}{2}. \tag{11.3}$$

The last expression is obtained by simply averaging over θ and assuming a uniform distribution. This simplifying assumption is actually well satisfied at sufficiently large $|K|$ (see [8]). At smaller K, even in the region of global instability, i.e., at $|K| > 1$, considerable regions of stable motion, i.e., of bounded quasiperiodic p oscillations, are preserved on the standard-mapping cylinder (Fig. 6). The

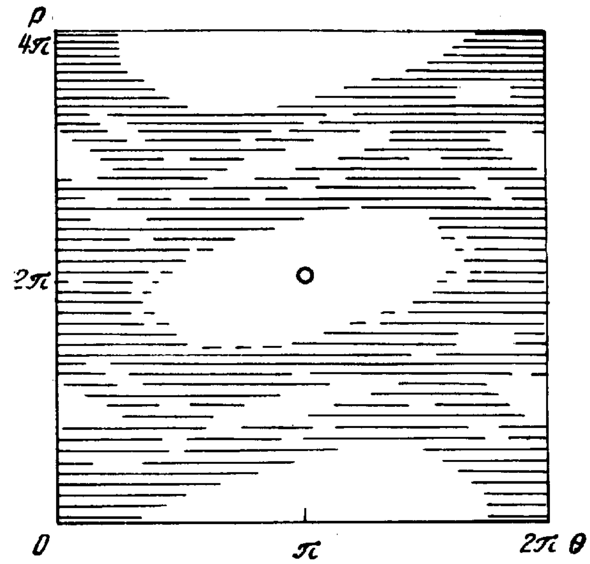

Fig. 6. Section of developed phase cylinder of standard mapping (9.3) at K = 1.13 (according to the data of [8]). The region of unrestricted motion in p (the stochastic component) is shaded. The circle marks a stable immobile point at the center of one of the integer resonances $p_r = 2\pi$.

largest regions surround stable periodic trajectories of the standard mapping with a period 1 (immobile points): $p_1/2\pi = r$, $\theta_1 = \pi$ (r is an arbitrary integer; K > 0). These points correspond to centers of integer resonances. An elementary analysis of the linear stability of these points (see, e.g., [8]) shows that the stable regions around them are preserved up to K = 4. At larger K there can also exist several other stable regions, but their area is small and we shall neglect them. This question was investigated in greater detail in [8] (at K = 5, for example, the relative area of stable regions is less than 2%). Accordingly, numerical simulation of the standard mapping shows [8] that the last expression in (11.3) for h is correct to within no more than 5% for K > 6.

The quantity h plays a major role in modern theory of dynamic systems and is called metric entropy (see, e.g., [26]) or sometimes KS entropy (the Krylov–Kolmogorov–Sinai entropy) [8]. It turns out that at h > 0, i.e., if local instability evolves exponentially, almost all the trajectories of a dynamic system, more accurately of the ergodic (stochastic) component of the motion, are random [27]. In the case considered, at $K > 1$ the stochastic component coincides with the region of global instability.

A more detailed discussion of the extremely interesting question of the physical meaning of such a dynamic fortuity, i.e., random motion of a deterministic dynamic system, is beyond the scope of this article. We confine ourselves only to brief remarks, referring the interested readers to the original papers [27] (a brief popular discussion of these questions can also be found in [28]).

In modern theory of dynamic systems, randomness of trajectories is associated with maximum complexity of the system. The latter means, roughly speaking, that there exists no (simpler) method of describing a given random trajectory other than specifying the trajectory itself. In other words, the equations of motion are utterly useless for the calculation of the trajectory over a sufficiently long time interval, since the entire complexity of the trajectory is contained in its initial conditions. It can be easily seen that this is directly connected with the exponential local instability of the motion, owing to which the trajectory is determined in the course of time by arbitrarily minute details of the initial conditions. A nontrivial fact here is the rigorous result that almost all the initial conditions of the motion correspond here precisely to random trajectories. The dynamic randomness is thus due in the final analysis to the continuity of the phase space, while the role of the dynamic system (of the equations of motion) reduces only to ensuring local stability of motion, which reveals the microscopic structure of the phase space [28].

It is important, within the scope of the considered problem of particle motion in a magnetic trap, that strong local instability makes it impossible to represent the motion in terms of trajectories and forces the use of a statistical description. The basis of the statistical description is the ergodicity of motion in the entire phase space or in part of it. In the latter case one speaks of the ergodic component of the motion. A sufficient albeit not necessary condition of ergodicity of motion is the local instability described above. The average time that an ergodic trajectory stays in any region of phase space is proportional to the invariant measure of this region. For Hamiltonian (canonical) dynamic system such an invariant (i.e., conserved in the course of motion) measure is known to be the phase volume (the Liouville theorem). This permits a quantitative determination of the probability of a state (more accurately, of a region of states) of the dynamic system as a quantity proportional to the phase volume of this region (the proportionality coefficient depends on the normalization used). This is one of the advantages of the canonical (Hamiltonian) equations of motion or of mappings. For the standard mapping, for example, the probability density is $dw = dpd\theta$.

All other statistical properties of a dynamic system depend substantially on the behavior of the correlations. Consider, for example, the correlations of the phase θ in standard mapping or, more accurately, consider the correlation function

$$C(\tau) = \langle \sin\theta(t) \sin\theta(t+\tau) \rangle, \qquad (11.4)$$

where the averaging is either over t on one almost arbitrary (random) trajectory, or else, since the motion is ergodic, directly over θ. At $h > 0$ all the correlations are damped irreversibly, i.e., $C(\tau) \to 0$ as $\tau \to \infty$, although not necessarily exponentially (see below).

If this damping is fast enough, a simple diffusive description of the motion is possible. Indeed, using the first equation of (9.3), we can write

$$(\Delta p)_t = K \sum_{t'=1}^{t} \sin\theta(t'),$$

where the time t is an integer (the number of the iteration) and $(\Delta p)_t$ is the change of p after t iterations. Neglecting the stable component of the motion (see above), it follows from the ergodicity that $\langle \sin\theta \rangle = 0$, meaning also that

$$\langle (\Delta p)_t \rangle = 0. \qquad (11.5)$$

Let us find $\langle (\Delta p)^2_t \rangle$. We have

$$\langle (\Delta p)^2_t \rangle = K^2 \sum_{t'=1}^{t} \sum_{t''=1}^{t} \langle \sin\theta(t') \sin\theta(t'') \rangle.$$

Recognizing that $\langle \sin^2\theta \rangle = 1/2$, we can represent the last expression as $t \to \infty$ in the form

$$\langle (\Delta p)^2_t \rangle \to tK^2 \left[\frac{1}{2} + 2 \sum_{\tau=1}^{\infty} C(\tau) \right]. \qquad (11.6)$$

If the last sum is finite, we have a simple statistical diffusion with respect to p at a rate

$$D_p = \lim_{t\to\infty} \frac{\langle(\Delta p)_t^2\rangle}{2t} = \frac{K^2}{4} R(K), \tag{11.7}$$

where R(K) is a correlation factor that can depend only on K, the only standard mapping parameter that determines all its dynamic and static properties. As $K \to \infty$, the KS entropy $h \to \infty$ and the correlations vanish even for neighboring values of the phase θ. In this limit we have $R \to 1$, and obtain

$$D_p^\infty = K^2/4. \tag{11.8}$$

Since K is constant for the standard mapping, the diffusion equation for the distribution function f(p, t) takes the simple form

$$\partial f/\partial t = D_p \partial^2 f/\partial p^2. \tag{11.9}$$

Its particular solution corresponding to the initial conditions $f(p, 0) = \delta(p)$ is the Gaussian distribution

$$f(p, t) = \frac{\exp\left(-\frac{p^2}{4D_p t}\right)}{\sqrt{4\pi D_p t}}. \tag{11.10}$$

Numerical simulation confirms well these simple considerations [8].

Note that for validity of any kinetic equation in general and of the simple diffusion equation (11.9) in particular, it is necessary that the diffusion time scale $T_D \sim p^2/D_p$, i.e., the characteristic evolution time of the distribution function f, be much longer than the dynamic scale $T_h \approx 1/h$, i.e., the correlation damping time [29]. This is necessary because D_p is simultaneously also a local (in time) parameter of the diffusion equation, i.e., in the scale of T_D, and asymptotic in the scale of T_h (11.7).* For standard mapping we have

*If sight is lost of this important physical condition, it is easy to arrive at a contradiction (see [30-32] and below).

$$\frac{T_D}{T_h} \sim \left(\frac{p}{K}\right)^2 \Big/ \ln K \sim \left(\frac{p}{K}\right)^2 \gg 1.$$

We now turn from the standard mapping to a mapping of type (8.7), which describes the initial problem more accurately. Since the latter mapping contains the same phase, the correlation properties of the motion remain unchanged, and we can write down right away the rate of diffusion in P:

$$D_P = \frac{(\Delta P)_m^2}{4} R(K) \tag{11.11}$$

with the same correlation factor R(K) (11.7). The last expression is obtained, of course, also from the general relation

$$D_P = D_p \left(\frac{dP}{dp}\right)^2, \tag{11.12}$$

since $K \div G_r'(\Delta P)_m^2$ and $dP/dp = 1/G_r'$. In particular, the rate of diffusion in μ, which is exactly the one we need, is

$$D_\mu = \mu (\Delta P)_m^2 R(K), \tag{11.13}$$

where $(\Delta P)_m$ depends on the type of magnetic trap (see Section 8).

We write finally the diffusion rate in ordinary continuous time (and not in terms of the number of iterations of the mapping). Obviously, it suffices for this purpose to divide the expressions derived above by $T/2 = \pi/\Omega$. For example,

$$D_\mu = \frac{\Omega\mu}{\pi} (\Delta P)_m^2 R(K). \tag{11.14}$$

In contrast to the standard mapping, however, the quantity D no longer suffices to set up a diffusion equation for the distribution function $f(\mu, t)$. The reason is that the Fokker–Planck–Kolmogorov (FPK) equation that describes the diffusion process at small changes of the diffusing quantity ($|\Delta\mu| \ll \mu$ in our case) contains, besides D_μ, also another function

$$U_\mu = \lim_{t\to\infty} \frac{\langle(\Delta\mu)_t\rangle}{t}, \tag{11.15}$$

called "drift." This quantity is sometimes called also "friction," but generally without justification, and can be called more readily the average rate (in terms of μ).

With the aid of the quantities U_μ and D_μ, we can write the FPK equation in the form (see, e.g., [33])

$$\left.\begin{aligned} \frac{\partial f}{\partial t} &= -\frac{\partial Q}{\partial \mu}, \\ Q &= -\frac{\partial}{\partial \mu}(D_\mu f) + U_\mu f, \end{aligned}\right\} \tag{11.16}$$

where Q is the probability flux. In the general case $U_\mu \neq 0$. Consider, for example, the mapping (8.7). As shown in Section 8, it is canonical just in the variables P and θ_0, but not μ and θ_0; i.e., at $|K| \gg 1$ the stochastic trajectory is uniformly distributed just on the P, θ_0 surface. Since $\mu = P^2$, we have $\Delta\mu = 2P\Delta P + (\Delta P)^2$. Hence,

$$U_\mu = \frac{\langle(\Delta\mu)_t\rangle}{t} = \frac{\langle(\Delta P)_t^2\rangle}{t} = 2D_P. \tag{11.17}$$

Comparing this expression with the diffusion rate D_μ (11.13) we arrive at the relation ($R \approx 1$):

$$U_\mu = \frac{1}{2}\frac{dD_\mu}{d\mu}, \tag{11.18}$$

which in fact solves the problem of finding the function U_μ and with it the complete FPK diffusion equation for the mapping (8.7). The question is, however, how accurately does this mapping describe the initial problem of particle motion in a trap? It is undoubtedly correct in first-order perturbation theory in the adiabaticity parameter $k \sim (\Delta P)_m$ (10.1). But $\mu U_\mu \sim D_\mu \sim (\Delta P)_m^2 \sim k^2$; i.e., the velocity U_μ is of second order of smallness. As we shall see later (see Section 13), the mapping (8.7) does not ensure such an accuracy, so that relation (11.18) is not correct.

The general method of finding U_μ will be considered in Section 13, and now we shall show that in the initial diffusion state the rate U_μ plays no role at all, and can be simply neglected. In fact, the change of μ consists of two parts: first, the diffusion proper or the scatter $(\delta\mu)_1 \sim \sqrt{D_\mu t}$ and, second, the average displacement $(\delta\mu)_2 \sim U_\mu t$. Their ratio is [see (11.18)]

$$\frac{(\delta\mu)_1}{(\delta\mu)_2} \sim \frac{\sqrt{D_\mu t}}{U_\mu t} \sim \frac{\mu}{(\delta\mu)_1} \gg 1 \tag{11.19}$$

so long as $(\delta\mu)_1 \ll \mu$, i.e., so long as the diffusion has a local character.

By way of example we consider diffusion in a thin stochastic layer in a multimirror trap. In the expression for the diffusion rate (11.13) (discrete t) we assume for simplicity that $R(K) \approx 1$. And since we have in a narrow layer $\mu \approx \mu_a$ (the value of μ on the adiabatic loss cone), the diffusion coefficient is $D_\mu \approx$ const, and we arrive at the simple diffusion equation (11.9). If the multimirror trap is long enough and the particle flux along the trap can be neglected, the diffusion in the layer leads simply to relaxation of the initial distribution, $f(\mu, 0) \to$ const. To determine the relaxation time, we note that the diffusion flux is zero on both boundaries of the layer, i.e., $\partial f/\partial\mu = 0$. This yields the eigenfunctions of the diffusion equation:

$$\left.\begin{aligned} f_n(\mu, t) &= \exp\left(-\frac{t}{\tau_n}\right)\cos(\pi n \nu), \\ \nu = (\mu - \mu_{cr})/\Delta_\mu; &\quad \tau_n = \Delta_\mu^2/\pi^2 n^2 D_\mu, \end{aligned}\right\} \tag{11.20}$$

where μ_{cr} is one of the boundaries of the layer, and Δ_μ is its total width. The equilibrium distribution corresponds to $n = 0$. The relaxation time is determined by the maximum $\tau_n = \tau_1$. Using the expressions for D_μ and for the layer width ($\Delta\mu/\mu = 4|\Delta\beta_0|/\beta_0^{(a)}$), we obtain for the relaxation time

$$\tau_1 \approx \frac{64}{\pi^2}\left(\frac{\lambda L}{\rho_m}\right)^2 \tag{11.21}$$

by iterating the mapping (8.7), i.e., of the passes of the particle between neighboring mirrors. We note that the next eigenfunction with $n = 2$ in (11.20) relaxes at a rate four times faster.

Let us digress somewhat. At equilibrium ($t \to \infty$, $f \to$ const) we have $\langle(\Delta\mu)^2\rangle$ = const. Since Eq. (11.6) remains valid also in this limit, we get $R(K) \to 0$ as $t \to \infty$. Clearly, this is due to the onset of long-range correlations on reflection of the particle from the layer boundaries. But it does not follow at all that the diffusion coefficient (11.7) in Eq. (11.9) is zero, as is sometimes assumed [30-32]. This would be too formal and straightforward an interpretation of the limit in (11.7). In fact, infinity in this limit is infinity in small, i.e., in a dynamic time scale $T_h \ll T_D$. In other words, the limit as $t \to \infty$ in (11.7) means in fact the strong double inequality $T_h \ll t \ll T_D$.

We now consider one section of a multimirror trap. In this case, the particles are confined only in the lower half of the layer. In the solution of the diffusion equation, the second boundary condition must therefore be $f(\mu_a, t) = 0$, i.e., the condition for absorption (emission) of the particles on the adiabatic cone. It is easily seen that the first eigenfunction of (11.20) satisfies this boundary condition (at $\nu = 1/2$). Therefore, expression (11.21) yields also the lifetime of the particles in the lower half of the layer. It is interesting to note that this time increases like the square of the magnetic field, whereas the layer width decreases exponentially with increasing field (10.25). Note also that the next eigenfunction, which satisfies the absorption condition at $\mu = \mu_a$, corresponds now to n = 3 and is damped nine times faster than the fundamental (n = 1).

12. Dynamic Correlations

Let us examine in greater detail the correlation factor R(K) in the expression for the diffusion rate in the case of standard mapping [see (11.7)]. We assume as before that if $|K| \gg 1$ we can neglect the stable component of the motion. Since the standard mapping is canonical in the variables p and θ, in this case the trajectories will fill uniformly the surface of the phase cylinder. Since the structure of the standard mapping is periodic not only in θ but also in p (with the same period 2π), it suffices in the calculation of the correlations to average over the phase square $2\pi \times 2\pi$ (developed part of the phase cylinder).

Let us find the first few correlations of the function $\sin\theta$ for the standard mapping. The quantity C(1) in (11.4) is obtained directly from the second mapping equation (9.3), and is equal to

$$C(1) = \langle \sin\theta \sin\bar{\theta} \rangle = \langle \sin\theta \sin[\theta + K\sin\theta + p] \rangle = 0 \quad (12.1)$$

upon averaging over p (for fixed θ). To find C(2), we express the succeeding ($\bar{\theta}$) and preceding ($\underline{\theta}$) phases in terms of θ and p in the present step:

$$\bar{\theta} = \theta + K\sin\theta + p, \quad \underline{\theta} = \theta - p.$$

Hence

$$C(2) = \langle \sin\underline{\theta} \sin\bar{\theta} \rangle = \frac{1}{2} \langle \cos(2p + K\sin\theta) \rangle - \frac{1}{2} \langle \cos(2\theta + K\sin\theta) \rangle$$

$$= -\frac{1}{2} \cdot J_2(|K|) \approx \frac{1}{\sqrt{2\pi|K|}} \cos\left(|K| + \frac{15}{8|K|} - \frac{\pi}{4}\right). \qquad (12.2)$$

In the last expression we used an improved asymptotic representation of the Bessel functions of $|K| \gg 1$ [22]. The entire derivation is apparently valid down to $|K| \approx 4$. At smaller $|K|$ there appears an appreciable stable region (see above) and simple averaging over θ and p is not valid.

Somewhat more cumbersome calculations yield for the following three correlations:

$$\left.\begin{aligned} C(3) &= \frac{1}{2}\left[J_3^2(|K|) - J_1^2(|K|)\right] \approx -\frac{4J_1J_2}{|K|} \sim |K|^{-2}, \\ C(4) &\approx \frac{1}{2} J_2^2(|K|) \sim |K|^{-1}. \end{aligned}\right\} \qquad (12.3)$$

The approximate equality means here retention of only the principal term of the expansion in the small parameter $|K|^{-1/2}$. Starting with C(4), the exact expressions contain infinite sums of Bessel functions, so that further progress by this method is impossible. Since, however, the correlations are rapidly damped at $|K| \gg 1$ (see below), the obtained values of $C(\tau)$ already approximate sufficiently well the correlation factor

$$R(K) \approx 1 - 2J_2(|K|) + 2J_2^2(|K|), \qquad (12.4)$$

where we have neglected the contribution of C(3). The decisive quantity here is the second term, which leads to characteristic slowly damped oscillations of the diffusion rate with increasing K. Such combinations were observed in numerical simulation of the standard mapping in [8] and in other papers. In [34] was calculated for the first time the correction (12.4) for the asymptotic diffusion rate $D_p^\infty = K^2/4$. The calculation was carried out by an entirely different method (actually, even by two different methods). In particular, ergodicity of the motion was not assumed. The result of [34] can therefore be regarded also as independent proof of the ergodicity of the standard mapping at $|K| \gg 1$.

The numerical values of the factor R(K), taken from [34], are compared in Fig. 7 with the theoretical relation (12.4). The latter differs from the result of [34] (first paper) in that the correlation C(4) is taken into account, thereby improving somewhat the agreement with the numerical data. This correction was introduced in several papers, including the second paper of [34], and also in [35], by a method close to that described above (and postulating likewise ergodicity of the motion).

Thus, the dependence of the first (short-range) correlations on K is explained quite satisfactorily and simply enough. Much less clear is the time dependence of the correlations. Numerical experiments show that this dependence is far from always the simply exponential

$$C(\tau) \propto \exp(-Ah\tau),$$

as was assumed at one time, even if the KS entropy $h > 0$. Figure 8 shows an example of correlation damping for standard mapping at $K = 7$. It can be seen that the function $C(\tau)$ with even τ can be fairly well fitted with the aid of the function

$$C(\tau) \approx \frac{1}{2} \exp(-\sqrt{\tau}). \tag{12.5}$$

The nature of this correlation damping remains unclear, although similar results were obtained analytically also for other dynamic systems, at any rate, as an upper bound estimate [36]. On the other hand, for similar mappings the damping of the correlations can also differ significantly from (12.5) (see [37]).

The behavior of the correlations becomes quite complicated as $|K| \sim 1$. A major role is assumed here by the boundary between the stochastic and stable regions with very complicated structure (see, e.g., [38]). We have seen in Section 10 that such a boundary is a distinguishing feature of the phase space of a particle in a hole. The diffusion rate falls off steeply near the boundary. This correlated with the dependence of the diffusion rate for the mapping on K as $K \to 1$. According to numerical data [8], the correlation factor in this region is

$$R(K) \propto (|K| - 1)^s, \quad s \approx 2.6. \tag{12.6}$$

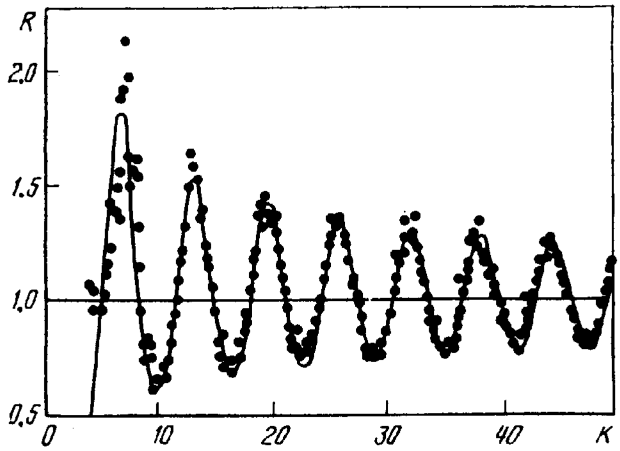

Fig. 7. Relative diffusion rate $R = 4D_p/K^2$ for the standard mapping vs. the mapping parameter K: points – numerical data from [34]; curve – calculated from Eq. (12.4).

By an entirely different method, numerical simulation of the motion in the stochastic layer yielded in [39] $s \approx 4$. Owing to the slow diffusion near the boundary, the trajectory remains stuck in this region for a long time, and this leads, in particular, to a slower decrease of the correlations. According to [39], the qualitative change of the character of the motion near the boundary sets in at $s > 2$. The diffusion to the boundary becomes, in this case, infinite; i.e., the stochastic trajectory does not reach the boundary of the stochastic component. This can be obtained from the following estimate [39]. Let x be the appropriately normalized distance from the boundary of the stochastic component and $d \langle (\Delta x)^2 \rangle /dt \sim D_x(x) \sim x^3$ [in a thin boundary layer we have $K(x) - 1 \propto x$; $K(0) = 1$ (12.6)]. Since the diffusion rate increases rapidly with x, the time required to leave a layer smaller than x will be determined by the time needed to diffuse over a distance of order x, i.e., $\langle (\Delta x)^2 \rangle \sim x^2$. Hence,

$$t > x^{2-s} \tag{12.7}$$

and for $s > 2$ we have $t \to \infty$ as $x \to 0$.

In the last case ($s > 2$) a qualitative change takes place also in the behavior of the correlation function. Indeed, x near the boundary is proportional to the relative phase volume (area) w of the boundary layer, meaning also to the probability of the trajectory landing in this region.

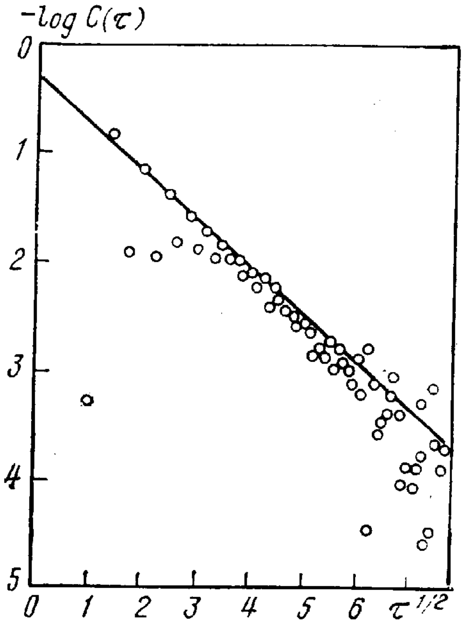

Fig. 8. Damping of the correlations $C(\tau)$ in the standard mapping at $K = 7$: τ – delay (number of iterations); the logarithm is to base 10. For $\tau = 1$ and $\tau \gtrsim 4$ the numerical values of $C(\tau)$ are determined by the fluctuations of averaging of (11.4) for one trajectory over 10^6 iterations. Straight line – the function $C(\tau) = 0.5 \exp(-\sqrt{\tau})$.

When expression (11.4) for the correlation function is averaged over the stochastic component, the fraction of trajectories remaining in the layer is less than $x(\tau) \sim \tau^{-1/(s-2)} \propto w(\tau)$, and determines the asymptotic behavior of the correlation as $\tau \to \infty$:

$$C(\tau) \to F(\tau)/\tau^{q}, \quad q = 1/(s-2). \tag{12.8}$$

This expression is valid only if $s > 2$ ($q > 0$), for otherwise the correlation is no longer determined by the boundary layer. The function $F(\tau)$ depends, generally speaking, on the behavior, in the boundary layer, of the functions $f(\theta, p)$ to which the correlations $C(\tau)$ pertain [e.g., $f = \sin\theta$ in (11.4)]. In particular, $F(\tau)$ can oscillate, so that $\langle F(\tau)\rangle = 0$ (the average over τ).

As already noted (see Section 11), for the standard mapping at $|K| \sim 1$ there exist sizable stability regions so that a power-law correlation decrease of type (12.8) can be expected. Such a behavior was indeed observed in numerical simulation, and it turned out that $q \approx 1$ ($K = 2.1$), corresponding to $s \approx 3$ (12.8). For $f = \cos\theta$, the mean value $\langle F(\tau)\rangle \neq 0$, and the integral of $C(\tau)$ diverges. In addition, the average over the stochastic component is $\langle\cos\theta\rangle \neq 0$, in view of the presence of stability. This, however, does not influence greatly the diffusion in p, since the latter is determined by the correlations of the function $f = \sin\theta$ (11.7), i.e., of the very same function that determines Δp in the mapping (9.3). In this case, $\langle F(\tau)\rangle = \langle\sin\theta\rangle = 0$ for any form of the stability region around the immobile point θ_f at which $\sin\theta_f = 0$. Indeed, the average over the stochastic component is

$$\langle\sin\theta\rangle_{sto} = \langle\sin\theta\rangle_0 - \langle\sin\theta\rangle_{stab},$$

where $\langle\sin\theta\rangle_0 = 0$ is the average over the entire phase square, and $\langle\sin\theta\rangle_{stab}$ is the average over the stable com-component. The latter, however, is also zero, since it is proportional to the average change of the momentum $\langle\Delta p\rangle = 0$ in the stable region. It can be similarly shown that in this case we also have $\langle F(\tau)\rangle = 0$. At larger $|K|$, namely at $K = 2\pi n$ ($n \neq 0$ an integer), there exist stable regions of another type, called "accelerational," with (θ_a) at their center, for which $\sin\theta_a \neq 0$, and for which $\langle\Delta p\rangle \neq 0$ [8]. We then have $\langle\sin\theta\rangle_{sto} \neq 0$; $\langle F(\tau)\rangle \neq 0$, and the diffusion becomes anomalously fast. It is possible that just this explains the appreciable spread of the points of Fig. 7 at the minimum of $R(K)$, which corresponds precisely to $K = 2\pi$. In the succeeding maxima the areas of the accelerational regions decrease rapidly, and with them their contribution to the average diffusion rate.

An anomalously slow decrease of the correlations is possibly contained also in the experimental data, described in [40], on electron confinement in a magnetic trap. Figure 9 shows a typical example of the experimental semilog plot of the flux ($-\dot{N}$) of the electrons leaving the trap versus time. The authors expected an exponential decrease of the flux (meaning also of the number N of the electrons remaining in the trap) with time. Such a dependence was indeed observed for some time ($\approx 2.5\tau_e$), but the subsequent decrease of the flow slows down (circles in Fig. 9). The authors fit the "tail" of the $\dot{N}(t)$ plot using a second exponential with larger τ_e.

Generally speaking, a relation in the form of a sum of several exponentials is not surprising, and is, on the con-

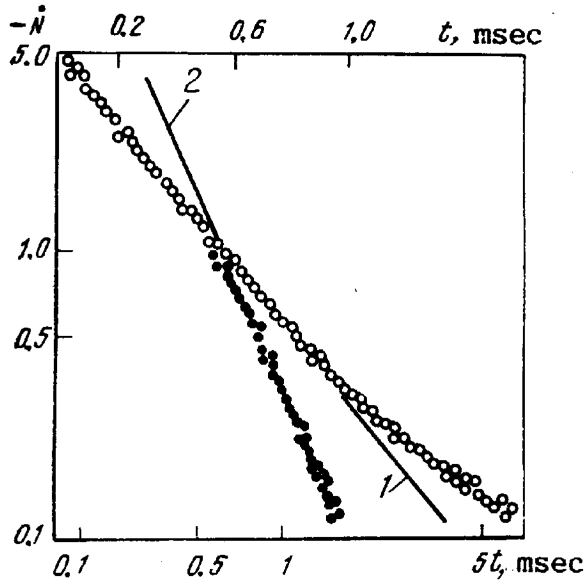

Fig. 9. Time dependence of electron flow from a magnetic trap according to the data of [40]: ($-\dot{N}$) is the flow of outgoing electrons (arbitrary scale). The circles show a semilog $\dot{N}(t)$ dependence (upper scale for t); curve 1 corresponds to the exponential relation $\dot{N} = A\exp(-t/\tau_e)$, $\tau_e \approx 0.36$ msec. The points show the same data (for $t \geq 0.6$ msec) in log–log scale (lower scale for t); curve 2 is the power-law dependence $\dot{N} = Bt^{-\gamma}$; $\gamma \approx 2.3$.

trary, typical of the solution of the linear equation in general and of the diffusion equation in particular (see Section 11). If, however, the data of [40] are plotted in log–log scale (points of Fig. 9), the "tail" of the $\dot{N}(t)$ plot fits even better a power law with exponent $\gamma \approx 2.3$. This is already unusual for a diffusion equation and denotes the absence of (nonsingular) eigenfunctions. The final choice between an exponential and a power-law dependence calls for additional experiments at longer t and in a better vacuum. The latter is needed because electron scattering by the residual gas assumes rapidly an increasing role with time, since the electrons are confined to a boundary layer of ever-decreasing thickness. The volume of this layer is approximately proportional to its thickness and to the number of electrons remaining in the stochastic component, a number that decreases with time like $t^{-\gamma+1} \approx t^{-1.3}$. The same law also governs the decrease of the correlations, i.e., $q \approx 1.3$ (12.8) and $s \approx 2.8$.

Although the exponents s and q given above differ noticeably, the possibility of a universal description of the asymptotic structure of the boundary layer as $x \to 0$, $t \to \infty$ is not excluded. This possibility is based in final analysis on the hierarchic structure of the nonlinear resonances (see [8], Section 4.4). The first successful attempts at a scale-invariant description of several characteristics of the pressure near the stochasticity boundary were undertaken in [23, 41, 42].

13. Global Diffusion

To describe prolonged diffusion (in μ or β_0) of a particle in a magnetic trap we must know the complete FPK equation (11.16) rather than its local variant with $U_\mu = 0$, $D_\mu = \text{const}$. It is necessary, therefore, first of all to find an expression for the average velocity U. As already noted above (see Section 11), direct calculation of U_μ in second-order perturbation theory is difficult. More convenient is the following simple procedure used in many papers (see, e.g., [33]). Let the equilibrium distribution function [$f_s(\mu)$ in our case] be known. For closed Hamiltonian systems it is easily obtained from a microcanonical distribution such as

$$F_e(\mu, J)\, d\mu dJ = \delta(H^0(\mu, J) - E)\, d\mu dJ, \tag{13.1}$$

where E is the given value of the energy. Note that we are using here the unperturbed actions μ and J and, accordingly, an unperturbed Hamiltonian. The perturbation, on the other hand, is assumed small enough to neglect the distortion it produces in the energy surface. In other words, we assume that the perturbation leads only to trajectory distribution over the entire unperturbed energy surface, with ergodic measure (probability density) $F_e(\mu, J)$. When necessary, it is possible (at least in principle) to change to the more precise actions $\mu^{(n)}$, $J^{(n)}$; the Hamiltonian is in general also altered in this case (see Section 5). Note that one more advantage of our choice of the unperturbed system (see Section 2) is the possibility of obtaining an equilibrium distribution function from the unperturbed Hamiltonian.

To obtain an equilibrium distribution in μ only, we integrate (13.1) over J:

$$f_s(\mu)\,d\mu = d\mu \int \delta\left(H^0(\mu,\ J) - E\right)\left(\frac{\partial J}{\partial H^0}\right)_\mu dH^0$$
$$= d\mu \int \frac{\delta\,(H^0 - E)\,dH^0}{\Omega\,(\mu,\ J)} = \frac{d\mu}{\Omega\,(\mu,\ E)}. \qquad (13.2)$$

In the last expression we expressed J in terms of μ and H^0 and assumed $H^0 = E$.

If, for example, $\Omega(\mu) \propto \sqrt{\mu}$, as in the short trap (3.12), the equilibrium density is $df_s \propto d\mu/\sqrt{\mu} \propto d\beta_0$ (at $\beta_0 \ll 1$), i.e., proportional to a planar-angle element rather than a solid-angle one as for a free particle. The reason is that as the angle β_0 increases, the frequency Ω of the longitudinal oscillations increases, their amplitude (given the energy E) decreases, and with it the "longitudinal part" of the phase volume. If, however, the magnetic field is uniform, then, $J \to p_{\|} = v_{\|}$, as well as $\Omega \to v_{\|} = v\cos\beta$ and $df_s \propto d\mu/v_{\|} \propto \sin\beta\, d\beta$, i.e., simply in proportion to the solid-angle element.

On the other hand, the equilibrium function $f_s(\mu)$ can be obtained from the FPK equation by equating the flux Q to zero. Hence,

$$U_\mu = \frac{1}{f_s}\frac{d}{d\mu}(D_\mu f_s) = \frac{dD_\mu}{d\mu} + D_\mu \frac{d\,(\ln f_s)}{d\mu}. \qquad (13.3)$$

This is in fact the general formula for the average velocity U_μ. We note that in its derivation it is quite immaterial whether an equilibrium distribution actually exists or not in this system. An equilibrium distribution may also not be reached for electrons in a trap, owing to their escape to the loss cone or to the fact that the function f_s is not normalizable, i.e., the total measure on the energy surface is infinite (see below). None of this influences in any way the limiting function $f_s(\mu)$. Relation (13.2) is simply an invariant measure of an ergodic Hamiltonian system on the basis of the Liouville theorem.

Returning to (13.3), we see that if f_s = const we get

$$U_\mu = dD_\mu/d\mu. \qquad (13.4)$$

This simple relation between the coefficients of the FPK equation was (implicitly) obtained in [43] from the seemingly rather general detailed balancing principle. Nonetheless, it does not always hold [44, 45]. Nor does it hold for our problem if only $d\Omega/d\mu \neq 0$.

The detailed balancing principle is usually associated with dynamic reversibility of motion. The probabilities of direct and reverse transitions in reversible dynamics are, of course, equal, but they must be calculated in full measure (i.e., with all the dimensions of phase space taken into account) of the ergodic component. In the present problem this is not at all the case. First, we disregard completely the phases that are conjugate to the actions. It is shown in [45] that this is permissible in the absence of stable regions. Second, we have excluded one of the actions (J) and, finally and most importantly, the ergodic component of the motion is bounded for a closed system by the energy surface. As a result of all this the density f_S of the probability (of the invariant measure) for the remaining variable μ, whose change we wish to describe by the FPK diffusion equation, is proportional to $\Omega^{-1}(\mu)$ and not to a constant, and relation (13.4) does not hold, nor, therefore, does the detailed balancing "principle" (for the same variable μ). The latter means simply that the transition probability is not proportional in this case to $d\mu$, but $df_S \propto d\mu/\Omega(\mu)$.

It is clear, therefore, that to use the reversibility of the motion in the form of the detailed balancing principle, the latter must be formulated in terms of adequate variables, which could be called ergodic [45]. In the general case they do not coincide with the unperturbed integrals of motion, as is sometimes assumed. In our problem, for example, the ergodic variable is a quantity (we designate it by Γ) proportional to the equilibrium distribution function, i.e., to the probability on the ergodic component. The variable Γ can be defined, for example, via the relation

$$d\Gamma = d\mu/\Omega(\mu). \tag{13.5}$$

The probabilities of the direct and reverse transitions between any two regions with identical $d\Gamma$ will then be equal (the detailed-balancing principle), $f_S(\Gamma)$ = const and $U_\Gamma = dD_\Gamma/d\Gamma$ (13.3). In the last equation we can now return to the variable μ with the aid of the equations

$$\left.\begin{aligned} D_\Gamma &= D_\mu (d\Gamma/d\mu)^2, \\ U_\Gamma &= U_\mu \frac{d\Gamma}{d\mu} + D_\mu \frac{d^2\Gamma}{d\mu^2} = \frac{U_\mu}{\Omega} - \frac{D_\mu}{\Omega^2}\,\frac{d\Omega}{d\mu}. \end{aligned}\right\} \tag{13.6}$$

In the calculation of U_Γ we must expand $\Delta\Gamma$ in terms of $\Delta\mu$ up to second order, inclusive. Hence,

$$U_\mu = \Omega \frac{dD_\Gamma}{d\Gamma} + \frac{D_\mu}{\Omega} \frac{d\Omega}{d\mu} = \frac{dD_\mu}{d\mu} - \frac{D_\mu}{\Omega} \frac{d\Omega}{d\mu}. \qquad (13.7)$$

This relation can, of course, be obtained also directly from (13.3).

Besides the dynamic variables, we can also transform the time. In particular, a new time τ can be chosen such that the new frequency $\Omega(\mu) = d\psi/d\tau = \text{const}$, for example, $d\tau = \Omega(\mu)dt$. According to (13.5), μ becomes, in this case, an ergodic variable, and the coefficients of the FPK equation for the function $f(\mu, \tau)$ satisfy the relation (13.4). This is precisely a property possessed by the discrete mapping time, which is measured in units of $T/2 = \pi/\Omega$. The same result can also be obtained in a more formal manner, by using (13.7). Indeed, putting

$$D_\mu = \frac{\Omega}{\pi} D_\mu^{(0)}, \quad U_\mu = \frac{\Omega}{\pi} U_\mu^{(0)}, \qquad (13.8)$$

where the quantities D_μ and U_μ pertain to the continuous time, and $D_\mu^{(0)}$ and $U_\mu^{(0)}$ to the discrete one, we get from (13.7)

$$U_\mu = \frac{\Omega}{\pi} \frac{dD_\mu^{(0)}}{d\mu} + \frac{D_\mu^{(0)}}{\pi} \frac{d\Omega}{d\mu} - \frac{D_\mu}{\Omega} \frac{d\Omega}{d\mu} = \frac{\Omega}{\pi} \frac{dD_\mu^{(0)}}{d\mu}$$

or

$$U_\mu^{(0)} = dD_\mu^{(0)}/d\mu. \qquad (13.9)$$

We note that (13.9) differs from the relation (11.18) obtained directly from the mapping (8.7). This mapping is thus valid only in first order in the small parameter k. It hence follows, in particular, that it is not suitable for numerical simulation of prolonged (global) diffusion ($\delta\mu \gtrsim \mu$), when the effect of the average velocity U_μ becomes significant (see Section 11).

The problem of an accurate diffusive description for the analogous problem (the Fermi stochastic acceleration model) was discussed from a variety of viewpoints in [46-48] (see also [9]).

Since (13.9) is known to simplify the FPK equation, it is expedient to solve the problem in discrete time. From (11.16) we get

$$\frac{\partial f}{\partial t} = \frac{\partial}{\partial \mu} \mu \frac{\partial f}{\partial \mu}, \tag{13.10}$$

where we have dropped the zero subscript of D_μ, with the latter given by (11.13).

By way of example we consider a magnetic trap in which the resonant $\Delta\mu$ and the stability parameter K can be estimated in the short-trap approximation (10.14). If $\beta_0^{(cr)} \gg \beta_0^{(a)} \approx \lambda^{-1/2} \ll 1$, we can neglect in first-order approximation the oscillations of the diffusion rates as functions of K and put $R(K) \approx 1$ in (11.13). Introducing a new time (which is likewise discrete)

$$s = t(\Delta P)_m^2 \lambda / 4\mu_0, \tag{13.11}$$

where $\mu_0 = v^2/2\omega_0$, and a new variable $x = \beta_0/\beta_0^{(a)}$, we write the equation for the eigenfunctions in the form [see (13.10)]

$$\frac{d}{dx}\left(x \frac{df_\varkappa}{dx}\right) + \varkappa^2 x f_\varkappa = 0 \tag{13.12}$$

with boundary conditions

$$f_\varkappa(1) = 0, \quad \left.\frac{df}{dx}\right|_{x=x_{cr}} = 0. \tag{13.13}$$

The first condition corresponds to the particles going off to the adiabatic cone $\beta_0 = \beta_0^{(cr)}$, and the second to the absense of a particle flux on the stochasticity boundary $\beta_0 = \beta_0^{(cr)}$ (10.15) ($x_{cr} = \beta_0^{cr}/\beta_0^{(a)}$). The smallest eigenvalue $\varkappa^2 \neq 0$ determines the lifetime of the particles in the trap under conditions when the motion is stochastic:

$$f(\mu, s) \to \exp(-\varkappa^2 s). \tag{13.14}$$

The solution of (13.12) is expressed in terms of Bessel functions (see, e.g., [22])

$$f_\varkappa(x) = CJ_0(\varkappa x) + N_0(\varkappa x). \tag{13.15}$$

The eigenvalue and the constant C are determined from the boundary conditions (13.13)

$$\left.\begin{aligned} CJ_0(\varkappa) + N_0(\varkappa) &= 0, \\ CJ_1(\varkappa x_{cr}) + N_1(\varkappa x_{cr}) &= 0. \end{aligned}\right\} \tag{13.16}$$

At $x_{cr} \gg 1$, the approximate solution of these equations can be written in explicit form by using the asymptotic expressions

$$\left.\begin{aligned} N_0(z) &\approx \frac{2}{\pi} J_0(z) \ln\left(\frac{\gamma z}{2}\right), \\ N_1(z) &\approx -\frac{2}{\pi z} + \frac{z}{\pi} \ln\left(\frac{\gamma z}{2}\right), \\ J_1(z) &\approx z/2 \end{aligned}\right\} \quad (13.17)$$

at $z \ll 1$; $\gamma = 1.78\ldots$ is the Euler constant. The small value of $\varkappa$ for $x_{cr} \gg 1$ follows directly from the fact that the first eigenfunction (13.15) must be positive everywhere. Therefore, $\varkappa x_{cr} \lesssim 1$ and $\varkappa \lesssim 1/x_{cr}$. Substituting (13.17) in (13.16), we get from the first of these equations

$$C = -\frac{2}{\pi} \ln\left(\frac{\gamma \varkappa}{2}\right)$$

and, from the second,

$$\frac{1}{\varkappa^2} = \frac{x_{cr}^2}{2} \ln x_{cr}. \quad (13.18)$$

Gathering together all the relations, we obtain for the characteristic lifetime of the particle (the number of passes through the trap):

$$\tau_e \approx \frac{\mu_{cr}}{(\Delta P)_m^2} \ln(\lambda\beta_{cr}^2) \approx \frac{16}{9\pi}\left(\frac{L}{r_0}\right)^{3/2} \frac{\exp(3q/2)}{q} \ln(\lambda\beta_{cr}^2), \quad (13.19)$$

where $\beta_{cr} \equiv \beta_0^{(cr)}$. The last expression was written using (8.8) and (10.15), i.e., for a short trap with addition of a narrow loss cone ($\lambda \gg 1$). With increasing mirror ratio λ, the lifetime of the particles increases slowly, just as, incidentally, in multiple scattering by a gas [1]. A similar relation is obtained also (in planar geometry) for field-reversed mirrors, likewise with addition of a finite loss cone.

The lifetimes of the particles in a trap can be estimated also by a different procedure, used in Budker's first paper [1] on adiabatic traps for multiple scattering of particles. Consider stationary diffusion of particles having sources inside the trap. From (13.10) we have

$$\frac{d}{d\mu} \mu \frac{df_q}{d\mu} + q(\mu) = 0, \quad (13.20)$$

where $q(\mu)$ is the source density, which we choose in the form

$$q(\mu) = \mu^{\alpha} \tag{13.21}$$

with a constant $\alpha > -1$. The particle flux in a trap is

$$Q(\mu) = D_{\mu} \frac{df_q}{d\mu} = -\int_{\mu_{cr}}^{\mu} q d\mu = \frac{\mu_{cr}^{\alpha+1} - \mu^{\alpha+1}}{\alpha+1}, \tag{13.22}$$

where $\mu_{cr} = \mu_0 x_{cr}^2/\lambda$ corresponds to the stochasticity limit and $Q(\mu_{cr}) = 0$. The total stationary particle flux from the trap is

$$Q_0 = Q(\mu_a) \approx \frac{\mu_{cr}^{\alpha+1}}{\alpha+1} = \frac{\mu_{cr} q(\mu_{cr})}{\alpha+1};$$

$\mu_a = \mu_0/\lambda$ is the value of μ on the adiabatic loss cone, and we assume that $\mu_a \ll \mu_{cr}$. On the other hand, from (13.22) we obtain the particle density in the trap

$$f_q(\mu) = \int_{\mu_a}^{\mu} \frac{Q d\mu}{D_{\mu}} \approx \frac{1}{(\Delta P)_m^2} \frac{\mu_{cr}^{\alpha+1}}{\alpha+1} \ln \frac{\mu}{\mu_a}, \tag{13.23}$$

by putting, as before, $D_{\mu} \approx \mu(\Delta P)_m^2$, $f(\mu_a) = 0$.

The total number of the particles in the trap in the stationary regime is

$$N = \int_{\mu_a}^{\mu_{cr}} f_q(\mu) d\mu \approx \frac{\mu_{cr}^{\alpha+2}}{(\alpha+1)(\Delta P)_m^2} \ln \frac{\mu_{cr}}{\mu_a}. \tag{13.24}$$

We can now introduce the average lifetime of the particle

$$\langle\tau\rangle \equiv \frac{N}{Q_0} \approx \frac{\mu_{cr}}{(\Delta P)_m^2} \ln \frac{\mu_{cr}}{\mu_a}, \tag{13.25}$$

which does not depend on the arbitrary parameter α (at $\alpha > -1$) and agrees exactly with τ_e, (13.19), since

$$\mu_{cr}/\mu_a = (\beta_{cr}/\beta_0^{(a)})^2 = \lambda\beta_{cr}^2.$$

This means that in the approximation considered ($\beta_{cr} \gg \beta_0^{(a)}$) the average particle lifetime $\langle\tau\rangle$ is determined for a large class of source distributions by the first diffusive mode (eigenfunction). Indeed, comparing expressions (13.23) and (13.15) [with allowance for (13.17)] we see that in the approximation considered the two distribution functions coincide:

$$f_\varkappa \propto f_q \propto \ln \frac{\mu}{\mu_a}.$$

For $\alpha < -2$ we can obtain similarly

$$\langle\tau\rangle \approx \frac{\mu_{cr}}{|1+\alpha|\,(\Delta P)_m^2}. \qquad (13.26)$$

The average lifetime now decreases with increasing $|\alpha|$, owing to the concentration of the sources on the adiabatic loss cone. A major role is assumed in this case by diffusion modes with constantly increasing numbers, since the stationary distribution function

$$f_q(\mu) \propto 1 - (\mu_a/\mu)^{|1+\alpha|}$$

has at $\mu \to \mu_a$ an abrupt break whose slope increases with $|\alpha|$.

In the relations obtained above for τ_e and $\langle\tau\rangle$, the particle lifetime unit is the number of passes through the trap or the number of reflections (from the magnetic mirrors). To transform to ordinary (continuous) time, the expressions obtained must be multiplied by the average half-period of the longitudinal oscillations of the particle

$$\left\langle \frac{T}{2} \right\rangle = \left\langle \frac{\pi}{\Omega(\mu)} \right\rangle = \pi \int \frac{f(\mu)\, d\mu}{\Omega(\mu)}. \qquad (13.27)$$

Here $f(\mu)$ is a normalized distribution function corresponding to the given motion regime, say a stationary regime with courses, or the first diffusion mode.

Near the adiabatic loss cone ($\mu = \mu_a$) we have

$$\frac{1}{\Omega} \propto \ln\left(16 \frac{\mu_a}{|\mu - \mu_a|}\right)$$

[see (3.26)]. If $f(\mu) \propto \mu - \mu_a$, this region makes no significant contribution to the integral (13.27). We can therefore use $\Omega(\mu)$ without allowance for the loss cone. Let, for example,

$$\Omega(\mu) = \Omega_{cr}\sqrt{\frac{\mu}{\mu_{cr}}}, \tag{13.28}$$

where Ω_{cr} is the frequency on the stochasticity boundary [see (3.12)]. Furthermore, let

$$f(\mu) = \frac{\ln(\mu/\mu_a)}{\mu_{cr}\ln(\mu_{cr}/\mu_a)} \tag{13.29}$$

be the diffusion distribution function (13.23) normalized to unity ($\mu_{cr} \gg \mu_a$). The integral (13.27) then yields

$$\left\langle \frac{T}{2} \right\rangle \approx \frac{2\pi}{\Omega_{cr}} = 2\,\frac{T_{cr}}{2};$$

i.e., the average period of the longitudinal oscillations of the particle is double the minimum value on the stochasticity boundary.

Now let

$$\Omega(\mu) = \Omega_{cr}\mu/\mu_{cr}$$

[field-reversed mirrors; see (3.37) and (3.38)], and let the distribution function be the same (13.29). In this case,

$$\left\langle \frac{T}{2} \right\rangle \approx \frac{T_{cr}}{4}\ln(\lambda\beta_{cr}^2) \tag{13.30}$$

and the average oscillation period diverges logarithmically as $\lambda \to \infty$. Note that the ergodic measure (13.2) also diverges here and no equilibrium is reached (at $\lambda = \infty$, i.e., in the absence of a loss cone). More accurately speaking, the relaxation is, in this case, nonexponential, and the probability density (the distribution function) tends everywhere to zero. A simple example of such a relaxation is longitudinal diffusion in infinite space. In the one-dimensional case $f(x, t) \propto t^{-1/2} \to 0$ as $t \to \infty$.

14. Cohen's Mapping

We have considered all the trap examples described in Section 3, except two: a long trap and opposing mirrors in cylindrical geometry. Particle motion in these last traps does not reduce to standard mapping. We consider below this new situation with cylindrical field-reversed mirrors as the example. Particle dynamics in a long trap was investigated in [49] (see also [4]).

A characteristic feature of particle dynamics in cylindrical field-reversed mirrors is the asymmetry, due to the different asymptotic forms of the effective potential as $s \to \pm\infty$ (3.42), of two half-periods of the longitudinal oscillations of the particle. This leads to a difference in time between successive transits through the field minimum, and hence to two different functions G(P) that characterize the successive changes of the Larmor phase at the field minimum. Comparing (3.36) with (3.42) and using (8.12), we can write

$$G_+(P) = \frac{1}{3}\,\frac{l_0 v^3}{\omega_0 P^4}, \quad G_- = \frac{2}{3}\,\frac{l_0 v^3}{\omega_0 P^4}, \tag{14.1}$$

where $G_\pm$ describes the change of the Larmor phase for motion in the regions of positive and negative s, respectively. These changes differ thus by a factor of two (at the same value of P). There is actually also another difference, because we need the Larmor phase not exactly at the field minimum, but at the point $s = s_1 \approx -\ell_0/19$ (7.38). At longitudinal-oscillation frequencies $a \gg \ell_0$, however, this effect can be neglected (see the end of this section).

Since the resonance $\Delta\mu$ is described in this case, as in the others, by one and the same expression (7.37) during both half-cycles of the longitudinal oscillations, we obtain, in lieu of (8.7), the two-step mapping

$$\bar{P} = P + (\Delta P)_m \sin\theta_1, \quad \bar{\theta}_1 = \theta_1 + G_\pm(\bar{P}). \tag{14.2}$$

Here θ_1 includes in the general case the additional phase shifts (7.37), and the functions $G_\pm$ alternate in succession. Therefore, (14.2) comprises in fact a system of four difference equations and describes the change of the dynamic variables during the entire period of the longitudinal oscillations of the particle. The functions $G_\pm(P)$ can be linearized in P, and the result is a new two-step mapping that is similar but does not fully conform to the standard mapping. It can be expressed in the form

$$\bar{p} = p + K_0 \sin\theta; \quad \bar{\theta} = \theta + \gamma_\pm \bar{p} + \alpha_\pm. \tag{14.3}$$

Here $\gamma_\pm$ are two different constants defined by the condition

$$\frac{G'_{\pm}(P_r)}{\gamma_{\pm}} = G'_0(P_r). \qquad (14.4)$$

The resonant value P_r is now obtained from the relation

$$G_+(P_r) + G_-(P_r) = 2\pi r, \qquad (14.5)$$

where r is an integer and the additional phase shifts are equal to

$$\left.\begin{aligned} \alpha_+ &= G_+(P_r) \mod 2\pi, \\ \alpha_- &= G_-(P_r) \mod 2\pi, \\ \alpha_+ + \alpha_- &= 0 \mod 2\pi. \end{aligned}\right\} \qquad (14.6)$$

The parameter (no longer unique) of the mapping (14.3) is

$$K_0 = (\Delta P)_m G'_0(P_r) \qquad (14.7)$$

and the variable is

$$p = G'_0(P_r)(P - P_r). \qquad (14.8)$$

In this form (with $\alpha_{\pm} = 0$) the two-step mapping (14.3) was first obtained by Cohen [49] in an analysis of particle motion in a long magnetic trap. Although this trap is symmetric about the z = 0 plane (see Section 3), the cause of the asymmetry of the mapping is that the principal singularities of the magnetic field are shifted from the trap center to the inner edge of the mirrors (see Section 7). Two steps of the mapping correspond in this case to transit of the particle between the singularities and its return to each of them after reflection from the corresponding mirror. Note that if such a trap were also intrinsically asymmetric (e.g., had different mirrors), the mapping would consist of three steps (six difference equations).

In our problem of opposing mirrors we have

$$\left.\begin{aligned} &G_0(P) = l_0 v^3 / 3\omega_0 P^4, \\ &\gamma_+ = 1, \quad \gamma_- = 2, \\ &\alpha_+ = 2\pi\gamma_+/\gamma, \quad \alpha_- = 2\pi\gamma_-/\gamma, \quad \gamma = \gamma_+ + \gamma_- \end{aligned}\right\} \qquad (14.9)$$

and $(\Delta P)_m$ is given by (7.37).

Proceeding to the analysis of the dynamics of the Cohen mapping (14.3), we consider first, following [49], the simpler case when $\gamma_+ \ll \gamma_-$. This situation is typical of long traps. In this case, the mapping (14.3) can lead approximately to a one-step mapping over the total period of the perturbation. To this end, we express the variables $\bar{p}$ and $\bar{\theta}$ in terms of $\underline{p}$ and $\underline{\theta}$, which precede the quantities p and θ by one complete period of the mapping (14.3). Writing the four difference equations in explicit form*

$$\left.\begin{aligned} \bar{p} &= p + K_0 \sin\theta, \quad \bar{\theta} = \theta + \gamma_- \bar{p}, \\ p &= \underline{p} + K_0 \sin\underline{\theta}, \quad \theta = \underline{\theta} + \gamma_+ p, \end{aligned}\right\} \tag{14.10}$$

we get

$$\bar{p} = p + K_0 [\sin\theta + \sin(\theta + \gamma_+ p + \gamma_+ K_0 \sin\theta)],$$
$$\bar{\theta} = \theta - \gamma_+ K_0 \sin\theta + \bar{p}(\gamma_+ + \gamma_-).$$

In the last equation we neglect the term $\sim K_0\gamma_+$, and in the first we rewrite the expression in the square brackets in the form

$$2\cos\left(\frac{p\gamma_+}{2} + \frac{\gamma_+ K_0}{2}\sin\theta\right)\cos\left(\theta + \frac{\gamma_+}{2}(p + K_0\sin\theta)\right) \approx 2\cos\left(\frac{p\gamma_+}{2}\right)\cos\theta .$$

The reason for retaining the term $(p\gamma_+/2)$ in the first cosine but dropping it from the second is the following. In the first case the quantity $p\gamma_+$ with large enough p can greatly increase the perturbation K_0, whereas in the second it leads only to an insignificant phase shift. Of importance in the dynamics of the phase is not the absolute value of the term $(p\gamma_+/2)$, but its change after one iteration of the mapping. This change is of the order of $K_0\gamma_+$, i.e., the same as of the remaining discarded terms. All these terms lead to the appearance of a second harmonic $\sim K_0\gamma_+ \sin 2\theta$ of the perturbation. For the standard mapping this harmonic appears in second-order perturbation theory, with relative amplitude $\approx K/16$ (see [8, Section 5.1]). This yields a roughly approximate condition for the validity of the considered approximation, viz., $\gamma_+ \lesssim 1/16$ (for $\gamma_- \sim 1$).

*If the phases $\alpha_\pm$ are proportional to $\gamma_\pm$, they can be eliminated by the momentum shift $p \to p + 2\pi/\gamma$.

Introducing the new variable

$$J = (\gamma_+ + \gamma_-)\, p = \gamma p, \tag{14.11}$$

we get the mapping

$$\bar{J} \approx J + K_1 \cos\theta, \quad \bar{\theta} \approx \theta + \bar{J}, \tag{14.12}$$

which is outwardly similar to the standard mapping [cf. (9.3)].

An essential property of the mapping (14.12) is, however, that its parameter

$$K_1 = 2\gamma K_0 \cos\left(\frac{\gamma_+}{\gamma}\,\frac{J}{2}\right) \tag{14.13}$$

depends now on the dynamic variable J. This leads to a qualitative change of the structure of the stochastic component, namely, it is all cut up into isolated strips by narrow gaps with stable motion. It follows from (14.13) that the gaps are located in the vicinity of $J = J_n$, where

$$\cos(J_n \gamma_+/2\gamma) = 0, \tag{14.14}$$

whence

$$J_n = \frac{\pi\gamma}{\gamma_+}(1 + 2n), \tag{14.15}$$

with n an integer. The width of the gap can be estimated from the condition that $|K_1| \approx 1$ on the gap boundary. Expanding the cosine in (14.13) at $J = J_n$ we obtain for the total width of the gap

$$\Delta J \approx \frac{2}{K_0\gamma_+} = \frac{2}{\pi K_m}\,|J_{n+1} - J_n|, \tag{14.16}$$

where $K_m = 2\gamma K_0$ is the maximum value of $|K_1|$. At $K_m \gg 1$ the relative gap width becomes small.

Of greater interest is the question of the size of the critical perturbation $|K_0| = K_g$, at which the gaps vanish and the isolated stochastic components of the motion merge into one. In [49] was proposed the criterion

$$K_g^2 \gamma_+ \gamma_- \sim 1 \tag{14.17}$$

based on the following simple consideration. At $|K_0| \sim K_g$ a gap of width $\Delta J \sim 1/K_g\gamma_+$ or $\Delta p \sim 1/K_g\gamma\gamma_+$ is overlapped on one step of the mapping (14.10), i.e., $(\Delta p)_g \sim K_g$; hence the estimate (14.17). This estimate, as well as the remaining simpler properties of the Cohen mapping, are well corroborated by his numerical simulation [49], as well as by our numerical data.

From the standpoint of the criterion for resonance overlap (see Section 10) the estimate (14.17) raises a definite problem. The overlap of the resonances means, in this case, that the gap width ΔJ (14.16) becomes smaller than the distance between the resonances ($\delta J = 2\pi$), or that the condition $|K_1| \gtrsim 1$ holds for all resonances inside a gap. From this we have $K_g \gamma_+ \sim 1$, which is larger than (14.17) by a factor $\gamma/\gamma_+ (\gg 1)$.

The reason why the resonance-overlap criterion leads in this case to a grossly incorrect result is apparently the following. In the vicinity of the gap the amplitudes of the resonances increase quite rapidly (linearly) with increasing distance from the gap center. Under this condition, an important role is assumed by one curious manifestation of interaction between resonances – their mutual repulsion. The physical meaning of the effect and an estimate of its magnitude can be easily followed by means of a simple example.

Consider the motion in the vicinity of one resonance in the pendulum approximation [see the Hamiltonian (10.3)]. Let $p_0 \gg \sqrt{K}$ be the unpertured (at $K = 0$) position of the second resonance, which we consider to be weak enough to neglect its influence on the first resonance. Yet the first resonance distorts the second in such a way that its unperturbed straight phase line $p = p_0 = \text{const}$ turns into the curve $p(\theta) = p_0 + \delta p(\theta)$. The distortion of the resonant trajectory $\delta p(\theta)$ is easily obtained in first order in K from the equation

$$\left.\begin{aligned} &p^2(\theta)/2 + K\cos\theta = p_0^2/2, \\ &\delta p(\theta) = p(\theta) - p_0 \approx -\frac{K}{p_0}\cos\theta. \end{aligned}\right\} \tag{14.18}$$

Since the maximum of the first-resonance separatrix is at $\theta = \pi$ [$K > 0$, see (10.4)], where $\delta p(\pi) > 0$, the resonance is repelled by an amount $\delta p(\pi) \approx K/p_0$.

Returning to the gap problem, we rewrite the last estimate in the form

$$\delta J_{kl} \sim F_l/(J_k - J_l), \tag{14.19}$$

where $J_k \sim k$ is the distance (in terms of J) from the center of the gap to the displaced resonance number k, while J_ℓ is the same for the displacing resonance; F_ℓ is the amplitude of the displacing resonance in a scale such that the overlap of the resonances correspond to $F \sim 1$, i.e., $F \sim |K_1|$. But the amplitude of the resonances near the gap is $F_\ell \sim F_0 \ell$, where F_0 is the amplitude of the weakest resonance near the gap center. According to (14.19), the displacement in each pair is then $\delta J_{k\ell} \sim F_0$. Since the motion is stochastic, the phases of the resonances are random and the total displacement of each of the resonances for a given value of the phase θ is $\delta J_k \sim F_0\sqrt{N}$, where N is the total number of resonances in the layer. The total displacement of the gap edge is δJ $\delta J_k\sqrt{N} \sim F_0 N$. But $F_0 N \sim K_m$ are the amplitudes of the resonances at the center of the layer. From the condition $\delta J \sim \Delta J$ [ΔJ is the gap width (14.16)] we obtain the estimate (14.17). Although the arguments presented above are excessively sketchy, it is quite likely that the resonance repulsion plays a major role in the problem considered.

This beautiful phenomenon was first considered qualitatively in [50] and later accurately calculated by the same author and others (see [41]). It should be noted that the statement made by the author in his title, that "primary (i.e., first-order-approximation) resonances do not overlap," has no bearing on this effect. This statement is, of course, correct in the sense that rather strong higher-approximation resonances do set in and ensure overlap prior (i.e., in weaker perturbation) to the tangency of the separatrices of the first-approximation resonances (see Section 10 and [8]). This, incidentally, is just the reason why the repulsion effect is negligible, for example, for two resonances of equal width. In fact, Eq. (14.18) leads, in this case, to the estimate

$$\left(\frac{2\delta p}{p_0}\right)_{cr} \approx \frac{2K_{cr}}{p_0^2} \approx 0.055,$$

where the numerical values of K_{cr} for the two resonances were taken from Section 4.1 of [8]. The same is confirmed by the results of [41], according to which $2K_{cr}/p_0^2 = 0.0612$. But the repulsion becomes substantial when the resonance widths are unequal. Thus, at a resonance-width ratio 3 the repulsion offsets completely the higher-approximation effects, and the critical value of the perturbation agrees with the result obtained by the primary-resonance overlap criterion [41]. For the maximum ratio 5 considered in that paper, the critical perturbation exceeds the last value by an approximate factor 1.7.

Note that in standard mapping there are no integer and half-integer resonances at all, owing to the symmetry of the mapping. The repulsion, however, shifts the resonances of higher (particularly third) order, lowering somewhat K_{cr} in this case. From a comparison of the analytic estimates of [8], where repulsion was not taken into account, with the actual value of K_{cr} it follows that the repulsion effect is, in this case, in the 10% range.

We now turn to particular motion in a trap with field-reversed mirrors. Since $\gamma_+/\gamma_- = 1/2$ in this case, the approximation considered above is not valid. However, at such a "round" ratio γ_+/γ_- the problem can be differently approached. We consider first the atandard mapping (9.3). The action of the perturbation can be regarded in this case as a periodic sequence of short "bumps" (Fig. 10a). This convenient method was used many times in the analysis of mappings (see, e.g., [8, 9]). In this approach the difference equations can be replaced by the exactly equivalent differential ones

$$dp/dt = K \sin\theta\delta_1(t), \quad d\theta/dt = p \tag{14.20}$$

with the Hamiltonian

$$H(p, \theta, t) = \frac{p^2}{2} + K\cos\theta\delta_1(t) = \frac{p^2}{2} + \frac{K}{2}\left\{\sum_{r=-\infty}^{\infty} \exp\left[i(\theta - 2\pi r t)\right] + \text{c.c.}\right\} \tag{14.21}$$

The time is measured here in numbers of mapping iterations; the fundamental frequency of the perturbation is accordingly 2π; $\delta_1(t)$ is a δ function with period 1 (Fig. 10a) and with a Fourier expansion that leads to the last expression of (14.21). We already know (see Section 9) that the standard mapping has a homogeneous system of resonances $(p_r/2\pi) = r$ (Fig. 10a). The overlap of these resonances (with account of the higher approximations) determines in fact the critical $K_{cr} \approx 1$.

Now consider the Cohen mapping (14.10) for $\gamma_-/\gamma_+ = 2$. In this case the perturbation takes the form of a perio-

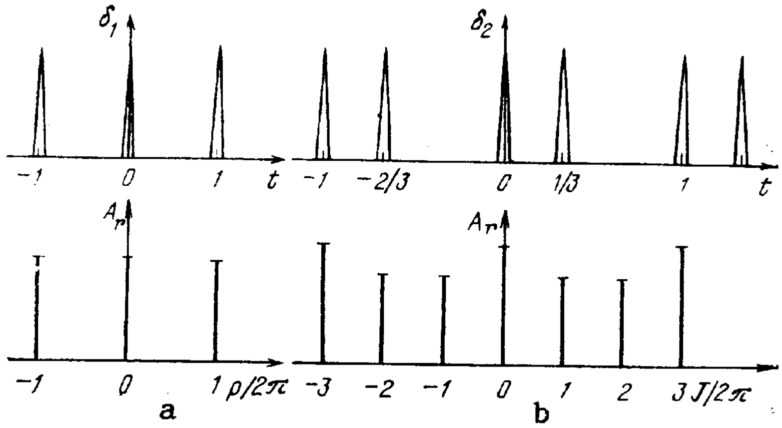

Fig. 10. The perturbation $\delta(t)$ and its spectrum A_r: a) for the standard mapping (9.3) – homogeneous system of resonances $r = p/2\pi$; b) for the Cohen mapping (14.10) for a particle in a magnetic trap with field-reversed mirrors. $\gamma_-/\gamma_+ = 2$, $r = J/2\pi$.

dic sequence of pairs of "bumps," and the four equations of (14.10) can be replaced anew by a pair of differential equations of form (14.20). If the unit of time is taken to be the total period of the perturbation, Eqs. (14.10) now become

$$dp/dt = K_0 \sin\theta\delta_2(t), \quad d\theta/dt = 3p, \tag{14.22}$$

since the phase changes after one full period by $(\gamma_+/\gamma_-)p = 3p$, and the function $\delta_2(t)$ is shown schematically in Fig. 10b. Introducing the new momentum $J = 3p$ we arrive at the Hamiltonian

$$H(J, \theta, t) = \frac{J^2}{2} + 3K_0 \cos\theta\delta_2(t) = \frac{J^2}{2} + \frac{3K_0}{2}\left\{\sum_r A_r \exp[i(\theta - 2\pi r t)] + \text{c.c.}\right\}. \tag{14.23}$$

In contrast to the standard mapping, the resonance amplitudes are now unequal (Fig. 10b):

$$|A_r| = \left|1 + \exp\left(\frac{2\pi i r}{3}\right)\right| = \begin{cases} 2, & r/3 - \text{integer}, \\ \sqrt{3}, & r/3 - \text{fractional}. \end{cases} \tag{14.24}$$

In first-order approximation, the critical value of the perturbation is then determined by overlap of two neighboring resonances of lower amplitude. Since the ratio of the amplitudes of the different resonances ($2/\sqrt{3} \approx 1.15$) differs little from unity, the higher-approximation correction and the resonance repulsion (both decrease somewhat the critical perturbation) are insignificant. But it follows hence that to determine the critical perturbation we can approximately replace the Cohen mapping (14.10) by the standard mapping

$$\bar{J} = J + 3\sqrt{3}\, K_0 \sin\theta, \quad \bar{\theta} = \theta + \bar{J}, \tag{14.25}$$

which corresponds to equal amplitudes of all the resonances ($|A_r| = \sqrt{3}$). Note that were we to use the directly mapping (14.12) with the parameter (14.13),

$$K_1 = 6K_0 \cos\left(\frac{\pi r}{3}\right) = \begin{cases} \pm 6K_0, & r/3 - \text{integer}, \\ \pm 3K_0, & r/3 - \text{fractional}, \end{cases}$$

the results would not differ too much from (14.25). This shows that the mapping (14.12) can be used for order-of-magnitude estimates at an arbitrary ratio γ_+/γ_-.

One more difference between the standard mapping (14.25) and the system (14.23) of interest to us should be noted. In the former case the amplitudes as well as phases of all resonances are equal, so that the overlap is determined by the maximum distance between the separatrix branches (see Fig. 1). Now, however, neighboring resonances are separated in phase by θ on $\Delta\theta = 60°$. Since the distance between the separatrix branches is proportional to $\cos(\theta/2)$ (10.4), its relative decrease by this shift is $\cos 30° = \sqrt{3}/2 \approx 0.87$, which increases the critical perturbation by approximately 13% and offsets in part the aforementioned decrease of the critical perturbation.

Neglecting all these corrections, we get from (14.25) for the critical perturbation in the Cohen mapping with $\gamma_-/\gamma_+ = 2$ the value

$$|K_0|_{cr} \approx \frac{1}{3\sqrt{3}} \tag{14.26}$$

or, in terms of the parameters of a trap with opposing mirrors [see (14.1), (14.7), (7.37)]:

$$\beta_0^{(cr)} \approx 2.6 q^{9/40} \exp(-q/5), \tag{14.27}$$

where $q = \omega_0 \ell_0 / 3v = \ell_0 / 3\rho_m$. This expression differs only by an insignificant numerical factor from relation (10.18) for planar opposing mirrors if the parameter q is suitably chosen (see Section 7).

In the estimate of the diffusion rate we confine ourselves to the case when $3\sqrt{3}|K_0| \gg 1$ and the correlations determine the critical perturbation we can approximately replace the Cohen mapping (14.10) by the standard mapping

$$\bar{J} = J + 3\sqrt{3}\,K_0 \sin\theta, \quad \bar{\theta} = \theta + \bar{J}, \qquad (14.25)$$

which corresponds to equal amplitudes of all the resonances ($|A_r| = \sqrt{3}$). Note that were we to use the directly mapping (14.12) with the parameter (14.13),

$$K_1 = 6K_0 \cos\left(\frac{\pi r}{3}\right) = \begin{cases} \pm 6K_0, & r/3 - \text{integer}, \\ \pm 3K_0, & r/3 - \text{fractional}, \end{cases}$$

the results would not differ too much from (14.25). This shows that the mapping (14.12) can be used for order-of-magnitude estimates at an arbitrary ratio γ_+/γ_-.

One more difference between the standard mapping (14.25) and the system (14.23) of interest to us should be noted. In the former case the amplitudes as well as phases of all resonances are equal, so that the overlap is determined by the maximum distance between the separatrix branches (see Fig. 1). Now, however, neighboring resonances are separated in phase by θ on $\Delta\theta = 60°$. Since the distance between the separatrix branches is proportional to $\cos(\theta/2)$ (10.4), its relative decrease by this shift is $\cos 30° = \sqrt{3}/2 \approx 0.87$, which increases the critical perturbation by approximately 13% and offsets in part the aforementioned decrease of the critical perturbation.

Neglecting all these corrections, we get from (14.25) for the critical perturbation in the Cohen mapping with $\gamma_-/\gamma_+ = 2$ the value

$$|K_0|_{cr} \approx \frac{1}{3\sqrt{3}} \qquad (14.26)$$

or, in terms of the parameters of a trap with opposing mirrors [see (14.1), (14.7), (7.37)]:

$$\beta_0^{(cr)} \approx 2.6 q^{9/40} \exp(-q/5), \qquad (14.27)$$

where $q = \omega_0 \ell_0 / 3v = \ell_0 / 3\rho_m$. This expression differs only by an insignificant numerical factor from relation (10.18) for planar opposing mirrors if the parameter q is suitably chosen (see Section 7).

In the estimate of the diffusion rate we confine ourselves to the case when $3\sqrt{3}|K_0| \gg 1$ and the correlations can be neglected, so that $R(K) \approx 1$ (see Section 12). In the mapping (14.2) we can now assume that both "bumps" are statistically independent. To describe diffusion in discrete time, we choose as the time unit again the half-period of the longitudinal oscillations. Expression (11.3) for D_μ then remains unchanged, and with it all other relations in Sections 11 and 13.

The correlation factor R(K) will, of course, be different now. It can be obtained in analogy with the procedure used in Section 12 for the standard mapping, but of course with allowance for the correlation of the two "bumps" in the mapping (14.2). We note, finally, that the period of the longitudinal oscillations is given in our case by the relation [see (3.37), (3.38), (3.42)]:

$$T = \frac{T_+ + T_-}{2} = \frac{3vl_0}{\mu\omega_0}, \qquad \Omega = \frac{2\pi}{T} = \frac{2\pi}{3}\,\frac{\mu\omega_0}{vl_0}. \tag{14.28}$$

In the approximation assumed, no gaps whatever appear in the stochastic component. The reason is that we have considered only longitudinal oscillations with large amplitude $a \gg \ell_0$, for which $\gamma_- / \gamma_+ = 2$. At lower amplitudes this ratio decreases and the resonance amplitude requires a slow dependence on p; this can lead to formation of gaps and to isolation of individual stochastic components of the motion. Generally speaking, gaps can exist also at very large oscillation amplitudes because the ratio γ_- / γ_+ is not exactly equal to 2, but is somewhat smaller because of the additional phase shift in (7.37). From (3.38) and (7.38) we get the estimate

$$\Delta = 2 - \frac{\gamma_-}{\gamma_+} \sim \frac{1}{20}\sqrt{\frac{l_0}{a}}.$$

Since this is a very small quantity, the number of resonances in the isolated part of the stochastic component, i.e., between the gaps ($\sim 1/\Delta$), can be comparable with the total number of resonances, and then the presence or absence of gaps is immaterial.

In a purely dynamic system any gap stops the diffusion completely and thus improves substantially the particle containment in the trap. In a real situation, however, this improvement is doubtful, since the gap is narrow and even insignificant multiple scattering of the particles will cause them to "infiltrate" through the gaps. This question deserves a more detailed investigation, all the more since the asymmetry needed for gap formation can be easily introduced in any trap.

We conclude this section by noting that the effect of a certain special perturbation in a tokamak is also described by Cohen mapping [51].

15. Remarks on Adiabatic Invariance

The Budker problem considered in this article, concerning the conditions and accuracy of conservation of the magnetic moment of a charged particle in an adiabatic magnetic trap, is a particular case of a general and, in a certain sense "perpetual," problem of classical mechanics – that of the adiabatic invariance of the action variables. This, as any other invariance, plays an important role in physics, even though it is, generally speaking, approximate. According to the most widely held notions, the basic condition of adiabatic invariance is associated with slowness of the perturbation. This notion dates back to the very beginning of the study of this phenomenon and was subsequently related to the averaging method used to establish adiabatic invariance. It became clear later that slowness of the perturbation does not by itself explain the mechanism whereby adiabatic invariance is violated. A vague idea arose that this mechanism is connected somehow with resonances between an external parametric perturbation and the natural oscillations of the system. During the burgeoning development of quantum mechanics, for which the action variables in general, and their adiabatic invariance in particular, play a special role, Born wrote, for example (as cited in [52]): "We regard as adiabatic such a system change which, first, is not related in any way with the period of the unperturbed system ..." This, however, was only intuition. The role of resonances for adiabatic invariance was first precisely formulated and solved in 1928 [52]. It was sufficient for this purpose to examine attentively, from the standpoint of physics, the well-known Mathieu equation and its solutions. Indeed, instability zone or regions of parametric resonance exist in the vicinity of any half-integer frequency ratio $\omega_0 / \Omega = r/2$, where ω_0 is the unperturbed frequency of the linear oscillator, Ω is the frequency of the harmonic parametric perturbation, and r is a positive integer. But as $r \to \infty$ we have $\Omega \to 0$ and the perturbation becomes adiabatic in accord with the slowness criterion. Nonetheless, once the oscillator becomes resonant, its energy (and action) can vary arbitrarily strongly with time, i.e., adiabatic invariance is violated no matter how slow the perturbation. This leads to a different concept of adiabatic perturbation as a nonresonant one (see Born's statement above). These two seemingly different concepts are in fact closely related, inasmuch as slowness of the perturbation ensures exponential smallness of the resonant harmonics (see Section 7). This holds true, in particular, also for the Mathieu equation:

$$J = J_0 e^{\gamma t}, \quad \gamma \approx r\Delta\Omega \approx \frac{\Omega}{3}\left(\frac{e^2\varepsilon^2}{8}\right)^r; \tag{15.1}$$

i.e., the rate of exponential growth in the resonance region is itself decreased exponentially with increasing frequency ratio $r = 2\omega_0/\Omega$. The frequency-modulation depth is determined here by the relation $\omega^2(t) = \omega_2{}^0(1 - \varepsilon^2 \cos\Omega t)$. An expression for the instability growth rate γ and for the total width $\Delta\Omega$ of the resonance zone is obtained from (7.1) at $r \gg 1$ if $\omega_x = 1 + x^2$ is replaced by $\omega(t)$, and takes the form (15.1) at $\varepsilon \ll 1$.

For a linear oscillator, the decisive of the two adiabaticity conditions is the nonresonance. The resonance zones in this case are very distinct and are determined only by the parameters of the system.

For a nonlinear oscillator, the nonresonance is governed by the initial conditions. Its role differs greatly with the number of degrees of freedom of the system. For a closed system with two degrees of freedom, and also for a linear oscillator with one degree of freedom and an external parametric perturbation, the decisive factor for the adiabatic invariant is the slowness of the perturbation. A result new in principle and at the same time rigorous is here the proof of existence of a finite critical slowness of the perturbation, below which the adiabatic invariant becomes an exact integral of the motion [10]. This result is strongly connected with the special topology of the resonance systems, which can be called ordered or one-dimensional. In this case the frequencies are in only one ratio that depends on one action variable (the second action is excluded in a closed system with the aid of the energy integral; see Section 8). Such an ordered topology is significant because an exact integral exists not for all initial conditions, but only for the "nonresonant" ones. This term has a special meaning in a nonlinear system, since the region at the very center of the resonance, i.e., at an action-variable value for which the resonance conditions are exactly satisfied (see Fig. 6), is here also nonresonant. Moreover, the region in question is as a rule even more stable in the sense that an exact integral is preserved here also when resonance overlap leads to development of global instability. The most unstable, however, is the vicinity of the separatrix of the nonlinear resonance, where a stochastic layer is produced and is preserved at arbitrarily small (and slow) perturbation (see, e.g., [8]). In the case when the nonlinear resonance can be described in the pendulum approximation, the stochastic layer in the vicinity of its separatrix is quite similar to the stochastic layer in a multimirror trap (see Section 10). The width of this layer, and accordingly the share of the "resonant" initial conditions, is exponentially small in terms of the slowness parameter of the perturbation. This region is nonetheless finite and contains no exact integral. Since the resonant structure is one-dimensional, however, the stochastic trajectory is strictly confined to the interior of the layer and collapse of the integral does not alter (with exponential accuracy!) the trajectory of the motion.

The situation changes radically, however, in the case of a multidimensional (even two-dimensional) or disordered topology of the resonance. The trajectory can now go from one stochastic layer to another (i.e., with different resonance), bypassing the nonresonant region with the exact integral of motion. This bypassing of the stable regions is made possible by the intersection of the resonances (and of their stochastic layers) in multidimensional space. In other words, if the dimensionality of the phase space is increased even by unity,* motion becomes possible not only across the layer, whose width is rigorously bounded and small, but also along the layer, which is in general bounded only by the energy integral. This beautiful phenomenon was predicted by Arnol'd, who constructed the first example of such a system [53]. A similar process was subsequently named Arnol'd's diffusion and investigated in great detail in [8] (see also [9, 54]).

---

*The dimensionality of the phase space of a closed Hamiltonian system is always even. If, however, the system is acted upon by a periodic perturbation, it is said to have one dimension (the phase of the perturbation) and a half-integer number of degrees of freedom.

From the standpoint of the adiabatic invariance discussed here (which is, of course, only a particular case of the general dynamic problem of the stability of motion), in a one-dimensional system the requirement that the initial conditions be nonresonant, is at least just as important as the requirement of slow perturbation. This last requirement, just as in order topology, ensures absence of resonance overlap and the existence of an exact integral for the overwhelming majority of nonresonant initial conditions.

In this situation, however, the probability of the stability of motion in general and adiabatic invariance in particular becomes, in the language of the mathematicians, an incorrect one, or simply physically meaningless. The point is that although the total volume of the stochastic layers in phase space is indeed exponentially small, they form everywhere a dense system. Of course, the same takes place in one-dimensional topology. For example, for standard mapping, any rational value of $p/2\pi$ is resonant (see Section 10). However, in view of the already described ordered structure of the resonances, the system motion is not affected. In the multidimensional case, however, unbounded Arnol'd diffusion sets in.

There are several methods of so-called regularization of the problem, i.e., of formulating it unambiguously and independently of the infinitely small changes of the initial conditions. One can, for example, pose the problem of adiabatic invariance over an arbitrarily large but finite time interval. Since the rate of the Arnol'd diffusion falls off extremely rapidly with increasing order of the resonances, any time limitation transforms right away the infinite and everywhere-dense system of resonances (and of their stochastic layers) into a finite one, and the problem acquires physical meaning. In this case, the nonresonance condition (with respect to the remaining "working" stochastic layers) is essential for adiabatic invariance.

Another regularization method consists of introducing in the problem an additional arbitrarily weak but finite external diffusion [8]. This again leaves a finite number of stochastic layers in which the Arnol'd diffusion is faster than the external diffusion. With the problem so formulated, the initial conditions of the motion are immaterial, since the external diffusion will continuously displace the dynamic trajectory.

REFERENCES

1. G. I. Budker, "Thermonuclear reactions in a system with magnetic mirrors. Contribution to the problem of direct conversion of nuclear energy into electricity," in: Collected Works [in Russian], G. I. Budker (ed.), Nauka, Moscow (1982), p. 72.
2. B. V. Chirikov, "The problem of stability of motion of a charged magnetic trap," Fiz. Plazmy, 4, No. 3, 521 (1978).
3. R. H. Cohen, "Orbital resonances in nonaxisymmetric mirror machines," Comments Plasma Phys. Controlled Fusion, 4, No. 6, 157 (1979).
4. B. V. Chirikov, "Adiabatic invariants and stochasticity in magnetic confinement systems," Proceedings Intern. Conf. on Plasma Physics, Nagoya (1980), Vol. II, p. 176.
5. R. H. Cohen, G. Rowlands, and J. H. Foote, "Nonadiabaticity in mirror machines," Phys. Fluids, 21, No. 4, 627 (1978).
6. B. V. Chirikov, "Homogeneous model of resonant diffusion of particles in an open magnetic trap," Fiz. Plazmy, 5, No. 4, 880 (1979).
7. G. I. Dimov, V. V. Zakaidakov, and M. E. Kishinevskii, "Thermonuclear trap with tandem mirrors," Fiz. Plazmy, 2, No. 4, 597 (1976); T. K. Fowler and B. G. Logan, "The tandem mirror reactor," Comments Plasma Phys. Controlled Fusion, 2, No. 6, 167 (1977).
8. B. V. Chirikov, "A universal instability of many-dimensional oscillator systems," Phys. Rep., 52, No. 5, 263 (1979).
9. A. J. Lichtenberg and M. A. Lieberman, Regular and Stochastic Motion, Springer, Berlin (1983).
10. V. I. Arnol'd, "Small denominators and the problem of stable motion in classical and celestial mechanics," Usp. Mat. Nauk, 18, No. 6, 91 (1963).
11. G. I. Budker, V. V. Mirnov, and D. D. Ryutov, "Influence of magnetic-field corrugation on expansion and cooling of a dense plasma," Pis'ma Zh. Eksp. Teor. Fiz., 14, No. 5, 320 (1971).
12. N. N. Bogolyubov and Yu. A. Mitropol'skii, Asymptotic Methods in the Theory of Nonlinear Oscillations [in Russian], Nauka, Moscow (1974).
13. R. W. B. Best, "On the motion of charged particles in a slightly damped sinusoidal potential wave," Physica, 40, No. 2, 182 (1968).

14. A. S. Bakai and Yu. P. Stepanovskii, Adiabatic Invariants [in Russian], Naukova Dumka, Kiev (1981).
15. J. E. Howard, "Nonadiabatic particle motion in cusped magnetic fields," Phys. Fluids, 14, No. 11, 2378 (1971).
16. A. M. Dykhne and A. V. Chaplik, "Change of adiabatic invariant of a particle in a magnetic field," Zh. Eksp. Teor. Fiz., 40, No. 2, 666 (1961).
17. M. Kruskal, Adiabatic Invariants [Russian translation], Inostr. Lit., Moscow (1962).
18. C. S. Gardner, "Magnetic moment in second order for axisymmetric static field," Phys. Fluids, 9, No. 10, 1997 (1966).
19. O. B. Firsov, "Repulsion of charged particle from regions with strong magnetic field. (Accuracy of adiabatic invariant)," in: Plasma Physics and the Problem of Controlled Thermonuclear Reactions [in Russian], Izd. Akad. Nauk SSSR, Moscow (1958), Vol. III, p. 259.
20. R. J. Hastie, G. D. Hobbs, and J. B. Taylor, "Non-adiabatic behavior of inhomogeneous magnetic fields," Plasma Physics and Controlled Thermonuclear Fusion Research, IAEA (1969), Vol. I, p. 389.
21. E. M. Krushkal', "Nonadiabatic motion of particles in nonuniform magnetic fields," Zh. Tekh. Fiz., 42, No. 11, 2288 (1972).
22. I. S. Gradshtein and I. M. Ryzhik, Tables of Integrals, Sums, Series, and Products, Academic Press, New York (1965).
23. J. M. Greene, "A method for determining a stochastic transition," J. Math. Phys., 20, No. 6, 1183 (1979).
24. F. M. Izrailev, B. V. Chirikov, and D. L. Shepelyanskii, "Dynamic stochasticity in classical mechanics," Preprint Inst. Nucl Phys., Siberian Branch, Acad. Sci. USSR, No. 80-209, Novosibirsk (1980).
25. M. N. Rosenbluth, "Superadiabaticity in mirror machines," Phys. Rev. Lett., 29, No. 7, 408 (1972).
26. I. P. Kornfel'd, Ya. G. Sinai, and S. V. Fomin, Ergodic Theory [in Russian], Nauka, Moscow (1980).
27. V. M. Alekseev and M. V. Yakobson, "Symbolic dynamics and hyperbolic dynamic systems," Suppl. to Methods of Symbolic Dynamics, R. Bowen (ed.) [Russian translation], Mir, Moscow (1979); A. A. Brudno, "Entropy and algorithmic complexity of trajectories of a dynamic system," Preprint of All-Union Inst. for System Research, Moscow (1980).
28. B. V. Chirikov, "Nature of stochastic laws of classical mechanics," in: Methodological and Philosophical Problems of Physics [in Russian], Nauka, Novosibirsk (1982), p. 181.

29. N. N. Bogolyubov, "Problems of dynamic theory in statistical physics," in: Selected Works [in Russian], Naukova Dumka, Kiev (1970), Vol. 2, p. 99.
30. J. L. Lebowitz, "Hamiltonian flows and rigorous results in nonequilibrium statistical mechanics," in: Statistical Mechanics. New Concepts, New Problems, New Applications, Univ. of Chicago Press, Chicago (1972), p. 41.
31. R. Balescu, Equilibrium and Nonequilibrium Statistical Mechanics, Wiley, New York (1975).
32. G. E. Norman and L. S. Polak, "Irreversibility in classical statistical mechanics," Dokl. Akad. Nauk SSSR, 263, No. 2, 337 (1982).
33. E. M. Lifshitz and L. P. Pitaevskii, Physical Kinetics, Pergamon Press, Oxford (1981).
34. A. B. Rechester and R. B. White, "Calculation of turbulent diffusion for the Chirikov–Taylor model," Phys. Rev. Lett., 44, No. 24, 1586 (1980); A. B. Rechester, M. N. Rosenbluth, and R. B. White, "Fourier-space paths applied to the calculation of diffusion for the Chirikov–Taylor model," Phys. Rev., A23, No. 5, 2264 (1981).
35. J. R. Cary, J. D. Meiss, and A. Bhattacharjee, "Statistical characterization of periodic measure-preserving mappings," Phys. Rev., A23, No. 5, 2744 (1981).
36. L. A. Bunimovich and Ya. G. Sinai, "Statistical properties of Lorentz gas with periodic configuration of scatterers," Commun. Math. Phys., 78, 479 (1981).
37. C. Grebogi and A. N. Kaufman, "Decay of statistical dependence in chaotic orbits of deterministic mappings," Phys. Rev., A24, No. 5, 2829 (1981).
38. G. V. Gadiyak and F. M. Izrailev, "Structure of transition zone of nonlinear resonance," Dokl. Akad. Nauk SSSR, 218, No. 6, 1302 (1974).
39. B. V. Chirikov and D. L. Shepelyanskii, "Statistics of Poincaré returns and structure of stochastic layer of nonlinear resonance," Preprint, Inst. Nucl. Phys, Siberian Branch, Acad. Sci. USSR, No. 81-69, Novosibirsk (1981).
40. D. Bora, P. I. John, Y. C. Saxena, and R. K. Varma, "Multiple lifetimes in the nonadiabatic leakage of particles from magnetic mirror traps," Plasma Physics, 22, No. 7, 653 (1980).
41. D. F. Escande and F. Doveil, "Renormalization method for computing the threshold of the large-scale stochastic instability in two degrees of freedom Hamiltonian systems," J. Stat. Phys., 26, No. 2, 257 (1981).

42. L. P. Kadanoff, "Scaling for a critical Kolmogorov–Arnold–Moser trajectory," Phys. Rev. Lett., 47, No. 23, 1641 (1981); S. J. Shenker and L. P. Kadanoff, "Critical behavior of a KAM surface: empirical results," J. Stat. Phys., 27, No. 4, 631 (1982).
43. L. D. Landau, "Kinetic equation for rarefied gases in strong fields," Zh. Eksp. Teor. Fiz., 7, No. 2, 203 (1937).
44. S. T. Belyaev, "Kinetic equation for rarefied gases in strong fields," in: Plasma Physics and Problem of Controlled Thermonuclear Reactions [in Russian], Izd. Akad. Nauk SSSR, Moscow (1958), Vol. III, p. 50.
45. B. V. Chirikov and D. L. Shepelyanskii, "Diffusion in multiple passage through nonlinear resonance," Preprint Inst. Nucl. Phys., Siberian Branch, Acad. Sci. USSR, No. 80-211, Novosibirsk (1980).
46. M. A. Lieberman and A. J. Lichtenberg, "Stochastic and adiabatic behavior of particles accelerated by periodic forces," Phys. Rev., A5, No. 4, 1852 (1972).
47. A. Brahic, "Numerical study of a simple dynamical system," Astron. Astrophys., 12, 98 (1971).
48. T. A. Zhdanova and F. M. Izrailev, "On Fermi statistical acceleration," Preprint Inst. Nucl. Phys., Siberian Branch, Acad. Sci. USSR, No. 121-74, Novosibirsk (1974).
49. R. H. Cohen, "Stochastic motion of particles in mirror machines," in: Intrinsic Stochasticity in Plasma, G. Laval and D. Gresillon (eds.), Edition de Physique, Orsay (1979).
50. D. F. Escande, "Primary resonances do not overlap," in: Intrinsic Stochasticity in Plasma, G. Laval and D. Gresillon (eds.), Edition de Physique, Orsay (1979).
51. R. J. Goldston, R. B. White, and A. H. Boozer, "Confinement of high-energy particles in tokamaks," Phys. Rev. Lett., 47, No. 9, 647 (1981).
52. L. I. Mandel'shtam, Complete Works [in Russian], Izd. Akad. Nauk SSSR, Moscow (1948), Vol. I, p. 297.
53. V. I. Arnol'd, "Instability of dynamic systems with many degrees of freedom," Dokl. Akad. Nauk SSSR, 156, No. 1, 9 (1964).
54. N. N. Nekhoroshev, "Exponential estimate of the stability time of nearly integrable Hamiltonian systems," Usp. Mat. Nauk, 32, No. 6, 5 (1977).